“New knowledge is the most valuable commodity on earth. The more truth we have to work with, the richer we become.”

-**Kurt Vonnegut**

University of Alberta

Investigating the Caspase Cleavage of the JunB Transcription Factor

by

Jason Kwok Ho Lee

A thesis submitted to the Faculty of Graduate Studies and Research
in partial fulfillment of the requirements for the degree of

Master of Science

in

Immunology

Medical Microbiology and Immunology

Spring 2013
Edmonton, Alberta

To my parents, for their endless support and encouragement.

ABSTRACT

The activation of caspases is an important step not only in apoptosis induction, but in cellular processes such as proliferation, differentiation, and the immune response. Here, we show that the AP-1 family transcription factor JunB is cleaved and dephosphorylated in a caspase-dependent manner in apoptotic cells. We demonstrate that JunB is cleaved directly by caspases, and identify aspartic acid 137 as the cleavage site. JunB cleavage separates the amino-terminal transactivation and carboxy-terminal DNA binding/dimerization domains to disrupt JunB transcriptional activity. Moreover, the carboxy-terminal cleavage fragment retains DNA binding activity, and the ability to dimerize with AP-1 proteins. This fragment interferes with full-length JunB binding to AP-1 sites and inhibits AP-1–dependent transcription. Finally, we show that the carboxy-terminal cleavage fragment impairs proliferation and promotes apoptosis when overexpressed in a T-cell lymphoma cell line. In summary, our findings reveal a novel mechanism of regulating the activity of an AP-1 family transcription factor.

ACKNOWLEDGMENTS

First and foremost, I would like to thank my supervisor, Dr. Robert Ingham, for taking a chance on me, and for the invaluable guidance, support, and patience he has provided over the course of my masters project. He has been a tremendous mentor who goes above and beyond for his students, and I am grateful for all of his support. I would also like to acknowledge Drs. Michele Barry and Hanne Ostergaard, my supervisory committee, for their help and support over the course of my project; Dr. Ing Swie Goping for agreeing to serve as the internal-external examiner for my thesis defense; and Dr. Jim Smiley for chairing my thesis defense.

I would also like to thank past and present members of the Ingham lab, who have made the lab a great place to be, both good days and bad. I would like to especially thank Joel Pearson, who has taught me everything I know, providing so much help and guidance, and without whom I would surely still be stuck at square one of my project. I would also like to thank Dr. Julinor Bacani and the members of the Baldwin and Lai labs for their input and feedback during our lab meetings. My thanks also go out to my friends both in and out the MMI department who have helped maintain some semblance of a life outside of the lab.

Finally, this would not have been possible without the loving help and support of my family who, despite not actually knowing what I do in the lab, continue to support my endeavours. I will forever be grateful for their support.

TABLE OF CONTENTS

LIST OF TABLES

Chapter 2: Materials and Methods

LIST OF FIGURES

Chapter 1: Introduction

Chapter 2: Materials and Methods

Chapter 3: Investigating the cleavage of JunB by caspases

Chapter 4: Discussion

LIST OF ABBREVIATIONS

AA	amino acid
ADP	adenosine diphosphate
Akt	protein kinase B
ALK	anaplastic lymphoma kinase
ALK+ ALCL	anaplastic lymphoma kinase positive, anaplastic large cell lymphoma
AP-1	activator protein 1
APS	ammonium persulphate
ASC	apoptosis associated speck-like protein containing a CARD
ATCC	American type culture collection
ATF	activating transcription factor
ATP	adenosine triphosphate
BCA	bicinchoninic acid protein assay
Bcl-2	B-cell lymphoma 2
BGH	bovine growth hormone
BH	Bcl-2 homology
BrdU	bromodeoxyuridine
BSA	bovine serum albumin
bZIP	basic region leucine zipper
CARD	caspase recruitment domain
CDK	cyclin dependent kinase
c-FLIP	FLICE-like inhibitory protein
CHAPS	3-[(3-cholamidopropyl)dimethylammonio]-1-propanesulfonate
CHOP	cyclophosphamide, hydroxydaunorubicin, oncovin and prednisone
CMV	cytomegalovirus
CRE	cyclic adenosine monophosphate (cAMP) response element
CREB	cAMP response element binding protein
CT	carboxy (C) terminal
DBD	DNA binding domain
DD	death domain
DED	death effector domain
DZD	dimerization domain
DISC	death-induced signalling complex
DNA	deoxyribonucleic acid
DNase	deoxyribonuclease
DTT	dithiothreitol
EB	elution buffer
EBV	Epstein-Barr virus
EDTA	ethylenediaminetetraacetic acid
EMSA	electrophoretic mobility shift assay
EPO	erythropoietin
ER	endoplasmic reticulum
ERK	extracellular signal-regulated kinase
ETS-1	E-twenty six-1
FADD	Fas-associated protein with a death domain
FAK	focal adhesion kinase

FBS	fetal bovine serum
Fbw7	F-box and WD repeat domain containing 7
FITC	fluorescein isothiocyanate
FOXO3a	forkhead box O3 a
Fra2	Fos-related antigen-2
GATA-1	GATA-binding factor 1
GSK-3	glycogen synthase kinase 3
HC	(immunoglobulin) heavy chain
HECT	homologous to the E6-AP carboxyl terminus
HRP	horseradish peroxidase
ICAD	inhibitor of caspase activated DNase
IFN-γ	interferon gamma
Ig	immunoglobulin
IL	interleukin
IMT	inflammatory myofibroblastic tumor
IP	immunoprecipitation
JAK	Janus kinase
JNK	c-Jun N-terminal kinase
K299	Karpas 299
LB	Luria broth
LC	(immunoglobulin) light chain
LS	large catalytic subunit (caspase)
MAPK	mitogen-activated protein kinase
M-CSF	macrophage colony-stimulating factor
MEK	MAPK kinase
MOMP	mitochondrial outer membrane permeabilization
NCBI	National Center for Biotechnology Information
NFAT	nuclear factor of activated T-cells
NF-κB	nuclear factor kappa-light-chain-enhancer of activated B cells
NK	natural killer
NLR	NOD-like receptor
NLS	nuclear localization signal
NOD	nucleotide-binding oligomerization domain
NP-40	Nonidet P-40
NPM	nucleophosmin
NPM-ALK	nucleophosmin anaplastic lymphoma kinase
NS	not significant
NSCLC	non-small cell lung cancer
NT	amino (N) terminal
OPG	osteoprotegerin
PAMP	pathogen-associated molecular patterns
PARP	poly (ADP-ribose) polymerase
PBS	phosphate buffered saline
PCR	polymerase chain reaction
PDGFRβ	platelet-derived growth factor receptor beta
PI	propidium iodide
PI3K	phosphatidylinositide-3 kinase
PIDD	p53-induced death domain protein

PIPES	piperazine-N,N'-bis(2-ethanesulfonic acid)
PKC	protein kinase C
PLC	phospholipase C
PMSF	phenylmethanesulfonyl fluoride
PRR	pattern recognition receptor
PS-SCL	positional scanning synthetic combinatorial libraries
PU.1	spleen focus forming virus (SFFV) proviral integration oncogene (spi1)
RAIDD	RIP-associated Ich-1/Ced-3-homologue protein with a death domain
RIG-I	retinoic acid-inducible gene 1
RING	really interesting new gene
RIP-1	receptor-interacting serine/threonine protein kinase 1
RNA	ribonucleic acid
RPMI	Roswell Park Memorial Institute medium
RPTP β/ζ	receptor protein tyrosine phosphate β/ζ
SCF	SKP1, CUL1 and F-box protein
SDS	sodium dodecyl sulphate
SDS-PAGE	sodium dodecyl sulphate polyacrylamide gel electrophoresis
siRNA	small interfering RNA
SS	small catalytic subunit (caspase)
STAT	signal transducer and activator of transcription
TAD	transactivation domain
TAE	Tris-acetate EDTA buffer
TBS	Tris-buffered saline
TBST	Tris buffered saline and Tween20
TCR	T-cell receptor
TE	Tris-EDTA buffer
TEMED	tetramethylethylenediamine
TK	tyrosine kinase
TNF	tumor necrosis factor
TNFR	tumor necrosis factor receptor
TPA	12-O-tetradecanoylphorbol-13-acetate
TRADD	Tumor necrosis factor receptor type 1-associated DEATH domain protein
TRAIL	TNF-related apoptosis-inducing ligand
TRE	TPA DNA responsive element
VV	Vaccinia Virus
WB	western blotting
WHO	World Health Organization
WT	wild-type
YY1	Yin Yang 1

CHAPTER 1: INTRODUCTION

1.1: ANAPLASTIC LYMPHOMA KINASE POSITIVE, ANAPLASTIC LARGE CELL LYMPHOMA (ALK+ ALCL)

Cancers of the immune system such as leukemias and lymphomas are responsible for a significant number of illnesses and deaths each year (1). Many of these cancers arise from mutations that result in the dysregulation of cell proliferation and survival. Anaplastic lymphoma kinase positive, anaplastic large cell lymphoma (ALK+ ALCL), a lymphoma of T-cell origin (2,3), is an example of how dysregulated signal transduction pathways can result in cancer pathogenesis.

1.1.1: Characteristics of ALK+ ALCL

First identified in 1985, anaplastic large cell lymphoma (ALCL) was described as a unique large cell lymphoma with a dedifferentiated cell morphology that expresses the CD30 (Ki-1) antigen, an activator antigen found in a number of other cancers (4). CD30, a member of the tumour necrosis factor (TNF) family of receptors, typically mediates signalling in activated T and B lymphocytes that leads to cell-type dependent consequences ranging from cell proliferation, cell survival, or apoptosis (5,6). CD30 is often found to be expressed in cancers such as Hodgkin lymphoma and ALCL (7), however its function in ALCL is not well understood. In Hodgkin lymphoma, the high expression of CD30 results in the constitutive activation of the NF-κB pathway to result in cell proliferation and survival. In ALCL however, the activation of CD30 generally results in cell cycle arrest and apoptotic cell death (8-10) – although it appears that the method and duration of CD30 stimulation can affect its signalling and the induction of apoptosis (11).

Further characterization of ALCL came with subsequent reports (12-15) that found recurrent chromosomal translocations in some of these lymphomas, determined

in 1994 to be a translocation between chromosomes 2 and 5, to result in the aberrant expression of the anaplastic lymphoma kinase (ALK) fusion protein (16). Under the current World Health Organization (WHO) classification Scheme for lymphomas (2,17), ALCL that expresses ALK is a distinct subset of T cell neoplasms known as ALK+ ALCL.

Although these lymphomas are characterized by the appearance of 'hallmark cells' with morphological features that include horseshoe or kidney shaped nuclei, dispersed nuclear chromatin, prominent perinuclear/Golgi staining, and occasionally multi-nucleated large cells (2,17), the definitive diagnosis of ALK+ ALCL is the detection of the expression of ALK by antibodies (18). It is now widely accepted that most ALCL tumour cells are derived from T-lymphocytes as these cells are reported to have undergone clonal rearrangements at the TCR locus (19). However, these cells are often characterized as T or null cell immunophenotype as they often do not express characteristic T-cell markers such as CD3 and ZAP70 (20). The specific subset of T-cells that ALCL cells are derived from remains unknown, as genome wide studies of ALK+ ALCL gene expression shows that these cells were equally different from CD8+ and CD4+ T-cells (21). Nevertheless, the expression of cytotoxic molecules such as granzyme B and perforin in ALK+ ALCL cells seems to suggest that these cells may be derived from cytotoxic lymphocytes (22,23).

In affected patients, ALK+ ALCL presents as an aggressive disease with infiltration of lymph nodes by dedifferentiated T/null lymphoid cells (5), with extranodal disease occurring in skin, bone, soft tissues, and in rare cases the CNS and GI tract as well to result in systemic disease (reviewed in (24)). ALK+ ALCL occurs mostly in children and young adults, but can also occur in older patients. In children, ALK+ ALCL represents 84-95% of pediatric cases of ALCL – making it the most common non-Hodgkin lymphoma

in children (25,26). ALK+ ALCL is typically treated with combination chemotherapy using the CHOP (cyclophosphamide, hydroxydaunorubicin/doxorubicin, oncovin, and prednisone) regimen (27). This regimen is typically used in the treatment of non-Hodgkin lymphomas and includes the DNA damaging agents cyclophosphamide (an alkylating agent) and hydroxydaunorubicin/doxorubicin (a DNA intercalating agent), the mitotic inhibitor oncovin that disrupts microtubule assembly, and the corticosteroid prednisone which likely functions as an immunosuppressant. The prognosis for patients diagnosed with ALK+ ALCL is generally quite good, with 5-year survival rates up to 85% in children, and 80% in young adults with conventional chemotherapy (28-31). More recently, both CD30 and NPM-ALK have been used as therapeutic targets, with the development of drugs that target these molecules, such as Brentuximab vedotin – a CD30 targeting monoclonal antibody-drug conjugate approved in 2011 for use in Hodgkin lymphoma and systemic ALCL (32); and Crizotinib – an ALK inhibitor that was approved in 2011 for use in ALK expressing non-small cell lung cancers (33), and currently undergoing clinical trials for advanced disseminated ALCL (34) and neuroblastoma (35).

1.1.2: The anaplastic lymphoma kinase (ALK)

The anaplastic lymphoma kinase (CD246) is a receptor tyrosine kinase of the insulin receptor superfamily, and is typically expressed in the cells of the central and peripheral nervous systems (25,36-38). The normal function of ALK is not well known, and ALK-deficient mice do not appear to have any overt developmental defects (39-42). However, in experiments conducted in *Drosophila melanogaster*, ALK has been found to function as a receptor for the neurotrophic factor jelly belly protein (Jeb) (43-45), and other studies have shown that ALK can act as a receptor for the mammalian proteins

pleiotrophin and midkine (46,47). The activation mechanism of ALK has been suggested to involve the removal of its inhibitor phosphatase, receptor tyrosine phosphatase β/ζ (RPTP β/ζ), following binding of pleiotrophin to RPTP β/ζ (48). Additionally, it was found that the expression of wildtype ALK induced apoptosis in rat neuroblast cells, although the addition of activating antibodies of ALK was able to reduce the apoptotic cell deaths of these cells (49). This led to the suggestion that ALK may function as a dependence receptor, a receptor that normally induces apoptosis when unbound, but suppresses apoptotic signalling when bound by its ligand (49,50). Outside of the nervous system, ALK is found to be aberrantly expressed in a number of cancers, most notably in ALK+ ALCL, non-small-cell lung cancer (NSCLC) (51-54), and inflammatory myofibroblastic tumours (IMT) (55-62). In many of these cancers, the aberrant expression of ALK is due to chromosomal translocations that results in the formation of an ALK fusion gene. Fusion partners of ALK vary from cancer to cancer, and common ALK fusion partners include echinoderm microtubule-associated protein-like 4 (EML4-ALK) in NSCLC (51), tropomyosin 3 (TPM3-ALK) in IMT (56,63), and the well characterized nucleophosmin (NPM-ALK) fusion in ALK+ ALCL. ALK expression can also be increased without chromosomal translocations, such as in the case in neuroblastomas, where ALK expression is dysregulated due to gene amplifications and activating mutations (64-69).

The most well characterized ALK gene fusion is in ALCL, where over half of all ALCL cases contain chromosomal translocations that result in the fusion of the Anaplastic Lymphoma Kinase (ALK) to another gene, usually *nucleophosmin* (*NPM*) (70). NPM, a carrier protein that shuttles proteins between the cytoplasm and nucleolus and is involved in a number of processes including ribosome biogenesis and transport, DNA repair, tumour suppression through the p53 pathway (71-74), is the fusion partner of

ALK in over 80% of the cases of ALK+ ALCL (75). The t(2;5)(p23;q35) chromosomal translocation generates a fusion gene under the control of the *NPM* promoter that contains the oligomerization domain of NPM, and the cytoplasmic tail and kinase domain of ALK (Figure 1.1). This gene fusion results in a expression of a constitutively active NPM-ALK fusion protein that activates down-stream signalling events to promote proliferation, survival, and migration in ALK+ ALCL (reviewed in (39,75,76)). Signalling pathways that are upregulated by NPM-ALK have been reviewed extensively in the literature (24,75,77), and include the JAK/STAT, MEK/ERK, PI3K/Akt, and PLCγ pathways (Figure 1.2). Among the many signalling molecules that are upregulated by NPM-ALK are a family of transcription factors known as AP-1 transcription factors, including proteins such as c-Jun and JunB, which have been shown to be important for the proliferation of ALK+ ALCL (78,79), and will be the subject of my thesis project.

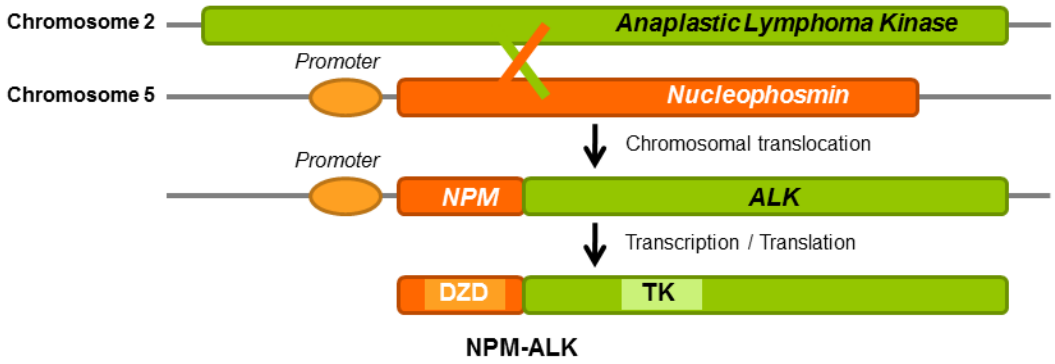

Figure 1.1: The chromosomal translocation that results in the formation of the NPM-ALK fusion protein in ALK+ ALCL.

ALK+ ALCL features recurrent chromosomal translocation that results in the aberrant expression of the anaplastic lymphoma kinase (ALK). Typically, chromosomal translocations between chromosomes 2 and 5 result in a fusion gene that driven by the *NPM* promoter to form a constitutively active fusion protein that contains the dimerization domain (DZD) of NPM and the tyrosine kinase (TK) domain of ALK.

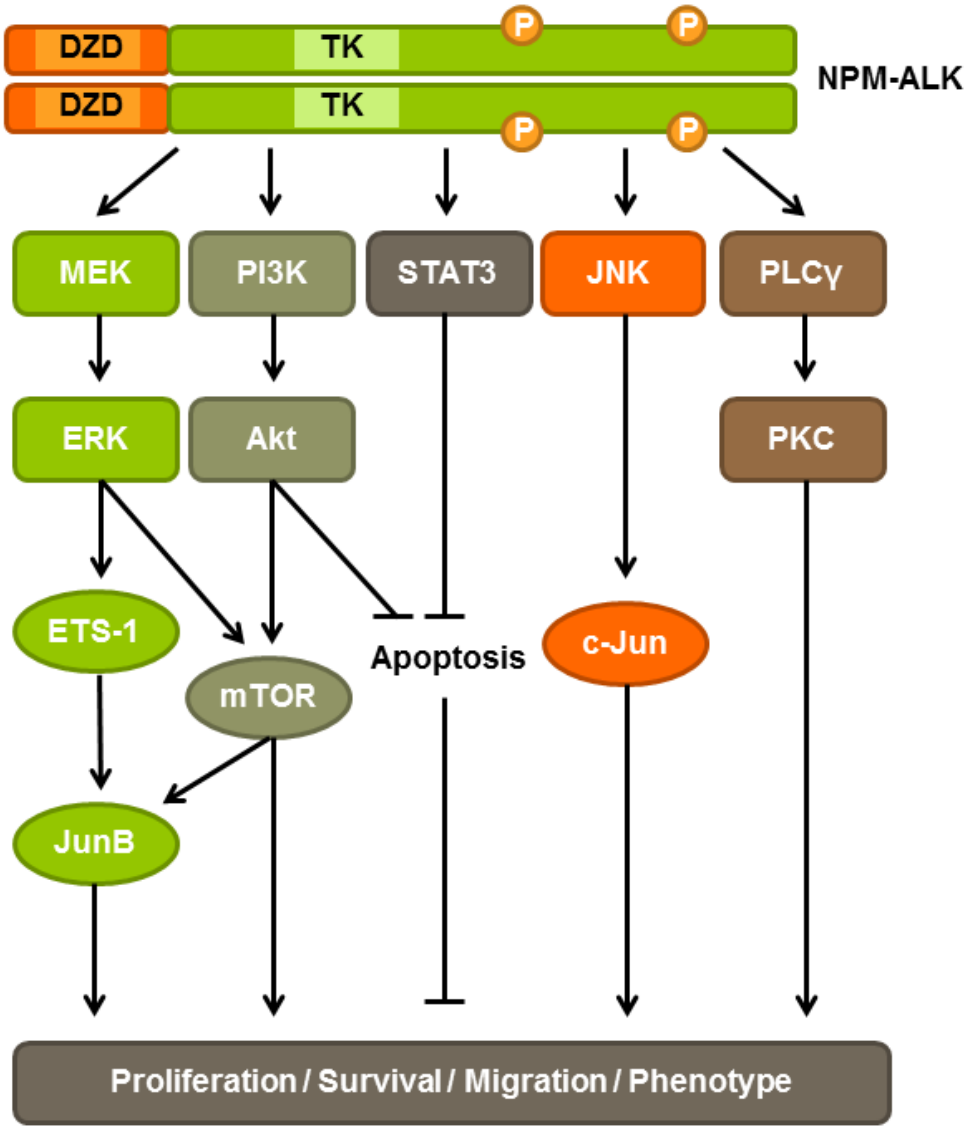

Figure 1.2: Signalling pathways affected by NPM-ALK in ALK+ ALCL cells.

NPM-ALK promotes the proliferation, survival, and migration of ALK+ ALCL cells through the MEK/ERK, PI3K/Akt, JAK/STAT, JNK, and PLCγ signalling pathways. The Jun proteins c-Jun and JunB, which promote the proliferation of ALK+ ALCL cells, are upregulated by NPM-ALK signalling through a number of pathways. c-Jun is upregulated by the activation of JNK, while JunB transcription is upregulated by the activation of the ETS-1 transcription factor by ERK. JunB translation is also promoted by mTOR, which is activated through both the MEK/ERK and PI3K/Akt pathways. Signalling through the PI3K/AKt and JAK/STAT pathways block apoptosis to promote survival.

1.2: THE AP-1 FAMILY OF TRANSCRIPTION FACTORS

1.2.1: Introduction

The Activator Protein-1 (AP-1) family of transcription factors are dimeric basic region-leucine zipper (bZIP) domain containing proteins that include Jun, Fos, activating transcription factor (ATF) and Maf family members (80-82). AP-1 transcription factors were first identified as proteins that bound to the promoter regions of genes stimulated by 12-O-tetradecanoylphorbol-13-acetate (TPA), a phorbol ester that activates protein kinase C (PKC) (83). These transcription factors dimerize through their leucine zippers to form homo and heterodimers that can bind to DNA through the basic domain of the proteins. Typically, dimers that are formed between Jun family members are unstable, while heterodimers between Jun and Fos family members are more stable and, as a result, more transcriptionally active (84-90). Fos family members, however, cannot homodimerize, and must form heterodimers with other AP-1 family member proteins (86,87,91). Dimerization between AP-1 proteins is essential for AP-1 activity and target specificity, and AP-1 dimers bind to specific TPA response elements (TRE; consensus sequence: TGACTCA (92,93) or cAMP response elements (CRE; consensus sequence: TGACGTCA (87)) within the promoter regions of genes. The composition of AP-1 dimers gives them dimer-specific DNA binding site preferences, and helps modulate the different genes that are regulated. For example, Jun/Fos dimers preferentially bind to TRE sites, while Jun/ATF dimers bind to CRE sites (94). These AP-1 dimers regulate the expression of a diverse group of genes involved in cellular processes such as growth and proliferation, apoptosis, and the immune response (82,95).

1.2.2: Structure of AP-1 proteins

AP-1 proteins can vary structurally between family members, although they retain an evolutionarily conserved bZIP motif where the basic and leucine zipper domains are responsible for DNA binding and dimerization respectively. The leucine zipper facilitates the dimerization of AP-1 proteins by forming parallel α-helices to form the coiled-coil structure of the AP-1 complex (96,97). Each half of the leucine zipper consists of regions containing characteristic heptad repeats with leucine residues in the 4^{th} position to form an amphipathic alpha helix with a hydrophobic region on one side, and a hydrophilic region on the other (98) (Figure 1.3A). This arrangement of amino acids allows for dimerization of the parallel α-helices along the hydrophobic ridge, at leucine residuesto form the leucine "zipper" (99) (Figure 1.3B). Additionally, the positively-charged DNA binding basic region, positioned N-terminally of the leucine zipper, is composed of positively-charged amino acids such as arginine and lysine to mediate the binding to the sugar-phosphate backbone of DNA (90,100) (Figure 1.3B). The basic region also contains the nuclear localization signal (NLS) to target these proteins to the nucleus in the cell following translation (101). In addition, AP-1 transcription factors may also contain transactivation domain(s) that contain phosphorylation sites or binding sites for cofactor proteins that can regulate their transcriptional activity, or target it for degradation. These transactivation domains are typically located on the N-terminal region of Jun family members (102,103) (Figure 1.3C) and are more variable in Fos family members (104-107). While there are many AP-1 family member proteins, because the main focus of this thesis project will be on the JunB transcription factor, the following sections will focus mainly on the function and regulation of the JunB transcription factor.

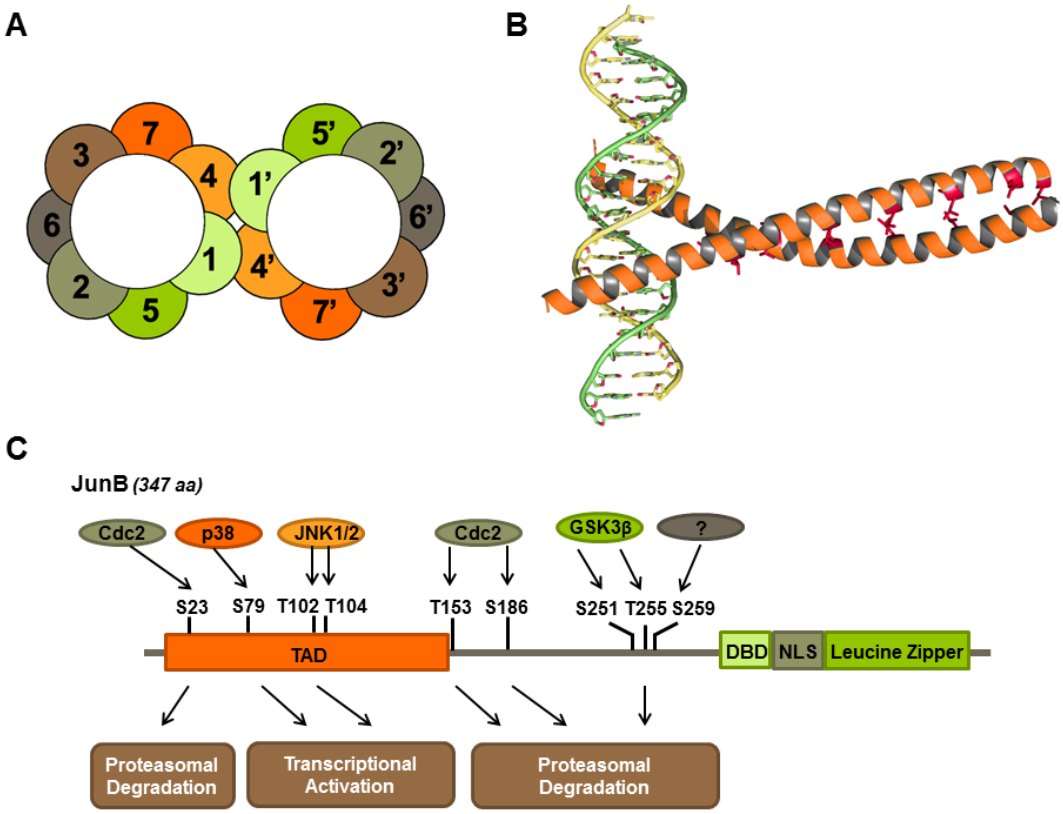

Figure 1.3: Structural domains and phosphorylation sites of JunB.

A. Helical wheel diagram of parallel alpha helices of a leucine zipper. The leucine residue, located on the 4th residue (4) of the heptad repeat, interacts with the other leucine residue (4') of the parallel alpha helix. Figure adapted from (108) **B.** Structure of DNA binding domain and leucine zipper of c-Jun and c-Fos bound to DNA (97) generated by the PyMol visualization program (109). The c-Jun/c-Fos dimer (orange) interact via leucine residues (red) to form the leucine zipper. The c-Jun/c-Fos basic domain binds to DNA (green/yellow) at the major groove of the molecule. **C.** Major structural domains of JunB are as indicated. JunB contains a highly conserved basic leucine zipper (bZIP) domain that contains the basic region which functions as a DNA binding domain (DBD), nuclear localization signal (NLS), and a leucine zipper that functions as a dimerization domain between AP-1 family members. JunB also contain an N-terminal transactivation domain (TAD). JunB function is regulated through phosphorylation, and the sites of phosphorylation, the kinases responsible for the phosphorylation, and the consequences of phosphorylation are indicated above.

1.2.3: JunB

JunB is a member of the activator protein-1 (AP-1) family of transcription factors, and was identified in 1988 shortly after the discovery of c-Jun (110). JunB is similar to c-Jun structurally and contains a bZIP domain in its c-terminal region that allows it to form homodimers with itself and form heterodimers with other AP-1 family members including members of the Jun, Fos, ATF, or Maf sub-families (81,82). JunB differs from c-Jun in the transactivation domain, resulting in a reduced ability to activate transcription (103). Indeed, JunB was first described as an antagonist of c-Jun for its ability to inhibit c-Jun transcriptional activity and block the transformation of fibroblasts by c-Jun (111,112), and was later shown to block the proliferation of the mouse fibroblast cell line 3T3 through the activation of the cyclin-dependent kinase inhibitor p16(INK4A) (113). While JunB has long been thought to function as a negative regulator of transcription by acting as an antagonist of c-Jun, JunB is not exclusively an antagonist of c-Jun, and has also been shown to promote cell cycle progression. For example, JunB can promote the expression of cyclin A to relieve a G_2/M impairment in mouse fibroblasts (114), and is important for cells to reach S-phase, as the injection of antibodies that blocked the function of JunB into mouse fibroblast cells was sufficient to significantly inhibit DNA synthesis (115).

JunB has also been found to play important roles in embryogenesis and development, as a JunB knockout in mice is embryonically lethal due to vasculature defects in embryonic tissue such as the placenta and yolk sack (116). Additionally, in c-Jun deficient mice, JunB was observed to rescue the lethal cell proliferation defects during development, as the introduction of JunB into these mice rescued developmental defects in the heart and liver in a dose-dependent manner (117). JunB also been

implicated in playing a role in myeloid cell differentiation as the conditional deletion of JunB in murine cells of myeloid lineage resulted in a chronic myeloid leukemia-like disorder (118). In addition, JunB is also important in bone development and resorption, as mice with a conditional JunB knockout in cells of macrophage-osteoclast lineage were born with an osteopetrosis–like disorder with symptoms including increased bone mass and osteopenia (119).

JunB and other AP-1 transcription factors also play an important role in the activation of T-lymphocytes. Following the encounter of antigen by a T cell, downstream signalling from the T-cell receptor results in the activation of Nuclear Factor of Activated T-cells (NFAT) transcription factors from calcium signalling, and AP-1 transcription factors from activated PKC signalling to promote the transcription of genes required for the immune response, such as the cytokine IL-2 (120-122). More specifically, JunB was found to play an important role in the differentiation of a subset of T-cells known as T-helper cells that play important roles in B-cell antibody class switching and the activation of cytotoxic T-lymphocytes (reviewed in (123)). Naïve T-helper cells can differentiate into different types of effector cells, including the IL-2 and IFN-γ producing Th1 cells involved in cell mediated immune responses; and the IL-4, IL-5, and IL10 producing Th2 cells that mediate the humoral immune response (124-129). The differentiation of T-helper cells into Th1 and Th2 cells is largely dependent on the cytokine environment, with IL-12 promoting Th1 cell differentiation and IL-4 promoting Th2 cell differentiation (130-134). JunB is selectively expressed in Th2 cells (132,135-137), and dimerizes with c-Maf to activate IL-4 expression (132). Overexpression of JunB in Th1 cells also resulted in the expression of the Th2 cytokines IL-4, 5, 6 and 10 (132), further supporting its role in promoting Th2 cell differentiation.

1.2.3.1: Regulation of JunB

JunB is typically expressed at low levels in the cell, but its expression can be upregulated during cell division and in response to external stimuli that activate MAPK signalling pathways, such as cytokines and growth factors (80). In resting cells, JunB protein levels increase from a very low basal level to a transient peak at the G_0/G_1 transition, before returning to an elevated level due to mitotic signalling such as MAPK signalling (138). In actively dividing cells, JunB expression increases as cells proceed through S phase, before returning to reduced levels in the G2/M and G1 phases (138).

Similar to c-Jun, JunB is regulated post-translationally by phosphorylation (Figure 1.3C). Unlike c-Jun however, JunB lacks the N-terminal serines present in c-Jun (S63 and 73) that are phosphorylated by Jnk (139), which led to the idea that JunB is not a JNK target. However, it was later discovered that JunB contains threonines residues (T102 and 104; corresponding to T91 and 93 in c-Jun) that are phosphorylated by JNK to promote the transcription of the cytokine interleukin 4 (IL-4) in T-helper cells (132,140). Additionally, phosphorylation of JunB on serine 79 by p38 MAPK was demonstrated to be important for JunB to associate with the p300 transcriptional co-activator in the MC3T3-E1 pre-osteoblast cell line (141). Moreover, JunB was found to be phosphorylated at serine residue 186 and a threonine residue homologous to threonine 153 in human JunB by Cdc2-cyclin B1 complexes during mid-/late G2 phase (142). These observations were also confirmed in murine JunB at similar sites (143). In both reports, these phosphorylation sites were found within consensus phosphorylation sites of cyclin dependent kinase (CDK) complexes, and the phosphorylation at these sites destabilizes JunB presumably by targeting the protein for proteasomal degradation (142,143).

JunB is also regulated by ubiquitylation. One of the more well characterized interactions with JunB and E3 ligases involves F-box and WD repeat domain containing 7 (Fbw7), a member of the SKP1, CUL1 and F-box protein (SCF) type ubiquitin ligase complex. Prior to Fbw7 binding, substrates are phosphorylated within a conserved motif known as the Cdc4 phospho-degron (CPD) motif by glycogen synthase kinase 3 (GSK3)(144). In JunB, the phosphorylation of serine 251 and threonine 255 in HeLa cells by GSK-3α/β appears to require a priming phosphorylation at serine 259 by an unknown kinase (145). Phosphorylation of these sites has been shown to be required for ubiquitin mediated degradation, as mutation of these three phosphosites to alanine attenuated the ability of the Fbw7 E3 ubiquitin ligase from interacting with and targeting JunB for degradation (145). Moreover, the phosphorylation of homologous sites in c-Jun was also found to interfere with DNA binding and negatively impact transcription (146). Other E3 ubiquitin ligases are known to interact with JunB, including homologous to the E6-AP Carboxyl Terminus (HECT) type ubiquitin ligases Itch and Smurf1, and really interesting new gene (RING) type ubiquitin ligase COP1 (147-150).

1.2.4: Role of AP-1 proteins in cancer

AP-1 transcription factors regulate many genes that are necessary for tumorigenesis, and dysregulation of AP-1 activity often results in diseases such as cancer (81,82). For example, in a study examining the transformation of chick embryo fibroblasts by AP-1 transcription factors, c-Jun was found to promote growth factor independence and inducing anchorage-independent growth by forming dimers with ATF-2 and c-Fos, respectively (151). Additionally, c-Jun was found to induce the transformation of rat embryo fibroblasts when expressed with Ras (152). c-Jun was also

found to promote cell motility, tumour formation in mice, and resistance to estrogen in the human mammary carcinoma cell line MCF7 (153).

While c-Jun is often seen as an oncogene, JunB was originally thought to lack transforming activity because early studies observed that JunB acted as an inhibitor to the transforming activity of c-Jun (111,113). It was also shown that JunB inhibits the transformation and proliferation of B-lymphoid cells by increasing the expression of the cyclin-dependent kinase inhibitor p16(INK4A) (154). Nevertheless, JunB has been shown to promote important signalling events in some lymphomas. For instance, JunB is highly expressed in Hodgkin lymphoma (155-157), CD30+ diffuse large B-cell lymphoma (156), anaplastic lymphoma kinase-negative, anaplastic large cell lymphoma (ALK– ALCL) (156), as well as ALK+ ALCL (155,156). Signalling pathways activated by NPM-ALK, and dysregulated GSK3β/Fbw7 function in ALK+ ALCL results in the increased expression and accumulation of JunB (79,145,158), which promotes the proliferation (79) and expression of proteins that contribute to the phenotypic characteristics of ALK+ ALCL including CD30/Ki-1 (159) and Granzyme B (160) (Figure 1.4). More recently, the up-regulation of c-Jun and JunB by NPM-ALK was found to promote the transcription of platelet derived growth factor receptor β (PDGFR-β) to promote the growth and spread of the lymphomas in an NPM-ALK transgenic mouse model (161) (Figure 1.4).

1.2.5: Role of Jun family transcription factors in ALK+ ALCL

One of the consequences of NPM-ALK signalling in ALK+ ALCL is the up-regulation of AP-1 transcription factor family members. The Jun family transcription factors c-Jun and JunB are often found to be highly expressed in CD30+ lymphomas including Hodgkin lymphoma, diffuse large B-cell lymphoma, and ALK+ ALCL (155,156,162). In ALK+ ALCL, NPM-ALK phosphorylates and activates JNK, which subsequently activates c-Jun by phosphorylating its serine 73 residue (78). Serine 73 phosphorylation is thought to activate c-Jun by recruiting the coactivator CREB binding protein (163). c-Jun was demonstrated to play an important role in the proliferation of ALK+ ALCL cells as the inhibition of either JNK or c-Jun in ALK+ ALCL cells was found to reduce cell growth and induce cell cycle arrest at the G_2/M transition through the downregulation of cyclin A and upregulation of p21 (78). Nevertheless, a subsequent study by Staber *et al* did not find any proliferation defect following c-Jun knockdown by siRNA (79). Staber *et al* instead suggested JunB as the main AP-1 transcription factor involved in the proliferation of ALK+ ALCL cells.

Activated MEK/ERK signalling in ALK+ ALCL activates the transcription factor ETS-1, which then promotes the transcription of JunB (158). Additionally, activated mTOR signalling in ALK+ ALCL cells results in the increased translation of JunB by targeting JunB mRNA to ribosome-rich polysomes (79). JunB, which is expressed at higher levels than c-Jun at the mRNA level in ALK+ ALCL cells (79), was shown to induce the expression of CD30 surface antigen in ALK+ ALCL and other CD30+ lymphomas (157,158,164), and also appears to play a role in regulating the cell cycle progression of ALK+ ALCL cells as the knockdown of JunB in ALK+ ALCL cells by siRNA resulted in a proliferation defect at the G_2/M stage (79).

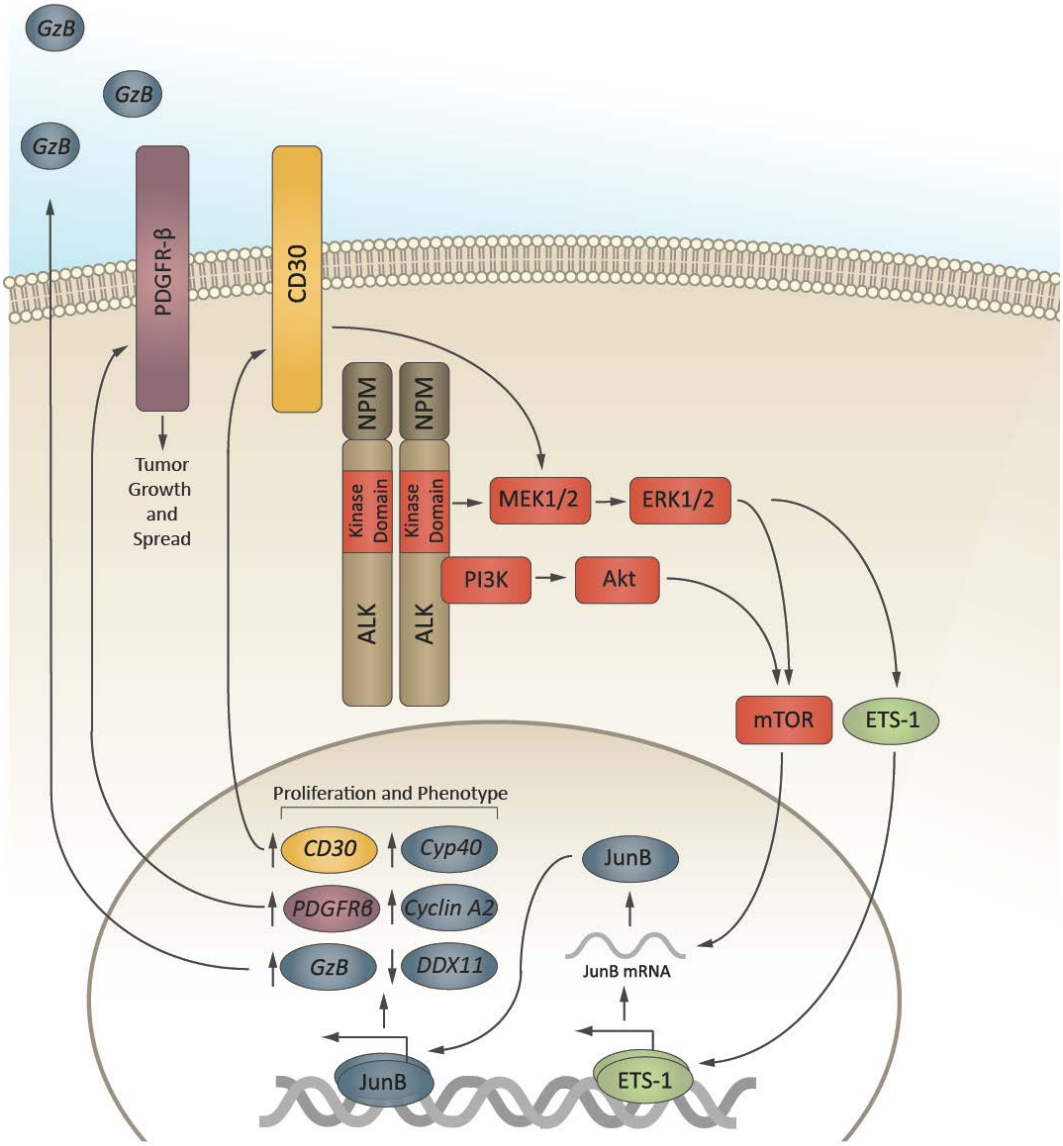

Figure 1.4: Role of JunB in ALK+ ALCL

The expression of JunB is upregulated in ALK+ ALCL cells both transcriptionally and translationally. NPM-ALK signalling activates MEK-ERK signalling which activates the transcription ETS-1 to promote the transcription of JunB. The upregulation of mTOR by both the MEK-ERK and PI3K/Akt pathways results in the increased translation of JunB. JunB has been shown to promote the proliferation and certain phenotypic characteristics of ALK+ ALCL, including the expression of CD30 and GzB. JunB has also been shown to promote the expression of PDGFR-β, which can promote tumor growth and spread.

1.3: APOPTOSIS

1.3.1: Overview of apoptosis

Apoptosis, a form of programmed cell death, plays important roles in maintaining tissue homeostasis and in the clearance of cancerous and virally-infected cells (165). Additionally, aberrant apoptosis contributes the pathology of neurodegenerative diseases (166), and dysregulated apoptosis often results in cancer (167,168) and autoimmune disorders (169,170). Apoptosis, a tightly regulated cell signalling pathway first characterized in 1972, is initiated by two evolutionarily conserved pathways. In the extrinsic pathway, external apoptotic stimuli activate members of the TNF family receptors (e.g. Fas and TNFRI/II) to initiate apoptosis, while the intrinsic pathway is activated by apoptotic stimuli from within the cell such as DNA damaging agents, cytotoxic drugs, or oncogenes (171). Apoptosis is characterized by well-defined biochemical and morphological changes in the cell, which result in the packaging of cellular contents into apoptotic bodies to be removed by phagocytic cells. These changes are largely mediated by aspartic acid-specific, cysteine proteases known as caspases, which can be induced by both apoptotic pathways (172).

1.3.2: Role of apoptosis

Apoptosis plays an important role in the development of multicellular organisms. During development, excess cells are removed during the developmental program through apoptosis, and apoptosis is important for the development of many multicellular organisms (173,174). The importance of apoptosis in animal development was first observed in studies of the cellular differentiation and developmental processes in the *Caenorhabditis elegans* (roundworm) model. In *C. elegans*, a transparent nematode roundworm, a number of cells are eliminated during development by a

genetically controlled apoptotic cell death program (175). Additional experiments using human anti-apoptotic proteins to block apoptosis in *C. elegans* demonstrated the evolutionary conservation of these apoptotic pathways (176). Indeed, apoptosis is involved in all stages of animal development from early embryogenesis to digit formation in the developing fetus (177,178). The importance of apoptosis in development was demonstrated in chickens embryos, where treatment of the developing embyro with caspase inhibitors blocked the removal of the intradigital web in the chick footpad (179). Additionally, organ remoulding both during development or in response to injury involves apoptotic mechanisms (180).

Apoptosis plays additional physiological roles beyond development, and is important in maintaining tissue homeostasis throughout the life of the organism. Approximately 50-70 billion human cells undergo apoptosis each day (174), and apoptosis is essential for the removal of these damaged, dying, or otherwise unwanted cells. Apoptosis also plays important roles within the immune system, and is involved in regulating the number of immune cells during the negative selection of T-cells, and also in the elimination of immune cells following clonal expansion post-infection (181). Moreover, during the cell-mediated immune response involving natural killer cells and cytotoxic T-lymphocytes (CTLs), virally-infected or cancerous cells are removed by the release of cytotoxic granules that initiate apoptosis in the target cells (182,183). Dead and dying cells are rapidly removed in vivo by macrophages and other neighboring phagocytic cells in a process known as efferocytosis (184). Apoptotic cells are recognized by phagocytic cells for engulfment by the exposure of phosphatidylserine residues on the cell surface (185-187). Thus, apoptotic cells are able to be eliminated without eliciting an inflammatory response (188-190).

1.3.3: Apoptotic pathways

1.3.3.1: Extrinsic apoptotic pathway

Apoptotic signalling is a tightly regulated process and can be initiated through two main pathways. One of these pathways – the extrinsic pathway – involves signalling through cell surface death receptors to activate apoptotic signalling pathways. These cell surface death receptors, characterized by a cysteine-rich extracellular region, and a cytoplasmic death domain (DD), are members of the tumor necrosis factor (TNF) receptor superfamily (191-194). The death domain, which is a conserved cytoplasmic fold, interacts with other apoptotic proteins (195,196).

There are a number of death receptors that have been identified in humans, all of which are all members of the TNFR family. The best characterized of these death receptors are the Fas receptor (also known as CD95/Apo1), which binds Fas ligand (FasL/CD95L/DAXX) (197), and TNF receptor I (TNFR1/p55/CD120a), which binds TNFα and lymphotoxin α (191,193,198,199). Other death receptors that have been identified include death receptor 3 (DR3/Apo3/TRAMP/WSL-1/LARD), which binds the ligand Apo3 (Apo3L/TWEAK) (200), and death receptor 4 (DR4) and 5 (Apo2/TRAIL-R2/TRICK2/KILLER), which binds TNF-related apoptosis-inducing ligand (TRAIL/Apo2L) (194,201).

Apoptotic signalling in the extrinsic pathway involves ligand binding to the death receptors, which subsequently result in the activation of caspase 8 and downstream executioner caspases. Following the ligation of FasL to the Fas receptor, Fas receptor clusters and undergoes conformational changes which allow the cytoplasmic DD of Fas to interact with the DD of the adaptor protein Fas-associating protein with death domain (FADD). FADD, which also possesses a death effector domain (DED) in addition

to its DD, then interacts with the DED of proenzyme procaspase-8 (202). This multi-protein complex of FasL, Fas, FADD, and procaspase-8 is known as the death inducing signalling complex (DISC), and in this complex, procaspase 8 dimerizes and activates itself by the proteolytic cleavage of its pro-domain and the inter-subunit linker between the large and small subunits. The activated caspase 8 can then activate downstream executioner caspases such as caspase 3, 6 and 7 to trigger apoptosis (Figure 1.5).

Similar to Fas/FasL signalling, the binding of TRAIL to DR4 and DR5 receptors result in downstream signalling that results in the formation of a DISC with the same protein components (203-205). Unlike Fas-mediated apoptosis, however, TRAIL appears to only induce apoptosis in cancer cells, as DR4 and DR5 receptors were found to be expressed at higher levels on tumour cells relative to normal cells. In addition, it was shown that normal cells express a number of decoy receptors that can bind to TRAIL. These receptors, which include decoy receptor 1 (DcR1/TRAIL receptor without intracellular domain (TRID)), decoy receptor 2 (DcR2), and osteoprotegerin (OPG) either lack a cytoplasmic domain (DcR1 and OPG), or have a truncated death domain (DcR2) to block apoptotic signalling following TRAIL binding (206-208). The expression of decoy receptors on healthy cells led to the idea that these cells are protected from TRAIL-mediated apoptosis, and suggests that the TRAIL pathway may be a possible target for anti-cancer therapy.

TNFα is typically produced by activated macrophages and T-cells following infection, and normally results in the induction of pro-inflammatory genes, although TNFα can also induce apoptosis (209). Previous studies have shown that signalling through the TNFR1 is not exclusively apoptotic and is thought to occur in two multi-protein complexes following TNFα binding (210). Complex I, which promotes the

activation of the NF-κB and MAPK pathways leading to cell survival and the inflammatory response, is a membrane bound complex made up of the TNFR-associated DD protein (TRADD), TNFR associated factors 2 and 6 (TRAF2 and TRAF6), the receptor interacting protein kinase (RIP1) and the cellular inhibitor of apoptosis protein 1 and 2 (cIAP1 and cIAP2) (211). Complex II, which is thought to promote apoptosis, contains TRADD, FADD, caspase 8, and caspase 10. The recruitment of procaspase 8 by FADD can result in the activation of procaspase 8 through dimerization and/or auto-proteolytic cleavage to result in the subsequent cleavage of downstream executioner caspases to trigger apoptosis (212). Whether signalling through the TNFR results in survival or cell death is a balance of the pro-survival and pro-apoptotic signals from each complex. While NF-κB activation typically suppresses apoptotic signalling, it is thought that other apoptotic signals (such as Fas signalling) can inhibit NF-κB to swing the balance towards apoptotic cell death (209,213).

1.3.3.2: Intrinsic apoptotic pathway

The second apoptotic signalling pathway – the intrinsic pathway – is initiated by intracellular stresses rather than external signals. These cellular stresses, such as ultraviolet radiation, aberrant growth signals, DNA damaging agents and cytotoxic drugs, can activate signalling that result in apoptosis (214). One of the ways this occurs is through the activation of tumor suppressor genes such as p53 – a transcription factor that can initiate DNA repair, cell cycle arrest and apoptosis (215). In healthy cells, p53 expression levels are kept at a low level through the interaction with its negative regulator MDM2, an E3 ubiquitin ligase which targets it for proteasomal degradation (216-218). In response to a variety of stress stimuli however, p53 becomes phosphorylated and dissociates from MDM2, resulting in its stabilization and

accumulation in the cell (219). p53 is then able to induce the expression of genes involved in DNA repair, cell-cycle arrest, and apoptosis. These genes include both TNF and Fas receptors, and pro-apoptotic proteins belonging to the Bcl-2 family including BAX, Noxa and Puma, which are a part of the intrinsic apoptotic pathway (220).

In mammalian cells, the Bcl-2 protein family is made up of approximately 25 members that are either anti-apoptotic or pro-apoptotic regulators, and is characterized by the presence of one to four Bcl-2 homology (BH) domains (221) (Figure 1.6). Anti-apoptotic members of the Bcl-2 family, such as Bcl-2, Bcl-XL, Bcl-w, Mcl-1 and A1 contain four BH domains (BH1, BH2, BH3, and BH4). Pro-apoptotic members of the Bcl-2 family may contain one BH domain (BH3-only), like Bim, Bik, Noxa, Puma, HRK, Bid, Bad, Bmf; or multiple BH domains (BH1, BH2, and BH3), such as Bak, Bax, and Bok (reviewed in (222)). Bcl-2 family members are able to regulate apoptotic signalling by controlling mitochondrial outer membrane permeability (MOMP) (223). MOMP, which is largely mediated by the pro-apoptotic Bcl-2 members Bax and Bak, is typically inhibited by the interaction of Bax and Bak with anti-apoptotic members of the Bcl-2 family (224). However, during the initiation of apoptosis, the BH3-only proteins relay pro-apoptotic signalling to the mitochondria by disrupting the interaction of Bax and Bak with the anti-apoptotic Bcl-2 family members (reviewed in (221,225)). Subsequently, the pro-apoptotic Bcl-2 members Bax and Bak can then translocate to the outer mitochondrial membrane and alter its permeability and integrity, which activates the mitochondrial permeability transition pore, and results in the release of the mitochondrial protein cytochrome c (226). The exception to this, however, is the BH3-only protein Bid, which can indirectly induce MOMP by interfering with Bax and Bak's interaction with anti-apoptotic Bcl-2 family members after translocating to the mitochondria following a

conformational change after cleavage by activated caspase 8 (227-229). The ability of caspase 8 to induce MOMP and the subsequent release of cytochrome c through Bid represents a point of crosstalk between the extrinsic and intrinsic apoptotic pathways – in that extracellular cues can engage the intrinsic apoptotic pathway.

Cytochrome c, a protein normally found inside the mitochondria, is able to interact with apoptotic protease activating factor-1 (Apaf-1) once it is released into the cytoplasm following MOMP (230). Apaf-1 consists of an N-terminal caspase recruitment domain (CARD), a central nucleotide oligomerization domain (NOD/NACHT), and C-terminal WD40 repeats that can bind cytochrome c (231,232). The WD40 repeats of Apaf-1, in the absence of cytochrome c, are thought to interact with the CARD domain to keep Apaf-1 in an inactive state. Upon cytochrome c binding to the WD40 repeats, a conformational change occurs to uncover the NOD domain of Apaf-1 to allow it to heptamerize to form a wheel-shaped platform which can recruit procaspase-9 through its CARD domains (233,234). This Apaf-1/cytochrome c/procaspase 9 complex is known as the apoptosome (Figure 1.7), and it is here that the dimerization of procaspase-9 results in its auto-activation, and subsequently the downstream activation of executioner caspases, such as caspases 3 and 7.

Another way that apoptotic pathways become activated is through cell-mediated killing by cytotoxic T-lymphocytes (CTLs) and natural killer (NK) cells. CTLs and NK cells are a part of the immune system that can kill infected cells (182,183). Apoptosis can be triggered through the engagement of both the extrinsic and intrinsic apoptotic pathways – through the binding of FasL to the Fas receptor on the target cell to activate the extrinsic pathway, or the release of cytotoxic granules that can activate the intrinsic apoptotic pathway of the target cell. CTLs and NK cells release cytotoxic granules that

contain the serine proteases granzyme A and B, and the membrane disrupting protein perforin, that function synergistically to induce apoptotic cell death in the target cell (235). Granzyme B has been shown to cleave similar substrates as caspases (236), and has also been shown to cleave and activate the executioner caspase, caspase 3, to induce apoptosis (237,238). Granzyme B can also induce apoptosis by the cleavage of Bid to induce cytochrome c release, which subsequently activates the intrinsic apoptosis pathway (239-241).

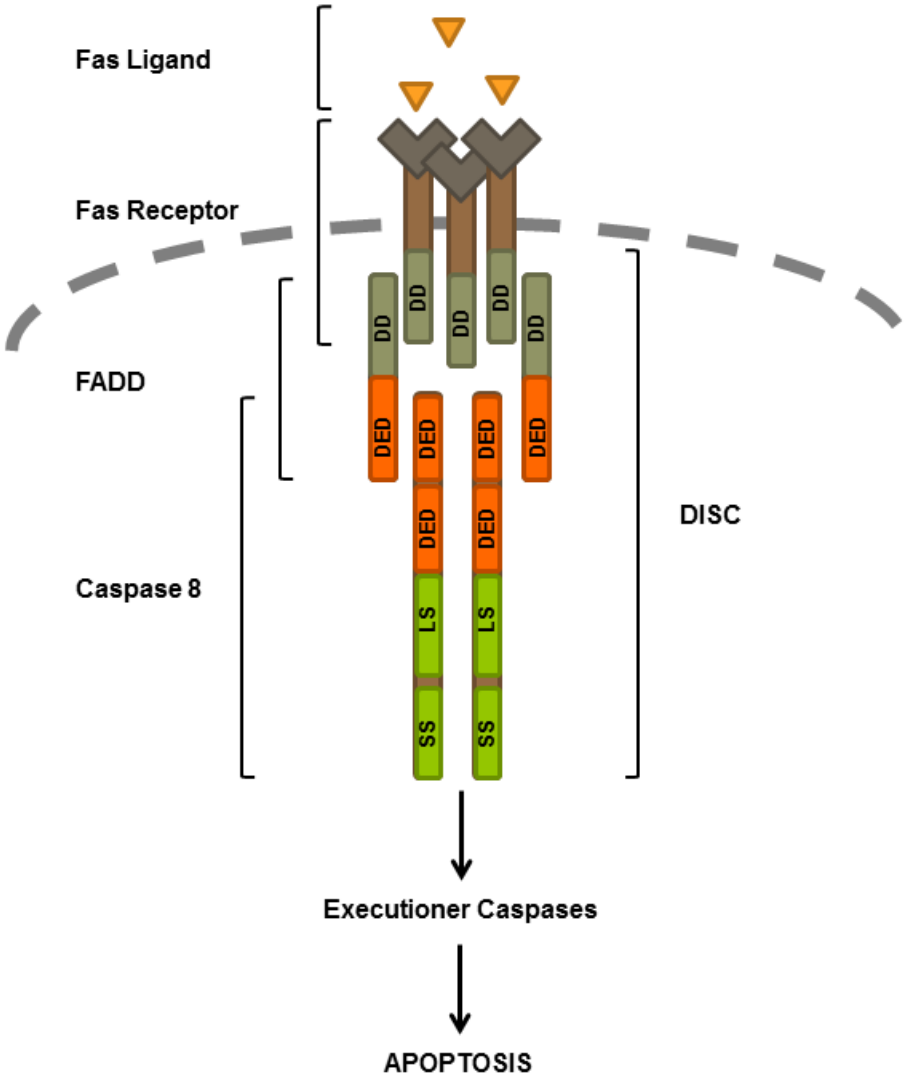

Figure 1.5: The extrinsic apoptotic pathway.

Activation of the Fas receptor represents one of the ways of activating the extrinsic apoptotic pathway. The binding of Fas ligand to the Fas receptor induces a conformational change that allows the recruitment of FADD through their death domains (DD). FADD then subsequently recruits caspase 8 through the interactions between death effector domains (DED) to form the death inducing signalling complex (DISC). Caspase 8 is then activated and can then cleave and activate executioner caspases to lead to apoptotic cell death.

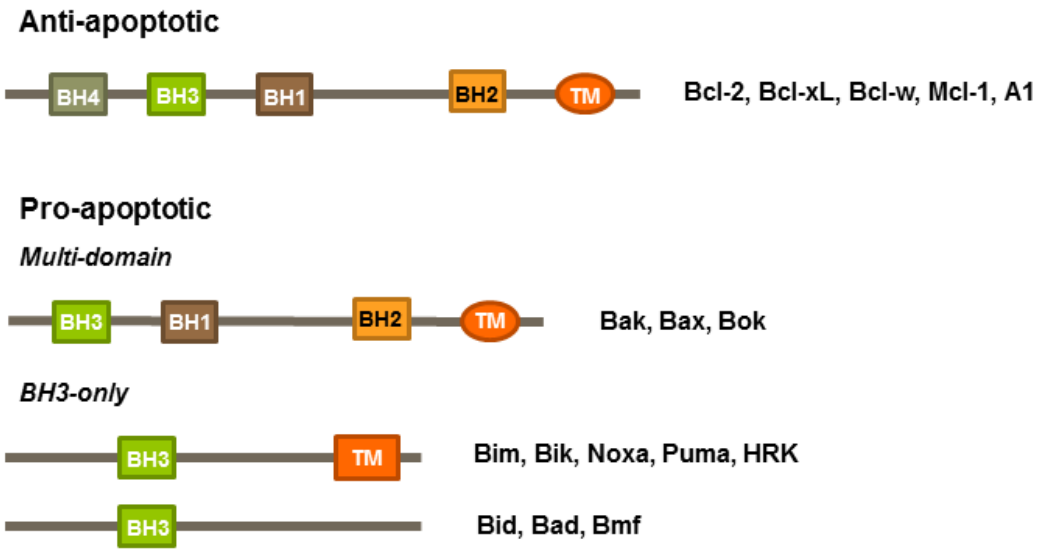

Figure 1.6: Members of the Bcl-2 family of proteins.

Mammalian Bcl-2 family members are either anti-apoptotic or pro-apoptotic. Anti-apoptotic Bcl-2 family members contain Bcl-2 homology (BH) domains 1-4 and, with the exception of A1, contain a C-terminal transmembrane domain. Pro-apoptotic members of the Bcl-2 family are further subdivided into multi-domain members, which contain BH1-3 domains, or BH3-only members. Pro-apoptotic Bcl-2 family members may also contain a C-terminal transmembrane domain, with the exception of Bid, Bad, and Bmf.

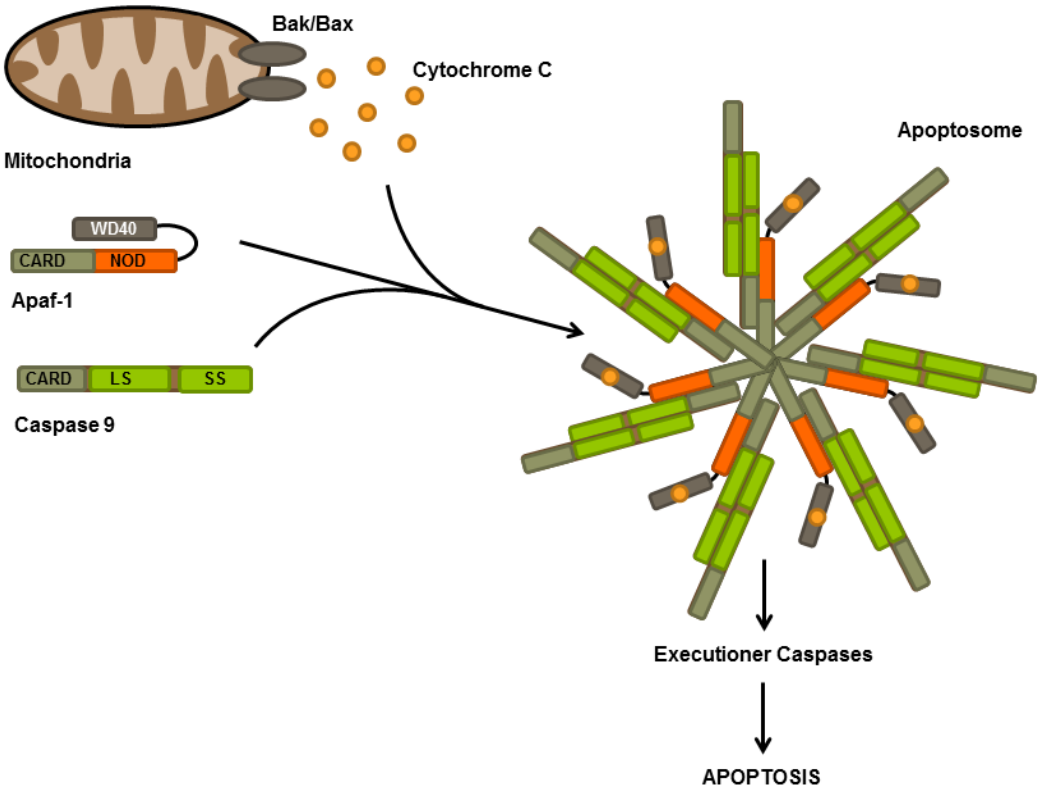

Figure 1.7: The intrinsic apoptotic pathway.

Intracellular stresses lead to the release of cytochrome c from the mitochondria by Bcl-2 family members Bak and Bax. In the cytoplasm, cytochrome C interacts with the WD40 domains of Apaf-1 to cause a conformational change to allow it to interact with caspase 9 via caspase recruitment domains (CARD). Apaf-1 then oligomerizes through its NOD domain to form a protein complex known as the apoptosome. Caspase 9 is activated in the apoptosome and subsequently activates executioner caspases – which eventually results in apoptotic cell death.

1.3.4: Types of caspases in humans

Twelve caspases have been identified so far in humans, and they are classified based on function and conserved protein domains (172,242-244) (Figure 1.8). While the majority of caspases that have been identified play a role in apoptosis (caspases 2, 3, 6, 7, 8, 9, 10), a small subset play a role in the inflammatory response (caspases 1, 4, 5 and 12). Apoptotic caspases can be subdivided into caspases involved in the initiation of apoptosis (apical caspases – 2, 8, 9 and 10) and downstream effector caspases (executioner caspases – 3, 6, and 7). Once activated, apical caspases cleave and activate the executioner caspases, which then proceeds to cleave various protein substrates to result in apoptotic cell death. Caspase 14 does not appear to be involved in either apoptosis or inflammation, and has been found to be involved in keratinocyte differentiation and the maintenance of skin cell integrity (245).

1.3.5: Apical caspases

The activation of the initiator/apical caspases (caspase 2, 8, 9 and 10) are important steps in both the intrinsic and extrinsic apoptotic pathways. Caspases 2 and 9 are activated in the intrinsic pathway, while caspases 8 and 10 are activated in the extrinsic pathway (244). Apical caspases are characterized by a long N-terminal pro-domain containing CARD and DED that allow for their recruitment to large, multi-protein complexes (243). In both apoptotic pathways, apical caspases dimerize as a part of these protein complexes to become activated. Following activation, apical caspases cleave and activate the executioner caspases 3, 6, and 7 to trigger apoptosis.

In the extrinsic pathway, death receptor signalling results in the activation of caspase 8 and 10 at the DISC. The oligomerization of the procaspases at the DISC is essential for the formation of active caspase dimers. It was originally thought that these

caspases had low intrinsic activity while in the procaspase form, and the cleavage of the pro-domain at the DISC during activation resulted in substantially increased enzymatic activity (246). However, more recent work has shown that the oligomerization of the caspases is the actual activation mechanism, and that the cleavage of the pro-domain simply stabilizes the dimeric caspase complex (212,247).

In the intrinsic pathway, caspase 9 is the primary apical caspase that is activated, and is activated in the apoptosome following cytochrome c release. The mechanism of the activation of procaspase 9 in the apoptosome is still not fully elucidated and is the subject of debate. While the monomeric form of procaspase 9 was originally suggested to be allosterically activated by Apaf-1 (248-250), more recent studies have shown that the direct dimerization of procaspase 9 is required for its activation by Apaf-1 (251). Once activated, caspase 9 cleaves procaspases 3, 6, and 7 to trigger apoptosis.

Caspase 2 is also involved in the intrinsic apoptotic pathway, although not in the canonical pathway involving the apoptosome. Caspase 2 has been observed to be activated following DNA damage, neurotrophic factor depletion during development, and beta amyloid toxicity in Alzheimer's disease (252,253). Caspase 2 contains an N-terminal CARD domain similar to caspase 9, and is recruited to the PIDDosome, a multi-protein complex thought to be capable of generating pro-apoptotic signals through caspase 2 activation (254). The PIDDosome is made up of the CARD and DD domain containing adaptor protein, RIP associated Ich-1/CED homologous protein with death domain (RAIDD), and p53 induced protein with a death domain (PIDD). The PIDDosome activates caspase 2 by an autocatalytic cleavage of the caspase, leading to apoptotic cell death (254-256). The PIDDosome also generates pro-survival signals through the activation of NF-κB, by forming an alternate complex with RIP1 and PIDD instead of

RAIDD (257). The differentiation between pro-apoptotic signalling and pro-survival signalling by the PIDDosome is largely based on the phosphorylation of PIDD at T788 by ATM, where phosphorylated PIDD can trigger apoptotic cell death, and un-phosphorylated PIDD can promote cell survival (258,259). Caspase 2 therefore appears to play a specialized role within the intrinsic apoptotic pathway in response to stimuli such as genotoxic stress. Nevertheless, caspase 2 has also been implicated in non-apoptotic roles such as DNA repair, ER stress, and the heat shock response, and suggest additional roles aside from cell death (260).

1.3.6: Executioner caspases

The extrinsic and intrinsic apoptotic pathways converge at the activation of the executioner caspases 3, 6, and 7. Structurally, the executioner caspases are characterized by a short N-terminal pro-domain (243), and do not associate with the multi-protein activation complexes. Executioner caspases are known to be cleaved by caspases 8, 9, 10, and also Granzyme B (261,262). Executioner caspases are activated when cleaved in the inter-domain linker region between the large and small subunits (263,264). Indeed, following cleavage by caspase 8, the catalytic activity of caspase 3 was found to be increased by over 10,000 times (262). In its procaspase form, the uncleaved linker region resides in the central cavity of the caspase and results in the misalignment of the substrate binding loops (263-266). Even following the activation of caspases 3 and 7, the active site does not become properly aligned until substrate binding (263,267). These findings suggest that the binding of substrate may be an additional component of executioner caspase activation.

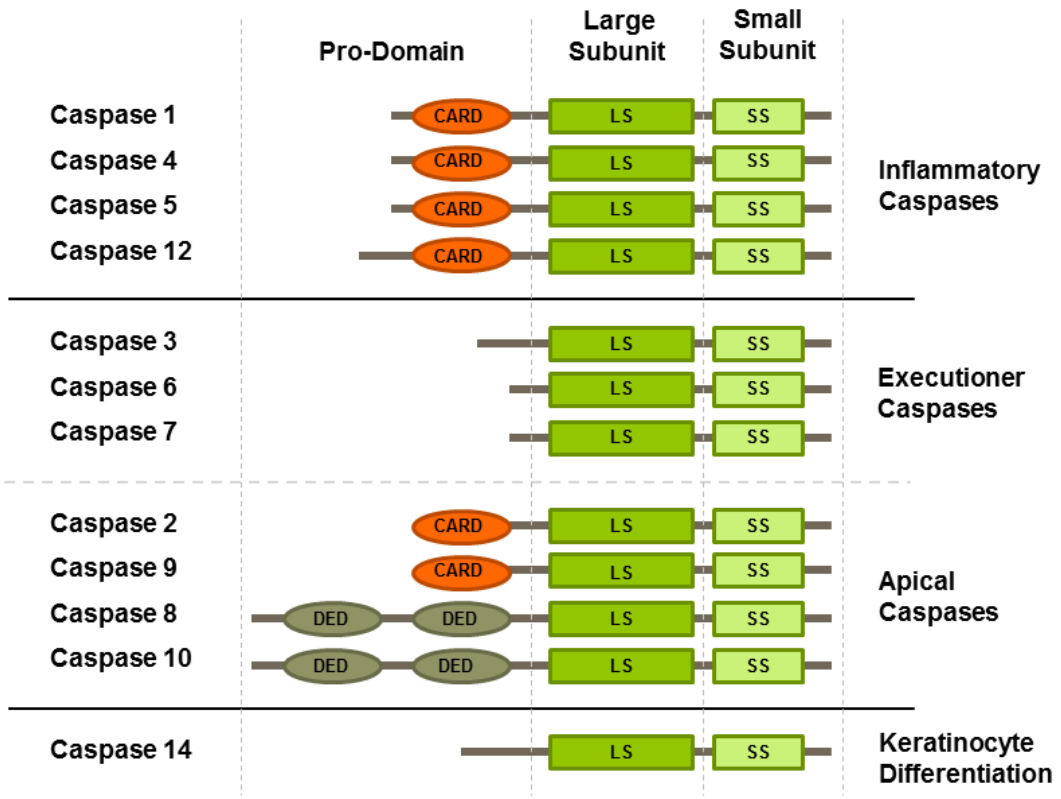

Figure 1.8: Structural domains of human caspases.

All caspases contain large and small catalytic subunits (LS/SS) and are grouped according to function. Caspases are involved in inflammation (inflammatory caspases 1, 4, 5, and 12), apoptosis (apical caspases 2, 8, 9, 10 and executioner caspases 3, 6, and 7), or in keratinocyte differentiation (caspase 14). Caspases also differ in the structural domains of their N-terminal pro-domain. The inflammatory caspases and the apical caspases involved in the intrinsic apoptotic pathway contain caspase recruitment domains (CARD), while the apical caspases involved in the extrinsic apoptotic pathway contain death effector domains (DED). All other caspases contain short N-terminal pro-domains.

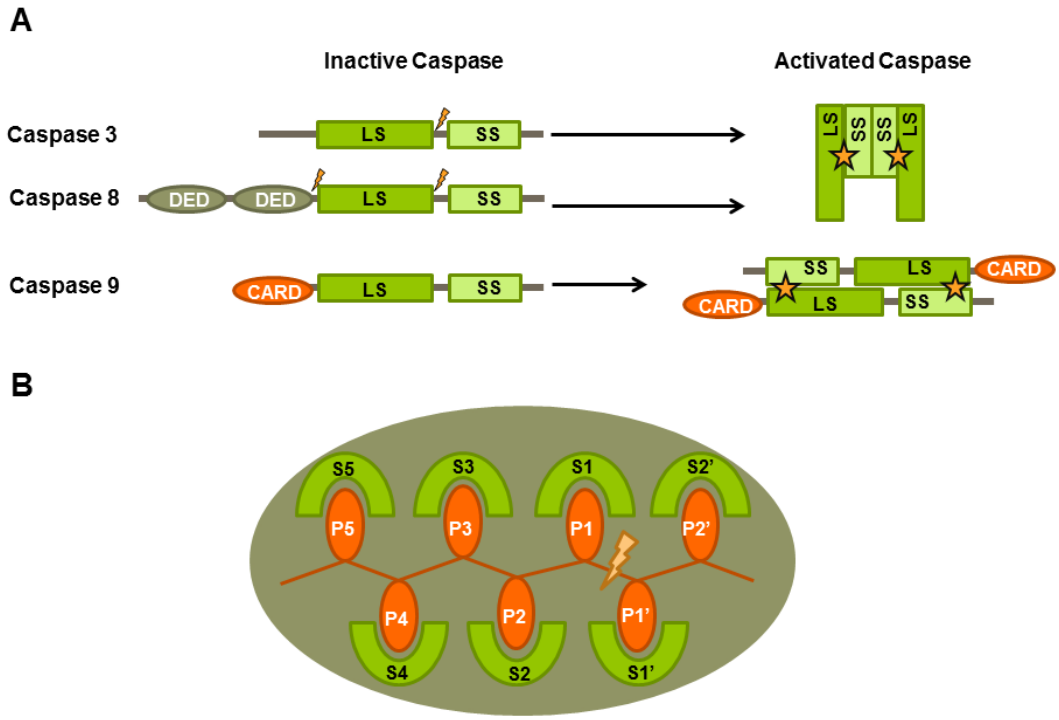

Figure 1.9: Caspase activation and substrate cleavage.

(A) Activation of executioner caspases and the apical caspase 8 requires cleavage between the large and small catalytic subunits and/or the N-terminal pro-domain. The large and small subunits oligomerize to form a complex with two active sites between the catalytic subunits. Caspase 9 is activated through the dimerization of the large and small catalytic subunit to form two active sites. The caspase recruitment domain (CARD) of one caspase 9 molecule then binds to Apaf-1 to form an apoptosome complex that stabilizes the caspase dimer. **(B)** Simple schematic diagram of the caspase active site. The protein substrate (light gray), is cleaved between the P1 and P1' residues. The amino acids N-terminal to the cleavage site are indicated as P1, P2, P3, and so on while the amino acids C-terminal to the cleavage site are indicated as P1', P2' P3' and so on. The corresponding binding sites within the caspase binding site are indicated as S1, S2, or S1' and S2' (figure adapted from (268)).

1.3.7: Caspase structure and catalytic activity

Caspases belong to the CD clan (containing the catalytic dyad histidine followed by cysteine) of cysteine proteases, and is further categorized into the C14 (caspase domain containing) peptidase family (269). Structurally, caspases typically contain large and small catalytic subunits on the C-terminal end of the protein, with the pro-domain making up the N-terminal end of the protein. Typically, pro-domains are regulatory domains containing CARD or DED domains, or simply a short N-terminal peptide extension, and are cleaved during caspase activation (243). The procaspase molecule, which contains both the large and small catalytic subunits, is enzymatically inactive. When activated however, caspases form dimers containing two catalytic units – each with its own large and small subunit – at either ends of the molecule (270,271) (Figure 1.9A).

The amino acid residues of caspase substrate proteins N-terminal of the cleaved peptide bond are named P1, P2, and so forth, while residues C-terminal of the cleaved peptide bond are named P1', P2', and so on (272). Similarly, the active site of caspases contain a large pocket that accommodates the P4-P1 residues, and the specific binding sites within the pocket are named S1-S4, with the S1 binding the P1 residue, and S2-S4 binding the P2-P4 residues (Figure 1.9B). The catalytic mechanism of caspases has been reviewed extensively (273), but briefly, within the active site, caspases contain a catalytic dyad consisting of histidine and cysteine residues which are required for the hydrolysis of the peptide bond. To hydrolyze the peptide bond, the thiol group of the catalytic cysteine undergoes de-protonation by the adjacent histidine's basic side chain, which then results in the nucleophilic attack on the P1 aspartic acid residue's carbonyl carbon by the anionic sulphur on the deprotonated cysteine. As a result, the portion of

the substrate C-terminal to the cleavage site (beginning with P1') is released as a fragment, the histidine residue is restored to a deprotonated form, and an intermediate thioester is formed between the catalytic cysteine and the substrate's new carboxy terminus. The thioester bond is then hydrolyzed to generate the c-terminal end of the cleaved substrate, and also to regenerate the caspase enzyme.

With very few exceptions, such as the Drosophila caspase DRONC which cleaves glutamate residues (274) or caspase 5 which cleaves the Max transcription factor at a glutamate residue (275), caspases cleave the peptide bond following an aspartic acid residue and therefore have a very strict specificity for aspartic acid for the P1 position (236,276-278). In addition, caspases prefer small residues such as glycine, alanine and serine for the P1' position (276,277). Previous studies have looked at the substrate profiles of caspases by generating libraries of labelled peptides and looking at its cleavage efficiency by caspases. Experiments using these libraries – also known as positional scanning synthetic combinatorial libraries (PS-SCL), were able to reveal trends in the P4-P2 specificity of caspases (236,278). For example, at the P4 position, executioner caspases prefer an aspartic acid residue, while apical caspases prefer leucine or valine residues, and inflammatory caspases prefer tyrosine and tryptophan (236,278). Not much is known in terms of in-vivo caspase substrate specificities, although inferences made from natural caspase substrates suggests that most cuts occur in loop regions, although they can also occur in alpha helices and beta sheets (276). Additionally, it has also been speculated that substrate recognition in-vivo may also involve an exosite – a site distant from the caspase cleavage site that makes contact with the caspase enzyme. A crystal structure of a the caspase substrate p35 (a viral caspase inhibitor) bound by caspase 8 showed contacts outside of the active site,

although this may be due to p35 functioning as a caspase inhibitor (279). It was also found that proteins are more likely to be cleaved by caspases when in complex with another caspase substrate (276), suggesting potential caspase substrate specificity through quaternary structure.

1.3.8: Caspase substrates and consequences of caspase cleavage

During apoptosis, cells undergo a number of well characterized morphological and biochemical changes (280). These changes, which include cell shrinkage, chromatin condensation, breakdown of the nucleus, membrane blebbing, DNA cleavage, and the formation of apoptotic bodies (reviewed in (281)), are largely mediated by caspases. Following activation, executioner caspases cleave a number of protein substrates in the cell, of which over 700 have been identified so far (282). These include a number of well–characterized substrates such as nuclear lamins (283-285), inhibitor of caspase-activated DNAse (ICAD) (286-288), and poly ADP ribose polymerase (PARP) (289-291). Cleavage of these substrates is largely responsible for the phenotypic changes associated with apoptosis, and the study of the consequences of caspase cleavage has been important for understanding cell death and other cellular processes. For example, it has been shown that during apoptosis, the cleavage of nuclear lamins is important for chromatin condensation and shrinkage of the nucleus (292). Additionally, the cleavage of ICAD relieves the inhibition of caspase-activated DNAse (CAD), which can then cleave genomic DNA into a characteristic DNA ladder (286-288). Many other proteins have also been observed to be cleaved by caspases, and these include proteins involved in almost all aspects of the cell (282,293). The cleavage of these proteins can result in either a gain or loss of function, and may also result in changes in cellular localization that may be important for the progression of apoptosis. It is also likely that some caspase substrates

are merely bystanders that become cleaved inadvertently during apoptosis. Nevertheless, the cumulative effect of the cleavage of caspase substrates results in an irreversible shutdown of cellular processes and dismantling of the cell that ultimately results in apoptotic cell death (282,293).

1.3.9: Inflammatory caspases and the inflammasome

Aside from cell death, some caspases play an important role in inflammation. Indeed the first caspase identified in mammals, caspase 1, was found to be involved in processing of IL-1β (294). Termed the inflammatory caspases because their known cleavage substrates are typically cytokines, these caspases (caspases 1, 4, 5, and 12) are structurally similar to caspase 9 and have an N-terminal CARD domain. The activation of inflammatory caspases also occur in a multi-protein complex known as the inflammasome, typically consisting of the adaptor protein apoptosis-associated speck-like protein containing a CARD (ASC or PYCARD), the NOD-like receptor, and caspase 1 and/or 5 (295,296)(Figure 1.10).

The innate immune system recognizes pathogen-associated molecular patterns (PAMPs) with a number of extracellular pattern recognition receptors (PRRs) such as Toll-like and C-type lectin receptors (TLRs and CLRs), and intracellular PRRs such as Nod-like and RIG-I like receptors (NLRs and RLRs) (297-302). Central to the formation of the inflammasome are NLRs, which are proteins that contain C-terminal leucine rich repeats (LRRs) that functions as sensors of PAMPs, a nucleotide oligomerization domain (NOD/NACHT), and additional CARD or Pyrin domains that can interact with other proteins (296,303,304). Upon the activation of PRRs, members of the NLR family assemble and oligomerize through the NOD domain, and subsequently recruit ASC to the protein complex through their pyrin domains. Inflammatory caspases are recruited

to the inflammasome either through CARD domains present in some NLRs or through the CARD domain of the adaptor protein ASC (305). Recruitment of procaspase 1 to the inflammasome results in its activation due to autocatalytic cleavage, and results in a number of cleaved, active caspase 1 dimers consisting of the large and small subunits (306). The activated caspase 1 then proceeds to cleave a number of protein substrates, including the cleavage of pro-IL-1β to IL-1β, cleavage of pro-IL-18 to IL-18 to activate T-lymphocytes and NK cells (295,307). The other inflammatory caspases are less well characterized, although it is thought that human caspases 4 and 5 arose from a gene duplication event from the mouse caspase 11 (296). Caspase 5 has been shown to be recruited to the inflammasome – suggesting that it may have similar functions as caspase 1 (295). Caspase 4 and 12 have also been implicated in the ER stress response, although their exact roles are not entirely known (308). Moreover, caspase 12 has also been suggested to be an antagonist of caspase 1 (309).

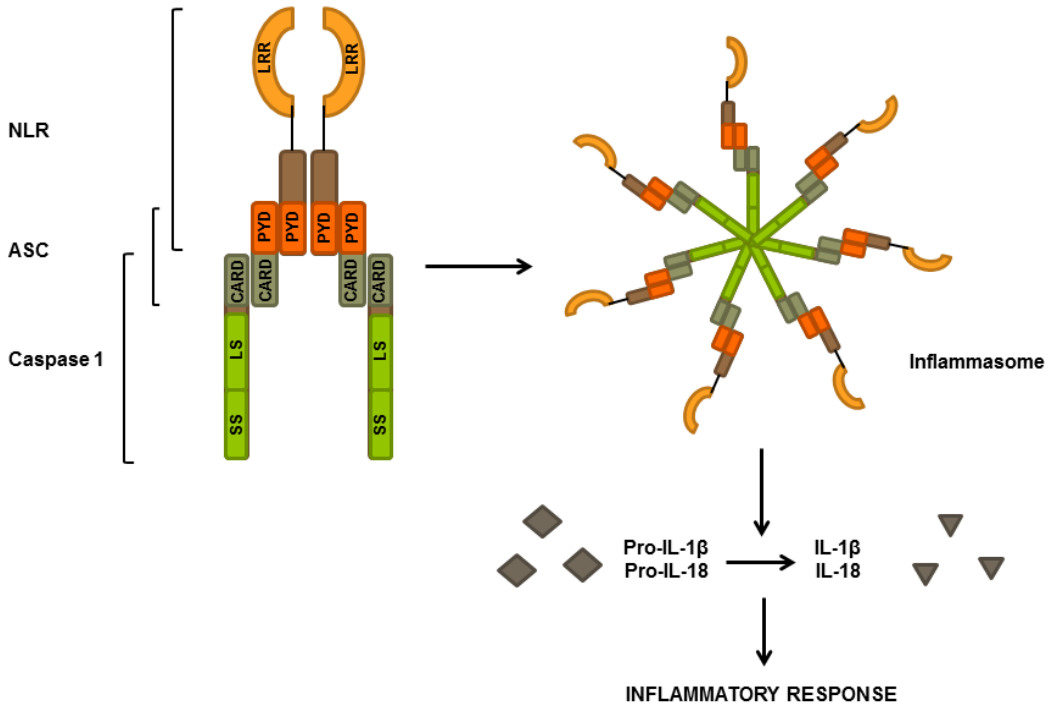

Figure 1.10: The Inflammasome.

Leucine rich repeats (LRR) of Nod-like receptors (NLR) can detect activation signals that lead to the formation of the inflammasome. The core structure of the inflammasome is made up of NLRs, which recruit the adaptor protein ASC through their pyrin domains (PYD). ASC can then recruit inflammatory caspases such as caspase 1 through their caspase recruit domain (CARD). This complex oligomerizes to form the inflammasome complex, which then cleaves and activates IL-1β and IL-18 to mediate the inflammatory response.

1.3.10: Role of AP-1 proteins in apoptosis

Many transcription factors play important roles in apoptosis, although the role of AP-1 proteins can be either pro- or anti-apoptotic depending on cellular context. c-Jun has been shown to promote apoptosis through the p53 and TNF-α pathways (82), and the inhibition of c-Jun or the expression of a c-Jun dominant mutant induces apoptosis in neuronal cells (310-312). The expression of a phosphorylation mutant of serines 63 and 73 to alanines in c-Jun was also able to protect neuronal cells from apoptosis (313). However, c-Jun was found to protect mouse hepatocytes from apoptosis during development and mouse fibroblasts that lacked c-Jun were more sensitive to apoptosis (314).

Similarly, the role of JunB in apoptosis is not clearly defined. There is evidence to suggest that JunB can be either a pro-apoptotic or an anti-apoptotic factor. JunB has been shown to inhibit cytokine-induced apoptosis by inhibiting ER stress in a pancreatic beta cell line (315), yet it has also been shown to promote apoptosis in HeLa cells by inhibiting pro-survival autophagy (316).

1.3.10.1: Apoptosis in ALK+ ALCL cells

The dysregulation of apoptotic pathways in cancer cells is a common occurrence and ALK+ ALCL does not appear to be an exception. Activated PI3K-Akt signalling results in the phosphorylation and subsequent inhibition of the pro-apoptotic Bcl-2 family member Bad to release the inhibition on the anti-apoptotic proteins Bcl-2 and Bcl-XL to promote the survival of ALK+ ALCL cells (317,318). Nevertheless, despite high expression levels of the anti-apoptotic proteins Bcl-2 and BAX in ALK+ ALCL samples, it was also found that the basal apoptosis rate of ALK+ ALCL cells were higher than that of ALK- ALCL tumors (319). In addition, the amount of activated caspase 3 was also greater in

ALK+ ALCL tumors (320). It has been suggested that the ability of ALK+ ALCL cells to undergo apoptosis readily explains its responsiveness to chemotherapy involving apoptosis inducing agents, and that it is likely caspase 9 and the intrinsic apoptotic pathway that is involved in the apoptosis of ALK+ ALCL cells in response to chemotherapy treatment (321).

1.4: THESIS OBJECTIVES

1.4.1: Rationale

Since JunB appeared to be play a major role in promoting the proliferation of ALK+ ALCL cells, previous work performed in our laboratory looked at whether or not JunB also played other roles in ALK+ ALCL pathogenesis. While performing experiments to see if JunB played a role in protecting ALK+ ALCL cells from apoptosis, an interesting observation was made in that we noticed that the electrophoretic mobility of JunB underwent changes as the cells underwent apoptosis. This cleavage was not observed when either JunB expression was knocked down with siRNA or when cells were treated with the general caspase inhibitor Z-VAD-FMK (unpublished results, J. D. Pearson and R. J. Ingham) – indicating that this is likely a JunB cleavage product, and that this cleavage was likely caspase dependent. These observations led us to hypothesize that JunB may be a novel caspase substrate – a potentially significant finding as JunB has not been previously described as a caspase substrate. Understanding the role of the caspase cleavage of JunB in its regulation and function was the main goal of my thesis.

1.4.2: Objectives

The overall goal of this study was to examine whether JunB is cleaved by caspases, and whether the cleavage modulates the activity of JunB. Our preliminary findings suggest that JunB may be cleaved as ALK+ ALCL cells undergo apoptosis.

The specific aims of this study were:

1. Characterize the cleavage of JunB and determine if caspases are responsible for the cleavage.
2. Identify the cleavage site(s) of JunB, and determine what cleavage fragments are formed.
3. Determine whether the cleaved JunB fragments have a functional role.

CHAPTER 2: MATERIALS AND METHODS

A portion of this chapter has been submitted for publication:

Lee JK, Pearson JD, Maser BM, and Ingham RJ. 2013. Cleavage of the JunB transcription factor by caspases generates a carboxy-terminal fragment that inhibits activator protein-1 transcriptional activity. *Journal of Biological Chemistry.* [undergoing revision]. Some methods described in this chapter were from experiments performed by J. Pearson. The original manuscript was written by J. Lee, J. Pearson, and Dr. R. Ingham.

2.1: CELL LINES

The cell lines used in this study are listed in Table 2.1. The ALK+ ALCL cell lines (Karpas 299 and SUP-M2) and Hodgkin lymphoma cell lines (KM-H2 and L428) were gifts from Dr. Raymond Lai (University of Alberta), the BJAB and Jurkat-TAg cell lines were gifts from Dr. Tony Pawson (University of Toronto), and the Jurkat and DG75 cell line was purchased from the ATCC (Manassas, VA). The ALK+ ALCL cell lines (Karpas 299 and SUP-M2), Jurkat, Jurkat-TAg, Burkitt lymphoma cell lines (BJAB and DG75), and Hodgkin lymphoma cell lines (L428 and KM-H2) were cultured in Roswell Park Memorial Institute (RPMI) 1640 media (GIBCO; Carlsbad, CA) supplemented with 10% heat-inactivated FBS (PAA; Etobicoke, ON, Canada), 1 mM sodium pyruvate (Sigma-Aldrich; St Louis, MO), 2 mM L-glutamine (Invitrogen; Carlsbad, CA), and 50 µM 2-mercaptoethanol (BioShop; Burlington, ON, Canada). The Hodgkin lymphoma cell lines (KM-H2 and L428) were cultured in media as described above except supplemented with 20% heat-inactivated FBS. The Epstein Barr Virus-transformed T cell line SIS (322) was cultured in a similar 10% FBS supplemented, RPMI media, except for the addition of 20 U/µl of recombinant human interleukin-2 (IL-2) (Sigma-Aldrich). All cells were incubated at 37°C in a 5% CO_2 atmosphere.

Table 2.1: Cell lines used in this study.

Cell Line	Cell Type	Cell Line Characteristics	Source
BJAB	B-lymphocyte	Burkitt lymphoma, established from tumour of African case of Burkitt lymphoma.	(323), Anthony Pawson
DG75	B-lymphocyte	Burkitt lymphoma, established from pleural effusion of 10-year-old male.	(324), ATCC
Jurkat	T-lymphocyte	Acute T cell leukemia, established from peripheral blood of 14-year-old male.	(325), ATCC
Jurkat-TAg	T-lymphocyte	Acute T cell leukemia; stably transfected with adenovirus large-T antigen	(326), Anthony Pawson
Karpas 299	T-lymphocyte	ALK+ ALCL, established from blast cells in peripheral blood of 25-year-old male.	(327), Raymond Lai
KM-H2	B-lymphocyte	Hodgkin lymphoma, cultured Reed-Sternberg cells from pleural effusion of 32-year-old male.	(328), Raymond Lai
L428	B-lymphocyte	Hodgkin lymphoma, cultured Reed-Sternberg cells from pleural effusion of 37-year-old female.	(329), Raymond Lai
SIS	T-lymphocyte	EBV-positive cell line established from peripheral blood of 1-year-old male.	(322)
SUP-M2	T-lymphocyte	ALK+ ALCL, established from cerebrospinal fluid from 5-year-old female.	(330), Raymond Lai

2.2: DNA METHODS

2.2.1: Polymerase chain reaction

Polymerase chain reaction (PCR) experiments were carried out in 50µl reaction volumes containing 1x *Pfu* buffer (Fermentas), 0.8 mM deoxynucleotide triphosphates (dNTPs) mix (Fermentas), 4 mM $MgSO_4$, 0.3 µM forward and reverse primers (Table 2.2) (IDT; Coralville, IA), and 0.5 U/µL of *Pfu* polymerase (Fermentas). Each reaction used 50 ng of plasmid DNA as template. The primers that were used are listed in Table 2.2. PCR reactions were carried out using either a PTC-100 Peltier thermal cycler (Bio-Rad; Hercules, CA) or a Biometra T-gradient thermal cycler (Biometra; Goettingen Germany). The typical PCR cycling parameters used for amplifying JunB were an initial denaturing step at 95°C for 5 min followed by 35 cycles of denaturing at 95°C for 40 seconds, annealing at 57°C for 40 seconds, and extension at 72°C for 3 min. A final extension step was carried out at 72°C for 5 min, followed by an indefinite hold at 4°C.

2.2.2: Agarose gel electrophoresis and gel extraction

PCR products, and restriction endonuclease digested DNA were resolved on 1% weight/volume (w/v) agarose (Invitrogen) gels prepared in 1x TAE buffer (40 mM Tris-acetate, 1 mM EDTA) with 1:10,000 SYBR Safe DNA gel stain (Invitrogen). Six times loading dye (Fermentas; Burlington, ON, Canaada) was added to samples before they were run on gels. The agarose gels were typically run at 140 V constant voltage for 30 min, and bands were then visualized using the Bio-Rad XR+ gel doc system.

Table 2.2: Oligonucleotides used in this study.

Name	Sequence (5' → 3')	Restriction Site*	Description	Source
JunB 5'	TTT TTT GAA TTC TGC ACT AAA ATG GAA	*EcoRI*	Used to generate JunB for cloning into pcDNA3.1a-Myc-JunB vector following NT Myc tag.	IDT
JunB 3'	TTT TTT GGT ACC TCA GAA GGC GTG TCC	*KpnI*	Used to generate JunB for cloning into pcDNA3.1a vector.	IDT
JunB (S251/T255/S259A) – 5'	GAG GCG CGC GCC CGG GAC GCC GCG CCG CCG GTG GCC CCC ATC	N/A	Used to mutate serine residues 251 and 259, and threonine residue 255 to alanine to generate JunB phosphorylation mutant.	IDT
JunB (S251/T255/S259A) – 3'	GAT GGG GGC CAC CGG CGG CGC GGC GTC CCG GGC GCG CGC CTC	N/A		IDT
JunB (D137/144/145A) – 5'	GGC TTC GCC GGC TTT GTC AAA GCC CTG GCC GCT CTG GCC GCT CTG CAC AAG	N/A	Used to mutate aspartic acid residues 137, 144, and 145 to alanine to generate JunB mutant.	IDT
JunB (D137/144/145A) – 3'	CTT GTG CAG AGC GGC CAG GGC TTT GAC AAA GCC GGC GGC GAA GCC	N/A		IDT
JunB (D144/145A) – 5'	GGC TCC GCC GAC GGC TTT GTC AAA GCC CTG GCC GCT CTG CAC AAG	N/A	Used to mutate aspartic acid residues 144 and 145 to alanine to generate JunB mutant.	IDT
JunB (D144/145A) - 3'	CTT GTG CAG AGC GGC CAG GGC TTT GAC AAA GCC GTC GGC GAA GCC	N/A		IDT
JunB (D137A) – 5'	GGC TTC GCC GCC GGC TTT GTC AAA GCC CTG GAC GAT CTG CAC AAG	N/A	Used to mutate aspartic acid residue 137 to alanine to generate JunB mutant.	IDT
JunB (D137A) - 3'	CTT GTG CAG ATC GTC CAG GGC TTT GAC AAA GCC GGC GGC GAA GCC	N/A		IDT

JunB (D31A) – 5'	TTT TTT GAA TTC TGC ACT AAA ATG GAA CAG CCC TTC TAC CAC GAC GAC TCA TAC ACA GCT ACG GGA TAC GGC CGG GCC CCT GGT GGC CTC TCT CTA CAC GCC TAC AAA CTC	*EcoRI*	Used to mutate aspartic acid residue 31 to alanine to generate JunB mutant. Primer contains restriction site, JunB start, and D31A mutation.	IDT
JunB NT Fragment – 3'	TTT TTT GAA TTC GGC TTT GTC AAA GCC CTG GAC GAT CTG CAC AAG	*KpnI*	Used to add stop codon after aspartic acid 137 to generate JunB N-terminal truncation mutant	IDT
JunB CT Fragment - 5'	TTT TTT GGT ACC CTA GTC GGC GAA GCC CTC CTG CTC CTC	*EcoRI*	Used to add start codon after aspartic acid 137 to generate JunB C-terminal truncation mutant	IDT

***Restriction site underlined in primer sequence.**

2.2.3: Agarose gel electrophoresis and gel extraction

To purify DNA from agarose gels, the bands of interest were excised from the gel and purified using the QIAquick Gel Extraction Kit (Qiagen; Germantown MD), per the manufacturer's protocol. Briefly, the excised gel fragment was dissolved in 3 volumes of solubilisation buffer at 50°C, and then transferred to a DNA-binding QIAquick spin column. The sample was then washed with an ethanol containing wash buffer, and the DNA was eluted in 30-50µl of the supplied elution buffer (EB) by centrifugation at maximum speed for 1 min. Eluted DNA was quantified using a NanoDrop 1000 spectrometer (Thermo Fisher; Waltham, MA).

2.2.4: Restriction endonuclease digestion

Restriction endonuclease digestions of 0.5-3 µg of plasmid DNA and PCR products were carried out in buffer containing 1x NEB (New England BioLabs; Ipswich, MA) or 1X FastDigest (Fermentas) buffer, 100 µg/ml of bovine serum albumin (BSA) (New England BioLabs), and 20-60U of various restriction enzymes for 1-3 h at 37°C.

2.2.5: DNA ligation

The restriction endonuclease digested PCR products were ligated into the pcDNA3.1a vector (Invitrogen) using 5-10U of T4 DNA ligase (Fermentas). Reactions were carried out in 1X T4 DNA ligase buffer (Fermentas) in 10-20µL volumes with an insert to vector molar ratio of 3:1 or 5:1. Ligation reactions were incubated overnight at room temperature.

2.2.6: Bacterial transformation

Chemically competent DH5α *Escherichia coli* (*E. coli*) were transformed with plasmid DNA by heat shock transformation (331). Briefly, competent DH5α cells were

incubated with plasmid DNA on ice for 30 min, heat shocked at 42°C for 1 min, and then allowed to recover for 5 min on ice. Transformed bacteria were then plated on Luria-Bertani (LB) broth agar plates (10 g/L tryptone, 5 g/L yeast extract, 10 g/L NaCl, 15 g/L agar, pH 7.4) containing 100µg/ml ampicillin (Sigma-Aldrich). LB agar plates were then incubated at 37°C for 16-20 h.

2.2.7: Isolation and purification of plasmid DNA

The isolation and purification of plasmid DNA was performed using either the Qiagen Qiaprep Spin Miniprep or the Plasmid Maxiprep kits as per the manufacturer's protocols. Briefly, an overnight culture of DH5α *E. coli* grown in LB media (10 g/L tryptone, 5 g/L yeast extract, 10 g/L NaCl, pH 7.4) supplemented with 100µg/ml ampicillin was harvested and lysed. After a neutralization step that precipitates the genomic DNA and proteins, the lysate containing the plasmid DNA was run through DNA binding column and purified through a number of washing steps in the supplied PE wash buffer. The DNA was finally eluted in either elution buffer (EB) or Tris-EDTA (TE) buffer, and quantified by the NanoDrop 1000 spectrometer.

2.2.8: DNA sequencing and analysis

DNA sequencing reactions were performed by The Applied Genomics Centre (TAGC) (University of Alberta) using the T7-forward and bovine growth hormone (BGH)-reverse sequencing primers supplied by TAGC. The resulting DNA sequences were analyzed by the basic local alignment search tool (BLAST) (National Center for biotechnology Information (NCBI)) and aligned using the MAFFT sequence alignment program (332) and the Protein Family Alignment Annotation Tool (PFAAT) (333).

Sequencing chromatograms were read using BioEdit (BioEdit (URL: http://www.mbio.ncsu.edu/BioEdit/)).

2.3: CLONING

2.3.1: Plasmids

Vectors used in this study are listed in Table 2.3. The pAP1-Luc AP-1 promoter firefly luciferase vector was purchased from BD Biosciences (Franklin Lakes, NJ), the pGL2 and phrl-tk-Renilla luciferase vectors were purchased from Promega (Fitchburg, WI). The pcDNA3.1a (-) Myc/His expression vector was purchased from Invitrogen. The pBlueScript-Myc2 cloning vector was purchased from Stratagene (La Jolla, CA). The pcDNA3-FLAG-c-Fos(WT) vector (334) was purchased from Addgene (Cambridge, MA; Addgene ID 8966). Other vectors were generated as described below.

2.3.2: Generation of Myc-tagged JunB

The pcDNA3.1a-Myc-JunB construct was generated by Joel Pearson. The construct was generated by first PCR amplifying human JunB from a FLAG-tagged JunB cDNA using the JunB 5' and JunB 3' PCR primers (Table 2.2). The JunB PCR product was then subcloned using the *EcoRI* and *SalI* sites of the PCR product into the pBlueScript-SK-MycII vector at the *EcoRI* and *XhoI* sites to add a 5' double Myc-tag. Myc-JunB was then isolated by digestion with KpnI and SalIm and cloned into the pcDNA3.1a(-)Myc-His eukaryotic expression vector at the *EcoRI* and *KpnI* restriction sites with a translational stop site before the C-terminal Myc/His tags (Note: the *SalI*/*XhoI* restriction sites were destroyed in the process). The Myc-JunB construct was verified by DNA sequencing.

2.3.3: Generation of Myc-tagged JunB cleavage site mutants

The putative caspase cleavage site mutants were generated by site-directed mutagenesis where aspartic acid residues 31, 137, 144, and/or 145 were mutated to alanine by PCR using pcDNA3.1a-Myc-JunB as template. For the D137A, D144/145A,

D137/144/145A JunB mutants (Figure 2.1), point mutations were introduced into the PCR product using DNA oligonucleotides designed with a mutant sequence by overlap extension PCR (335). Each half of the PCR product was generated by PCR using a 5' or 3' JunB flanking primer (JunB 5' and 3') and a 3' or 5' mutagenic primer (JunB (D137A) 5' and 3', JunB (D144/145A) 5' and 3', and JunB (D137/144/145A) 5' and 3' primers). Following PCR, a small amount of the 2 PCR products were mixed together, annealed and PCR amplified using the 5' and 3' JunB flanking primers. For the JunB D31A mutant, because of the proximity of the site of mutagenesis to the 5' end of JunB, a large primer was designed to be both the flanking and mutagenic primer spanning the N-terminus and the sequence to be mutated. To generate the JunB D31A mutant, one round of PCR was performed using the JunB (D31A) 5' and JunB 3' for pcDNA primers. The full length PCR products containing the mutation(s) were then cloned into the pcDNA3.1a expression vector using the *EcoRI* and *KpnI* restriction sites of the PCR product. All JunB cDNAs generated were verified by DNA sequencing.

2.3.4: Generation of Myc-tagged JunB truncation mutants

Using the Myc-tagged JunB as template for PCR, the N-terminal truncation mutant (Figure 2.1) was generated by introducing a stop codon following aspartic acid 137, while the C-terminal truncation mutant (Figure 2.1) was generated by introducing a start codon immediately following aspartic acid 137. Primer pairs used for the PCR reaction were JunB 5' and JunB NT fragment 3' primers for the N-terminal JunB fragment, and the JunB CT fragment 5' and JunB 3' primers for the C-terminal JunB fragment. The PCR products were then cloned into the pcDNA3.1a expression vector using the *EcoRI* and *KpnI* restriction sites of the PCR product. All JunB cDNAs generated were verified by DNA sequencing.

Table 2.3: Vectors used in this study.

Plasmid	Characteristics	Source
pBlueScript-SK-Myc2	Cloning vector containing N-terminal double Myc-tag	Stratagene
pcDNA3.1a	Expression vector with T7 and CMV promoters	Invitrogen
pcDNA3.1a-Myc-JunB	Double Myc-tagged wild-type JunB	Joel Pearson
pcDNA3.1a-Myc-JunB(D31A)	Myc-tagged JunB with D31A mutation	This study
pcDNA3.1a-Myc-JunB(D137A)	Myc-tagged JunB with D31A mutation	This study
pcDNA3.1a-Myc-JunB(D144/145A)	Myc-tagged JunB with D144/145A mutations	This study
pcDNA3.1a-Myc-JunB (D137/144/145A)	Myc-tagged JunB with D137/144/145A mutations	This study
pcDNA3.1a-Myc-JunB-NT (1-137)	Myc-tagged N-terminal JunB (terminating at D137)	This study
pcDNA3.1a-Myc-JunB-CT (138-347)	Myc-tagged C-terminal JunB (start after D137)	This study
pcDNA3-FLAG-c-Fos	FLAG-tagged wild-type c-Fos	Addgene (334)
pGL2	Luciferase reporter vector	Promega
phRL-TK-Renilla	Renilla luciferase	Promega
pAP1-Luc	AP-1 luciferase reporter	BD

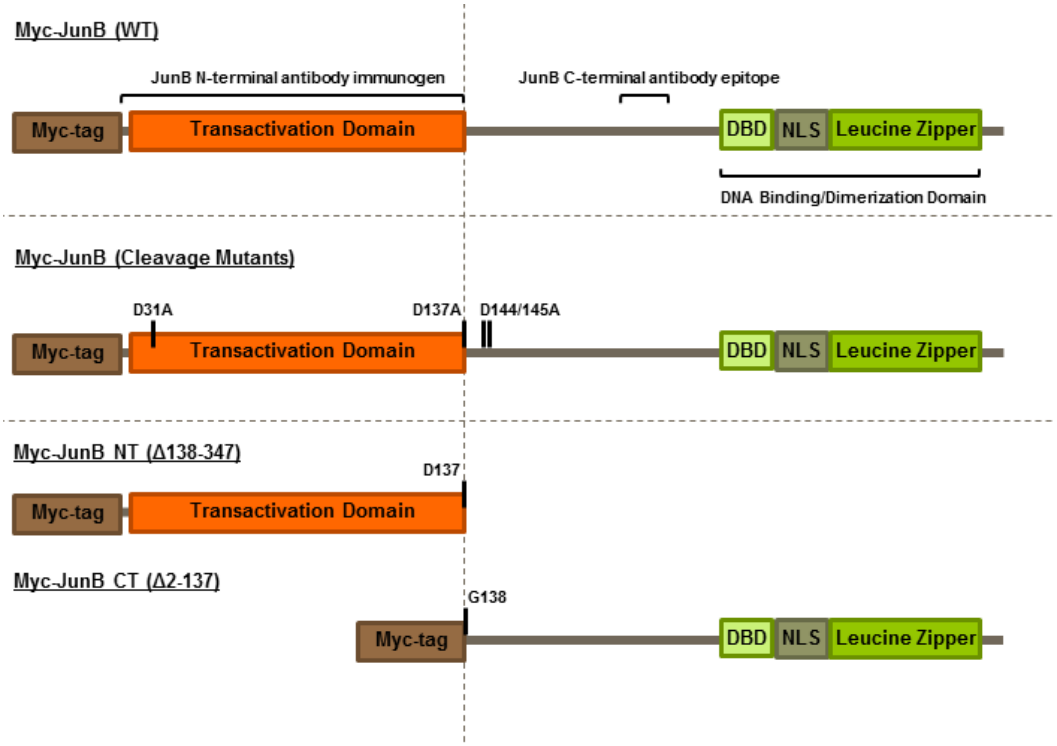

Figure 2.1: JunB mutants generated in this study.

The schematic diagram of wild-type Myc-JunB is illustrated with its Myc-tag, transactivation domain, and the DNA binding/dimerization domain (containing the DNA binding domain, nuclear localisation signal (NLS), and leucine zipper). The epitope recognized by the JunB C-terminal antibody, and the immunogen of the N-terminal JunB antibody are also shown. The JunB (1-137) and (138-347) mutants are the N and C-terminal truncation mutants, respectively, of JunB at the D137 site. Point mutations were made in D31, 137, or 144/145 to generate the putative JunB cleavage site mutants.

2.4: TRANSFECTIONS

2.4.1: General transfection protocol

Cells ($1–2x10^7$ cells/ml) were transfected by electroporation in 500 µl of complete RPMI media in a 4 mm gap cuvette (VWR International; Mississauga, ON, Canada). Electroporations were carried out using a BTX ECM 830 square wave electroporator (BTX; San Diego, CA) with the following settings: 225V, 3 pulses, 8 ms pulse length, 1 s between pulses. Cells were allowed to rest for 5 min following electroporation, then resuspended in 10-15 ml of RPMI media, and then incubated at 37°C in a 5% CO_2 atmosphere. The transfection of the BJAB Burkitt lymphoma cell line was performed as described above, with the exception that cells were resuspended in cold RPMI media and kept on ice throughout the transfection process to reduce cell death.

2.5: PROTEIN METHODS

2.5.1: Antibodies

Antibodies used in this study are listed in Table 2.4. The anti-caspase 3 mouse monoclonal antibody (mAb) (3G2), and rabbit anti-cleaved caspase 3 polyclonal antibody (pAb) (9661) were purchased from Cell Signalling Technology (Danvers, MA). The mAbs against c-Jun (60A8), JunB (C-11 and 204C4a), JunD (329), Fra2 (Q-20), c-Fos(C-10), FosB(102), Myc (9E10), tubulin (DM1A), and PARP-1 (5A5) were purchased from Santa Cruz Biotechnology (Santa Cruz, CA). The mouse anti-β-actin mAb (AC-15) was purchased from Sigma-Aldrich, the rabbit anti-pJunB (S259) pAb (ab30628) was purchased from Abcam (Cambridge, MA), and the rabbit anti-caspase 3 pAb (used in Figure 1A) was a gift from Dr. Michele Barry (University of Alberta) (336). For western blotting, antibodies were diluted to the specified working concentration (Table 2.4) in 1x Tris-buffered saline (TBS) (20 mM Tris base, 137 mM NaCl, pH 7.5) with 0.02% NaN_3.

2.5.2: Putative caspase cleavage site prediction

The computational identification of caspase substrate cleavage sites in JunB and other AP-1 family proteins was performed by the Cascleave webserver (http://sunflower.kuicr.kyoto-u.ac.jp/~sjn/Cascleave/webserver.html), using a number of sequence encoding schemes that take into account protein sequence and predicted protein structure to make the caspase cleavage site predictions (337).

Table 2.4: Antibodies used in this study.

Antibody	Species	Working concentration	Source
Actin (AC-15)	Mouse	1:5,000	Santa Cruz
Caspase 3	Rabbit	1:5,000	(336), Michele Barry
c-Fos (C-10)	Mouse	1:200	Santa Cruz
c-Jun (60A8)	Rabbit	1:1,000	Santa Cruz
Cleaved-Caspase-3 (9661)	Rabbit	1:2,000	Cell Signalling
FLAG M2	Mouse	1:1,000	Sigma
FosB (102)	Rabbit	1:200	Santa Cruz
Fra2 (Q-20)	Rabbit	1:200	Santa Cruz
JunB (204c4a)	Mouse	1:200	Santa Cruz
JunB (C-11)	Mouse	1:200	Santa Cruz
JunD (329)	Rabbit	1:200	Santa Cruz
Myc (9E10)	Mouse	1:200	Santa Cruz
PARP (5A5)	Mouse	1:5,000	Santa Cruz
pJunB (S259)	Rabbit	1:200	Cell Signalling
Pro-Caspase-3 (3G2)	Mouse	1:1,000	Cell Signalling
Tubulin (DM1A)	Mouse	1:5,000	Santa Cruz
Goat α-Mouse HRP	Goat	1:10,000	Bio-Rad
Goat α-Rabbit HRP	Goat	1:5,000 – 1:10,000	Bio-Rad

2.5.3: Cell lysis

Cells were collected by centrifugation at ~700*g*, washed in PBS (137 mM NaCl, 2.7mM KCl, 10 mM $Na_2HPO_4.2H_2O$, 2 mM KH_2PO_4, pH 7.4), and lysed in a 1% Nonidet P-40 (NP-40) lysis buffer (1% NP-40, 50 mM Tris pH 7.4, 150 mM NaCl, 2 mM EDTA, 10% glycerol) containing 1 mM PMSF (BioShop), 1 mM sodium orthovanadate (Sigma), and protease inhibitor cocktail (Sigma-Aldrich). Cell lysates were cleared of detergent-insoluble material by centrifugation at ~20,000*g* for 10 min, and stored at -80°C.

2.5.4: Apoptosis Induction

Cells ($5x10^5$-$1x10^6$ cells/ml) were induced to undergo apoptosis by treatment with either 5 µM of doxorubicin for 12 h or 2 µM of staurosporine for 6 h (ALK+ ALCL) or 8 h (BJAB) at 37°C. For time course and dose response experiments, the treatment times and drug concentrations are indicated in the respective figures. Staurosporine and the pan–caspase inhibitor, Z-VAD-FMK, were purchased from Enzo Life Sciences (Plymouth Meeting, PA). Doxorubicin was purchased from Sigma-Aldrich. Following drug treatment, cells were lysed as previously described and cell lysates used for SDS-PAGE and western blotting.

2.5.5: Immunoprecipitations

For immunoprecipitations, cleared lysates were incubated with 1-2 µg of antibody and Protein G-Sepharose beads (Sigma-Aldrich) for 1-2 h on a nutator at 4°C. Beads were then washed with 1% NP-40 lysis buffer containing 1mM PMSF. Proteins were eluted by boiling in SDS-PAGE sample buffer. Immunoprecipitates and cell lysates were resolved on SDS-PAGE gels before being transferred to nitrocellulose membranes.

2.5.6: Dephosphorylation assays

$6x10^6$ Karpas 299 cells were lysed in 1 ml of 1% NP-40 lysis buffer with inhibitors. Immunoprecipitations were performed, and immunoprecipitates were washed in 1% NP-40 lysis buffer without EDTA and sodium orthovanadate followed by a wash in FastAP buffer (Fermentas). JunB was then dephosphorylated by incubating immunoprecipitates with 2U of FastAP Thermosensitive Alkaline Phosphatase (Fermentas) in FastAP buffer for 1 h at 37°C. Immunoprecipitations were again washed in FastAP buffer, before proteins were eluted by the addition of SDS-PAGE sample buffer.

2.5.7: Nuclear/cytoplasmic fractionation

Nuclear/cytoplasmic lysates to be used for western blotting and EMSAs were prepared using either the ProteoJET cytoplasmic and nuclear protein extraction kit (Fermentas) or the NE-PER nuclear and cytoplasmic extraction reagent (Thermo Fisher) using the manufacturer's protocols. Cytoplasmic and nuclear extracts collected by both kits were stored at -80°C

With the ProteoJET kit, cells were first collected by centrifugation at ~650*g*, washed in PBS, and lysed in the supplied cell lysis buffer, supplemented with 1 mM PMSF, 1 mM sodium orthovanadate, and protease inhibitor cocktail. The cytoplasmic fraction was then isolated by collecting the supernatant following centrifugation at 20,000*g*. The pellet, containing the nuclear fraction, was then washed with the supplied nuclei washing buffer (with 1 mM PMSF, 1 mM sodium orthovanadate), resuspended in nuclei storage buffer (with 1 mM PMSF, 1 mM sodium orthovanadate), and lysed in the supplied nuclei lysis reagent. The nuclear fraction was collected from the supernatant following centrifugation at 20,000*g*.

With the NE-PER kit, cells were similarly collected and washed with PBS. The cell pellet was then resuspended in the supplied cytoplasmic extraction reagent (CER) I buffer, vortexed, and then mixed with the supplied CER II buffer, and vortexed again. The cytoplasmic fraction was then collected from the supernatant following centrifugation at 20,000*g*. The nuclear fraction was then extracted from the pellet by resuspended it in the supplied nuclear extraction reagent (NER) buffer, vortexing, centrifugation at 20,000*g*, and collecting the supernatant.

2.5.8: Electrophoretic mobility shift assay

For EMSA experiments, Karpas 299 cells were transfected with 5 µg pcDNA3.1a empty vector, pcDNA3.1a-Myc-JunB (WT or Myc-JunB C-terminal fragment). For competitor experiments, Karpas 299 cells were transfected with empty vector (20 µg) or 5, 10 or 20 µg Myc-JunB C-terminal fragment. Empty vector was added where necessary to bring the total DNA per transfection to 20 µg. Nuclear fractions were collected 24 h as described previously. EMSA experiments were performed using the LightShift chemiluminescent EMSA kit (Thermo Fisher). Binding reactions were performed with a biotinylated probe containing repeating AP-1 binding sites (GGG TTC CTG CTCTGG GCT GAATAG GTG GTC CACTCT GAGTCA TCA GCT GTG GGT GAT G), 3.5 µg of nuclear extract and 1 µg of the indicated antibody. The nuclear extract and antibodies were pre-incubated on ice for 15 min prior to addition of the biotinylated probe. EMSA experiments were performed by Joel Pearson.

2.5.9: In-vitro caspase cleavage assay

Assays were performed as previously described (338). Briefly, Myc-tagged JunB was produced using the T_NT T7 Quick Coupled Transcription/Translation System

(Promega), with 1 µg of the pcDNA3.1a empty vector or pcDNA3.1a-Myc-JunB (WT or site mutants) plasmid DNA (all containing T7 promoters) as template. The DNA was incubated with the T_NT kit components (1x T_NT Quick master mix and 20 µM unlabelled methionine) in a 50 µl reaction at 30°C for 1-1.5 h. Transcription of the plasmid DNA to RNA was carried out by T7 RNA polymerases, and translation to protein by rabbit reticulocyte lysate.

Two microliters of this reaction mixture was incubated with 256 ng of recombinant, active caspase 3 (Sigma-Aldrich) (134 or 268 pM; ~$9x10^{-4}$-$1.8x10^{-3}$ U) in cleavage buffer (20 mM PIPES, 100 mM NaCl, 40 mM DTT, 1 mM EDTA, 0.1% CHAPS, 10% Sucrose) for the indicated times. Reactions were stopped by the addition of SDS-PAGE sample buffer. Recombinant human caspases used for the cleavage experiment in Figure 3.11 was purchased from Millipore (Billerica, MA), and cleavage reactions were performed as described above with the exception that 2 U of each of the caspases was incubated with 0.5 µl TNT extract.

2.5.10: Protein quantification by bicinchoninic acid assay

The protein concentration of the cleared lysates was determined using the bicinchoninic acid (BCA) Protein Assay Kit (Thermo Fisher) based on manufacturer's protocol. Ten µL of diluted cell lysates (1:5 in water), along with a standard curve of increasing concentrations of bovine serum albumin (BSA) was mixed with 90 µL of BCA reagent were loaded in triplicate in a 96-well plate and incubated at 37°C for 30 min. Samples were read using a FLUOstar OPTIMA microplate reader (BMG Labtech; Ortenberg, Germany). A standard curve was generated using the BSA standards and used to determine the protein concentration of samples.

2.5.11: Protein quantification by Bradford assay

The protein concentrations of the nuclear and cytoplasmic fractions were determined using the Bradford assay (339). Ten µL of protein standard or extract was incubated with 250 µL of Bradford Dye Reagent (Bio Rad) at room temperature for 15 min. Samples were loaded in triplicate in a 96-well plate and read using a FLUOstar OPTIMA microplate reader (BMG Labtech). A standard curve was generated using the BSA standards and used to determine the protein concentration of samples.

2.5.12: SDS-polyacrylamide electrophoresis

Cell lysates were prepared in either a 5x sample buffer or 2x sample buffer (4% SDS, 20% glycerol, 10% 2-mercaptoethanol, 0.004% bromophenol blue, and 125mM Tris-HCl pH 6.8), and boiled at ~95°C for 5 min. Samples were resolved on SDS-PAGE gels using a Hoefer SE260 mini-vertical gel electrophoresis unit (Hoefer; Holliston, MA) at 25 mA constant current for approximately 1.5 h. Gels were run in a running buffer made up of 25 mM Tris base, 192 mM glycine and 0.1% SDS. SDS-PAGE gels were made up of a 5% acrylamide stacking gel (125 mM Tris base, 0.1% SDS, pH 6.8; 5% acrylamide, 0.05% ammonium persulphate (APS) and 0.1% tetramethylethylenediamine (TEMED)) and an 8-14% acrylamide resolving gel (375 mM Tris base, 0.1% SDS, pH 8.8; 8-14% acrylamide, 0.05% APS and 0.1% TEMED). All empty wells were loaded with 1x sample buffer and a PAGEruler prestained protein ladder (Fermentas) was used as a molecular mass indicator.

2.5.13: Semi-dry transfer

The semi-dry transfer of proteins from the SDS-PAGE gel to nitrocellulose membranes were performed with a Bio-Rad TransBlot SD transfer apparatus at a constant voltage of 15 V for 30-60 min. Prior to transfer, both the SDS-PAGE gel and nitrocellulose membrane were equilibrated in 1X transfer buffer containing 25 mM Tris base, 192 mM glycine, and 20% methanol for 10 min prior to transfer. Following transfer, membranes were stained with 0.1% Ponceau S stain (Sigma-Aldrich) – a reversible protein dye – to check the quality of the transfer and equal protein loading. The Ponceau S stain was then removed by washes with 0.05% TBST (1x TBS with 0.05% Tween-20).

2.5.14: Western blotting

The nitrocellulose membranes were blocked in 5% non-fat milk powder in 1x TBS for 30 min before being probed with primary antibody for 1 h at room temperature, then overnight at 4°C with shaking. Blots were then washed 3 times for 10 min each with 0.05% TBST, and probed with horseradish-peroxidase (HRP) -conjugated secondary antibodies (Bio-Rad) for 30 min at room temperature. Membranes were then washed 3 more times for 10 min each with 0.05% or 0.1% TBST. Proteins were visualized by incubating membranes for 5 min with SuperSignal West Pico Chemiluminescent Substrate (Thermo Fisher), and then exposed to autoradiography film (Clonex; Markham, ON, Canada). Films were developed using an M35A X-OMAT film developer (Kodak; Rochester, NY). Reprobed blots were first stripped in a 0.1% TBST, pH 2 stripping solution with 3 washes of ~30 min each, followed by 2 washes with 0.05% TBST at 5 min each, before being reprobed as described above.

2.6: ADDITIONAL ASSAYS

2.6.1: Luciferase assays

Cells were transfected with the indicated amounts of pGL2 vector, pcDNA3.1a vector, or Myc-JunB (WT/NT/CT) cDNAs; 5 μg of the pAP1-Luc AP-1 promoter firefly luciferase vector; as well as 1 μg of the CMV promoter-driven *Renilla* luciferase construct which is constitutively expressed and used as an internal control for transfection efficiency. Cells were collected by centrifugation at ~650*g* and counted 24 h post-transfection. $1x10^6$ cells were analyzed in triplicate in a 96-well plate for *Renilla* and firefly luciferase activity using the Dual-Glo Luciferase Assay System (Promega) in a FLUOstar OPTIMA microplate reader (BMG Labtech). Briefly, the cells were first mixed with the Dual-Glo luciferase reagent and incubated at room temperature for 10 min prior to the firefly luminescence reading. The firefly luminescence was then quenched by the addition of the Dual-Glo Stop & Glo reagent (made by diluting the Stop & Glo substrate 1:100 in Stop & Glo buffer) for 10 min at room temperature. The addition of the Stop & Glo reagent is also a substrate of the *Renilla* luciferase to produce the luminescence to be read by the plate reader. The firefly to *Renilla* luciferase activity ratio was calculated for each sample and then averaged for the triplicate measurements. Results are expressed relative to the vector alone–transfected cells and represent the average and standard deviation of at least three independent experiments. Statistical significance was determined by paired, one-tailed *t*-tests.

2.6.2: Resazurin-based viability assay

Karpas 299 cells were transfected with 20 μg of empty vector (pcDNA3.1a) or the indicated JunB constructs, and resuspended to $5x10^4$ cells/ml. Cell viability was then measured using a resazurin–based cell viability assay (340). At the indicated time points

after transfection, 100 µl of transfected cells were loaded in triplicate in a 96-well plate and mixed with resazurin (Sigma-Aldrich) to a final concentration of 44 µM. Cells were incubated at 37°C for 2-4 h before the fluorescence reading – until a colour change was observed. Fluorescence was then measured on a BMG Labtech FluoStar Optima Plate Reader (excitation – 544 nm, emission – 590 nm). Each sample was assayed in triplicate, the triplicate measurements averaged, and the cell viability expressed relative to empty vector–transfected cells. Statistical significance was determined by paired, one-tailed *t*-tests. Viability assays were performed by Joel Pearson.

2.6.3: Apoptosis and proliferation assays

Karpas 299 cells were transfected with 20 µg of empty vector or the indicated JunB constructs. Apoptosis was assessed 48 h after transfection using the Annexin V-FITC Apoptosis Detection Kit I (BD Biosciences). Briefly, $1x10^5$ cells from each sample were washed with PBS, stained with FITC-conjugated Annexin V and propidium iodide (PI), and incubated for 15 min at room temperature in the dark. Cells were also left unstained, stained with Annexin V-FITC alone, or PI alone for compensation controls. The stained cells were then mixed with 1x binding buffer, and analyzed by the FACScalibur flow cytometer (BD Biosciences). Statistical significance was determined by paired, two-tailed *t*-tests. The apoptosis assays were performed by Joel Pearson.

To measure cell proliferation, cells were transfected as described in the apoptosis assay, and were then assayed by measuring BrdU incorporation 48 h after transfection using the FITC BrdU Flow Kit (BD Biosciences). Briefly, were incubated with 10 µM of BrdU solution at a density of $1.5\text{-}3x10^5$ cells/ml for 4 h at 37°C. Cells were then fixed and permeabilized, DNase treated, and stained with antibody before being

analyzed for BrdU incorporation using the FACScalibur flow cytometer (BD Biosciences). Statistical significance was determined by paired, one-tailed *t*-tests. Proliferation assays were performed by Joel Pearson.

CHAPTER 3: INVESTIGATING THE CLEAVAGE OF JUNB BY CASPASES

A portion of this chapter has been submitted for publication:

Lee JK, Pearson JD, Maser BM, and Ingham RJ. 2013. Cleavage of the JunB transcription factor by caspases generates a carboxy-terminal fragment that inhibits activator protein-1 transcriptional activity. *Journal of Biological Chemistry*. [undergoing revision]

The pcDNA3.1A-Myc-JunB(WT) vector was generated by J. Pearson. The experiments contained in this chapter were performed by J. Lee, J. Pearson, and Dr. R. Ingham. Experiments in figures 3.8B, 3.11, 3.20, 3.22-27 were performed by J. Pearson, and experiments in figure 3.8A was performed by R. Ingham. The original manuscript was written by J. Lee, J. Pearson, and Dr. R. Ingham.

3.1: CHANGES TO JUNB ELECTROPHORETIC MOBILITY IN APOPTOTIC ALK+ ALCL CELL LINES

Previous experiments performed in the laboratory to examine whether JunB protects ALK+ ALCL cell lines from apoptosis caused by the apoptosis-inducing drug doxorubicin resulted in the observation of changes to the electrophoretic mobility of the anti-JunB immunoreactive bands. This was similar to the changes observed following treatment with the apoptosis-inducing drug staurosporine (Figure 3.1A). The characteristic JunB bands observed in untreated cells, which typically appeared as a doublet of ~43 kDa in size, was not evident in the staurosporine–treated cells. We instead observed a single band with the same electrophoretic mobility as the lower molecular weight band in the untreated samples at approximately 43 kDa. Moreover, we observed the appearance of an additional anti-JunB immunoreactive band of approximately 28 kDa (Figure 3.1A). We also observed similar results probing lysates from another staurosporine–treated ALK+ ALCL cell line, SUP-M2 (Figure 3.1B).

3.1.1: Caspase dependence of electrophoretic mobility change

Since the loss of the JunB doublet and the appearance of the ~28kDa JunB immunoreactive band in staurosporine–treated cells correlated with the activation of caspase 3, (Figure 3.1A and B), we next examined whether the change in JunB electrophoretic mobility was dependent on caspases. Co-treatment of Karpas 299 or SUP-M2 cells with staurosporine and the pan–caspase inhibitor, Z-VAD-FMK (341), blocked the appearance of the ~28 kDa anti-JunB immunoreactive band and preserved the JunB doublet (Figure 3.2). These results thus demonstrate the caspase dependence of the changes in JunB electrophoretic mobility.

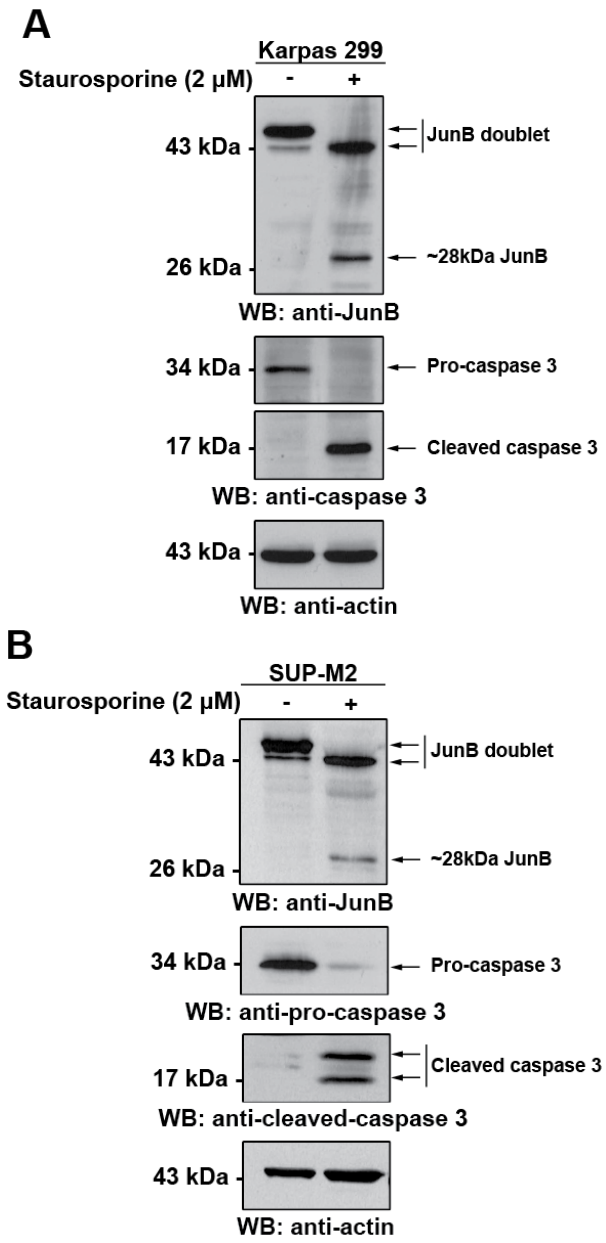

Figure 3.1: The electrophoretic mobility of JunB is altered in lysates of ALK+ ALCL cell lines treated with staurosporine.

Lysates from Karpas 299 cells **(A)** or SUP-M2 cells **(B)** treated with (+) or without (-) staurosporine were western blotted (WB) with an anti-JunB antibody. The efficacy of apoptosis induction in all panels was determined by the disappearance of pro-caspase 3 and the appearance of cleaved, active caspase 3. Anti-actin blots are included to demonstrate protein loading. The electrophoretic mobility of molecular mass standards are indicated to the left of blots.

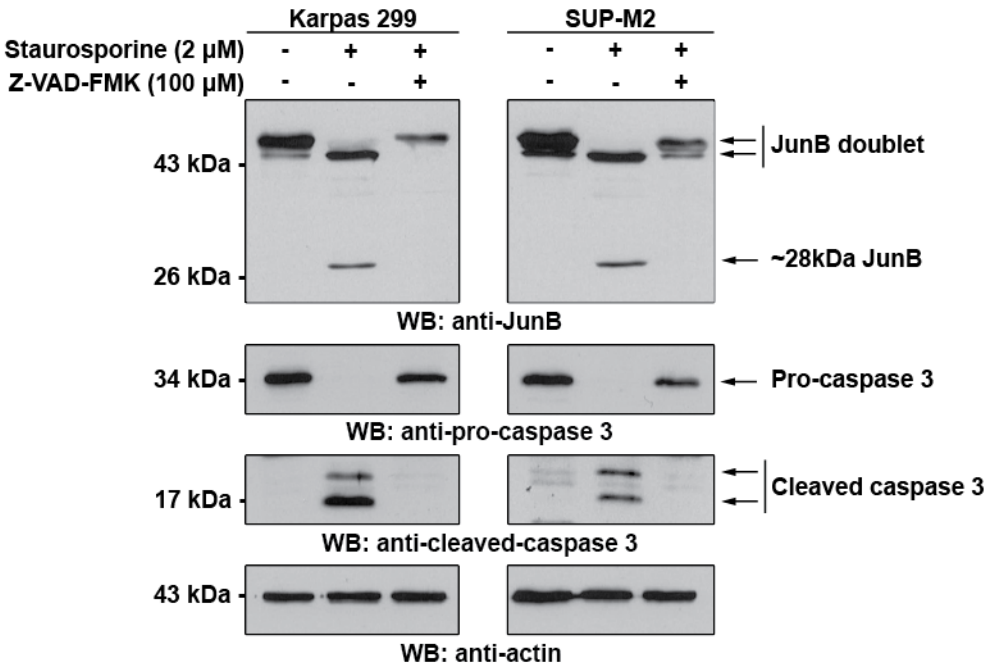

Figure 3.2: The electrophoretic mobility of JunB is altered in a caspase–dependent manner in lysates of ALK+ ALCL cell lines treated with staurosporine.

Karpas 299 and SUP-M2 cells were untreated, treated with staurosporine, or co-treated with staurosporine and Z-VAD-FMK. Lysates from these cells were then probed with an anti-JunB antibody. The efficacy of apoptosis induction in all panels was determined by the disappearance of pro-caspase 3 and the appearance of cleaved, active caspase 3. Anti-actin blots are included to demonstrate protein loading. The electrophoretic mobility of molecular weight standards are indicated to the left of blots.

3.1.2: Time and dosage dependence of electrophoretic mobility change

We further investigated the altered JunB electrophoretic mobility by examining the time and dosage dependence of drug treatment on the changes in JunB electrophoretic mobility. Staurosporine time–course (Figure 3.3A) and dose–response (Figure 3.3B) experiments further revealed a correlation between the appearance of the ~28kDa anti-JunB immunoreactive band and the activation of caspase 3. The appearance of the ~28kDa anti-JunB immunoreactive band also correlated with cleavage of the caspase substrate, PARP. The disappearance of the JunB doublet was also time and dosage dependent (Figure 3.3A and B).

3.1.3: Changes following doxorubicin treatment

We next examined whether other apoptosis–inducing agents could similarly affect the electrophoretic mobility of JunB in ALK+ ALCL cell lines. Doxorubicin promotes apoptosis in ALK+ ALCL cell lines (320,342,343), and is one component of the CHOP (cyclophosphamide, hydroxydaunorubicin (doxorubicin), oncovin, and prednisone) chemotherapy regimen used clinically to treat ALK+ ALCL (27). Similar to staurosporine treatment, we found that the treatment of both Karpas 299 and SUP-M2 cell lines with doxorubicin resulted in the appearance of the ~28 kDa JunB protein and a single band in place of the JunB doublet (Figure 3.4A and B). The change in JunB electrophoretic mobility induced by doxorubicin was also dependent on caspase activation, as both the appearance of the ~28 kDa band and the loss of the JunB doublet were blocked by the co-treatment of cells with Z-VAD-FMK (Figure 3.4A and B). Thus, our findings suggest that JunB may be cleaved by caspases in apoptotic ALK+ ALCL cells induced by the apoptosis inducing agents staurosporine and doxorubicin.

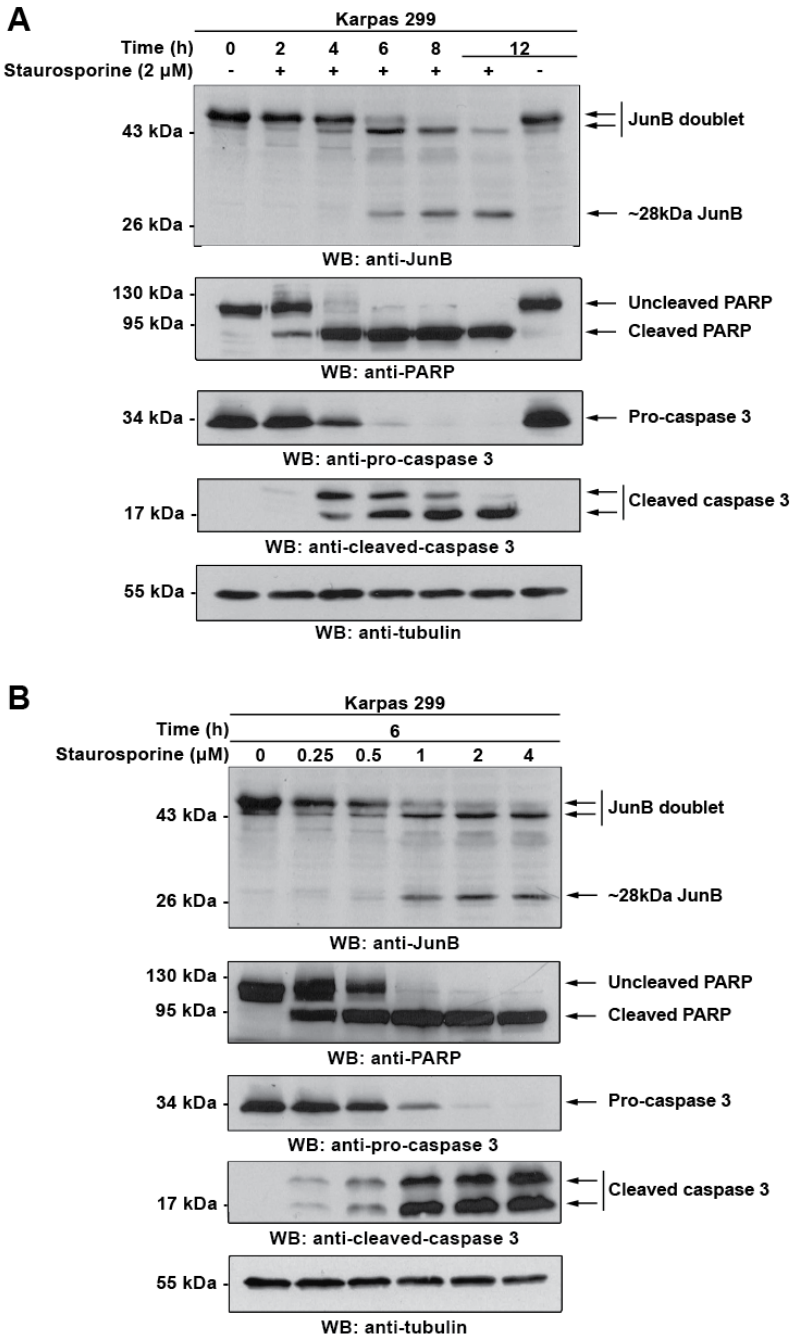

Figure 3.3: The electrophoretic mobility of JunB is altered in a time– and dosage–dependent manner in lysates of ALK+ ALCL cell lines treated with staurosporine.

Karpas 299 cells were treated for increasing times **(A)** or with increasing concentrations **(B)** of staurosporine, and lysates from these cells were probed with an anti-JunB or anti-PARP antibody. The efficacy of apoptosis induction in all panels was determined by the disappearance of pro-caspase 3 and the appearance of cleaved, active caspase 3. Anti-tubulin blots are included to demonstrate protein loading. The electrophoretic mobility of molecular weight standards are indicated to the left of blots.

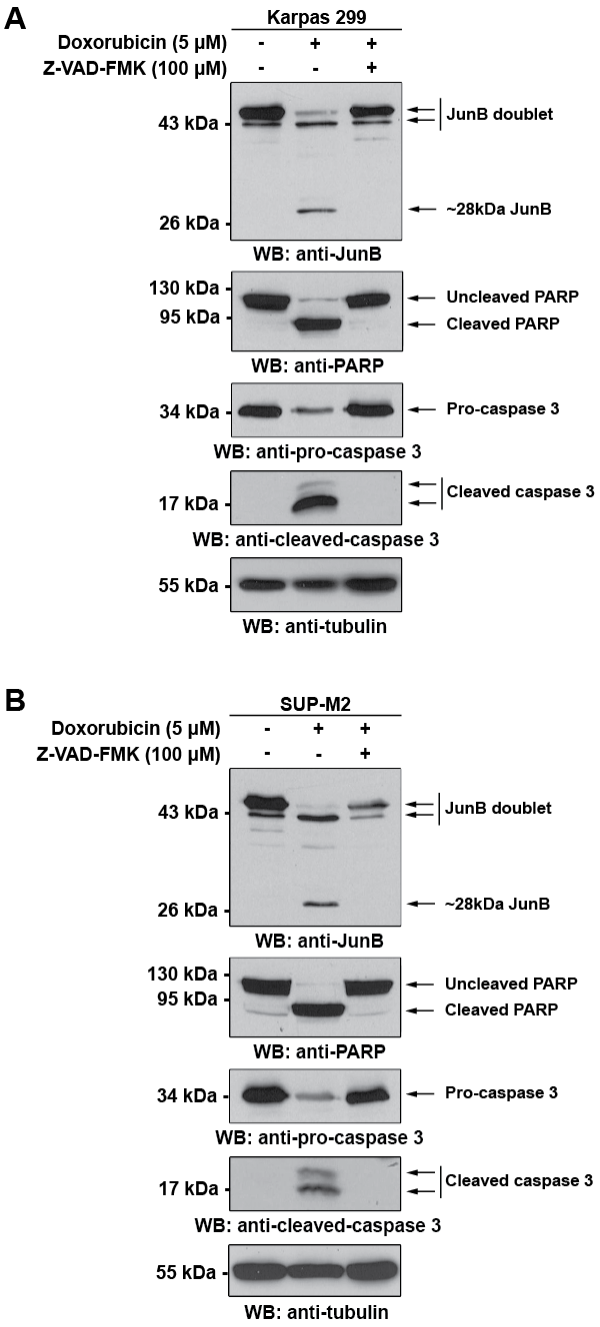

Figure 3.4: Doxorubicin treatment alters the electrophoretic mobility of JunB in a caspase–dependent manner in ALK+ ALCL cell lines.

Karpas 299 **(A)** or SUP-M2 **(B)** cells were left untreated, treated with doxorubicin, or treated with doxorubicin and Z-VAD-FMK. The efficacy of apoptosis induction in all panels was determined by the disappearance of pro-caspase 3, the appearance of cleaved, active caspase 3, and the cleavage of PARP. Anti-tubulin blots are included to demonstrate protein loading. The electrophoretic mobility of molecular weight standards are indicated to the left of blots.

3.1.4: Changes in electrophoretic mobility of other AP-1 family proteins

We also investigated whether the electrophoretic mobility of other AP-1 family members were altered in staurosporine–treated cells. Although staurosporine treatment significantly reduced c-Jun levels, we observed no bands of altered electrophoretic mobility (Figure 3.5). We also observed no alteration in FosB electrophoretic mobility in response to staurosporine treatment. We did observe 2 lower molecular weight anti-c-Fos immunoreactive bands in staurosporine–treated cells, and the appearance of this band could be blocked by the co-treatment of the cells with Z-VAD-FMK. However, these bands were only evident with longer exposure times, and much less prominent than was observed for JunB (Figure 3.1).

The electrophoretic mobility of JunD also did not appear to be significantly affected following staurosporine treatment, although the Fra2 doublet appeared to collapse in a similar manner as what we had observed in JunB. Interestingly, we only observed these changes at the 12 h time point but not at any of the previous time points (Figure 3.6). However, there were numerous bands detected by both the JunD and Fra2 antibodies both with and without staurosporine treatment, making it difficult to determine whether these are non-specific bands or potential JunD and Fra2 cleavage products (Figure 3.6).

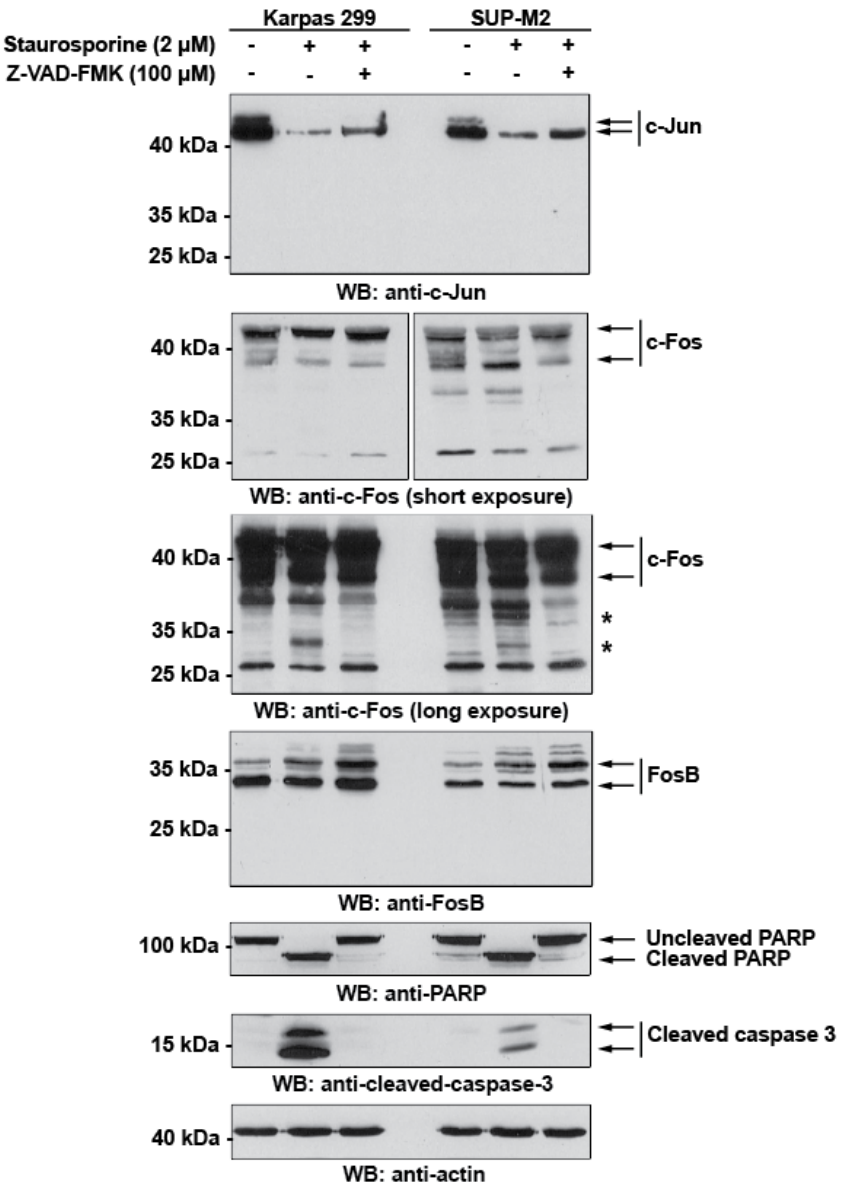

Figure 3.5: The electrophoretic mobility of c-Jun, c-Fos and FosB in lysates of ALK+ ALCL cell lines treated with staurosporine.

Karpas 299 and SUP-M2 cells were untreated, treated with staurosporine, or co-treated with staurosporine and Z-VAD-FMK. Lysates from these cells were then probed with an anti-c-Jun, c-Fos, or FosB antibody. The asterisk **(*)** indicates new c-Fos immunoreactive bands following staurosporine treatment. The efficacy of apoptosis induction in all panels was determined by the appearance of cleaved, active caspase 3 and PARP cleavage. Anti-actin blots are included to demonstrate protein loading. The electrophoretic mobility of molecular weight standards are indicated to the left of blots.

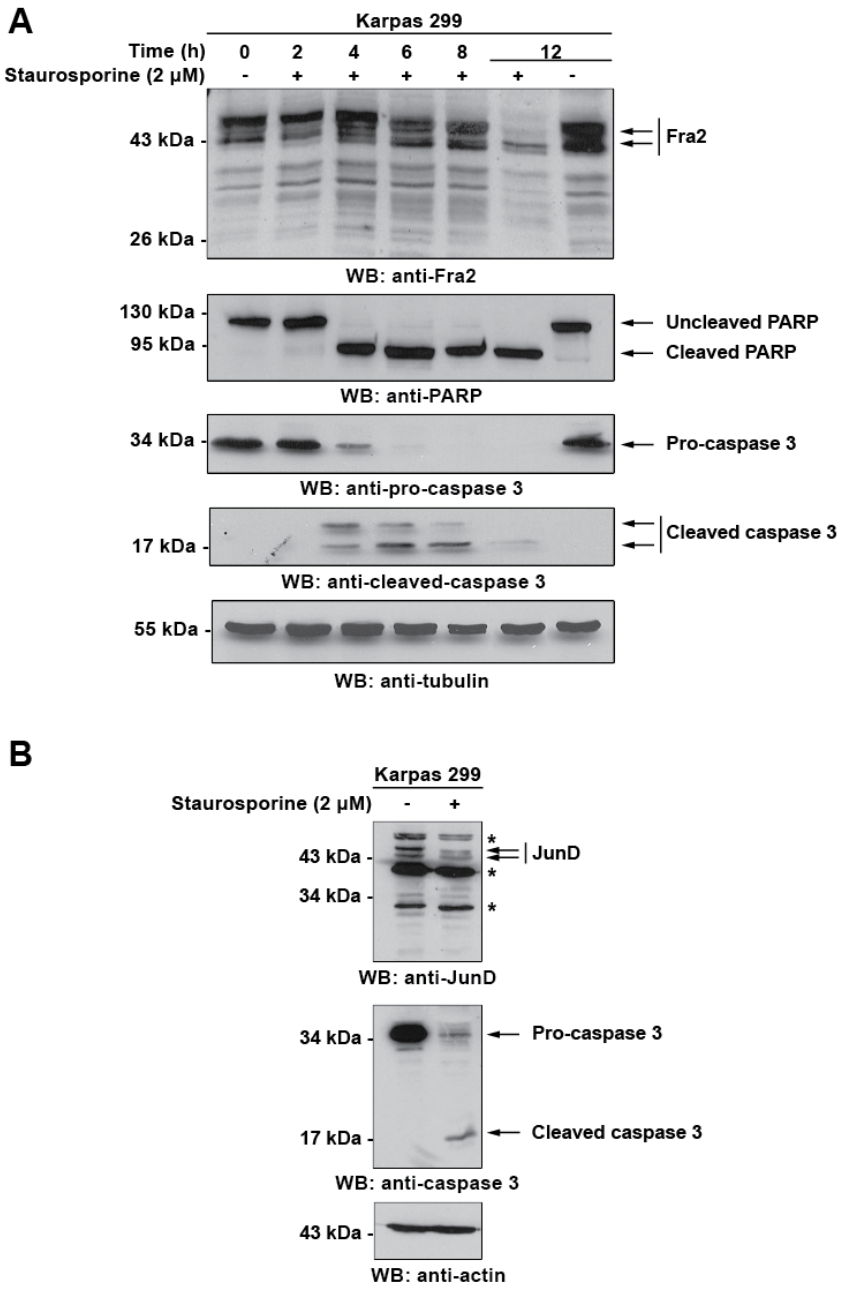

Figure 3.6: The electrophoretic mobility of Fra2 and JunD in lysates of ALK+ ALCL cell lines treated with staurosporine.

Karpas 299 and SUP-M2 cells were untreated or treated with staurosporine. Lysates from these cells were then probed with an anti-Fra2 **(A)** or JunD **(B)** antibody. The efficacy of apoptosis induction was determined by the disappearance of pro-caspase 3, the appearance of cleaved, active caspase 3 and/or PARP cleavage. Asterisks **(*)** indicate non-specific bands detected by the JunD antibody. Anti-tubulin and anti-actin blots are included to demonstrate protein loading. The electrophoretic mobility of molecular weight standards are indicated to the left of blots.

3.1.5: Changes in JunB electrophoretic mobility in other cell types

To determine if the electrophoretic mobility of JunB can be affected in other cells upon the induction of apoptosis, we co-treated two JunB-expressing Hodgkin lymphoma cell lines (KM-H2 and L428) with staurosporine and the tyrosine kinase inhibitor AG17 (Tyrphostin) – a combination which has previously been shown to induce apoptosis in Hodgkin lymphoma cell lines (344). Following treatment with either staurosporine, or staurosporine and AG17 together, the protein levels of both JunB and pro-caspase 3 decreased in KM-H2 cells but not the L428 cells, possibly indicating that more KM-H2 cells were undergoing apoptosis compared to L428 cells (Figure 3.7A). Nevertheless, the ~28 kDa JunB band typically observed in apoptotic Karpas 299 cells was not observed in both Hodgkin lymphoma cell lines (Figure 3.7A). Drug treatment of the SIS EBV-positive T-cell line, which also expresses JunB endogenously, resulted in similar observations. Some apoptosis was observed with drug treatment based on the cleavage of PARP, but no changes in JunB electrophoretic mobility was observed, although JunB protein levels appeared to decrease with staurosporine treatment (Figure 3.7B). The electrophoretic mobility of the JunB doublet also did not appear to change (Figure 3.7B). However, the limited apoptosis induction in the L428 Hodgkin lymphoma cell line likely affected the changes in JunB electrophoretic mobility, and the overall low expression levels of endogenous JunB in the SIS cells likely affected our ability to draw conclusive results from the data. Additionally, the KM-H2 results may also suggest that JunB may not always be cleaved under apoptotic conditions.

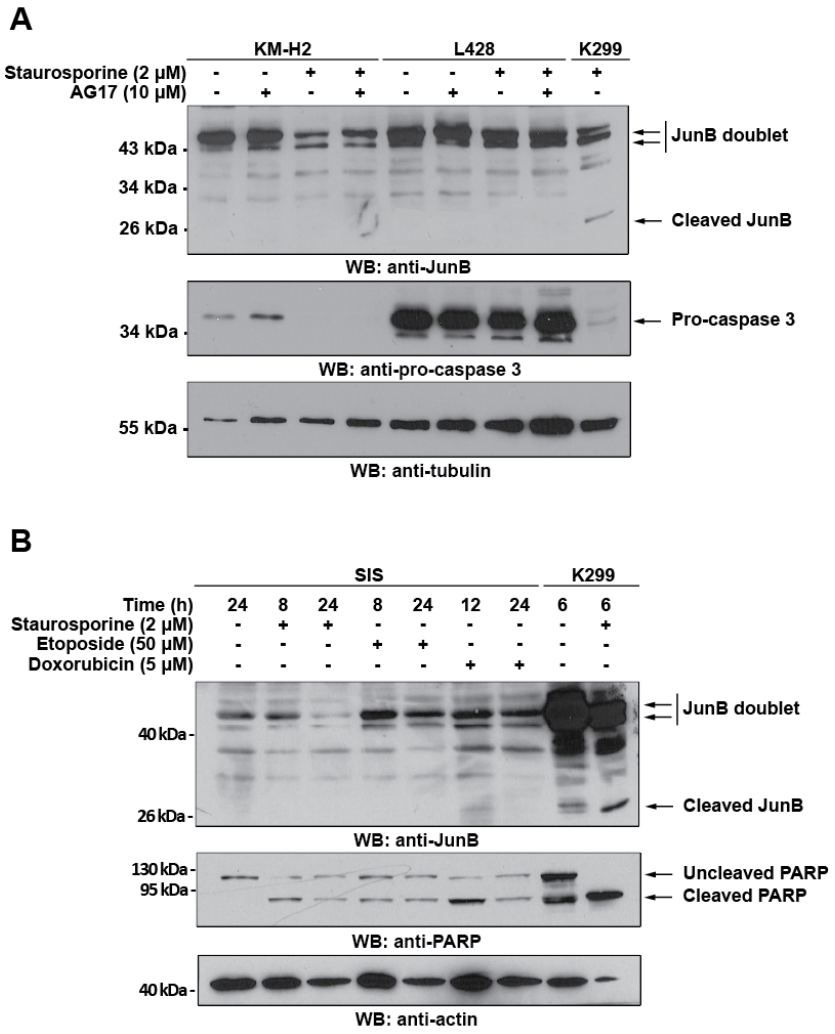

Figure 3.7: Electrophoretic mobility of JunB in drug-treated ALK+ ALCL, Hodgkin lymphoma, and EBV positive T-cell cell lines.

A. The Hodgkin lymphoma cell lines KM-H2, L428, and the ALK+ ALCL cell line Karpas 299 left untreated, treated with staurosporine, treated with AG17, or co-treated with staurosporine and AG17 as indicated, while the **B.** The SIS EBV-containing T-cell line or was either treated with or without staurosporine, etoposide, or doxorubicin for the times indicated, while the Karpas 299 (K299) cell line was treated with or without staurosporine for 6 h. Lysates were then western blotted (WB) with an anti-JunB antibody. The efficacy of apoptosis induction in all panels was determined by the disappearance of pro-caspase 3 or cleavage of PARP. Anti-tubulin or actin blots are included to demonstrate protein loading. The electrophoretic mobility of molecular weight standards are indicated to the left of blots.

To examine whether the electrophoretic mobility of JunB was altered in other apoptotic cells which express little endogenous JunB, we used an N-terminal Myc-tagged wild-type JunB construct. We first investigated whether the Myc-tagged JunB can be induced to undergo electrophoretic mobility changes similar to the endogenous JunB in staurosporine treated Karpas 299 cells (Figure 3.8A). Indeed, expression of the Myc–tagged JunB construct in Karpas 299 cells resulted in the appearance of a doublet band, which despite being shifted in molecular weight from the Myc epitope tag, was very similar to the endogenous JunB doublet in these cells (Figure 3.8A). In staurosporine–treated Karpas 299 cells expressing Myc-JunB, we observed a loss of the Myc-JunB doublet and the appearance of a single band of ~55 kDa which had the same electrophoretic mobility as the lower molecular weight band in the untreated samples (Figure 3.8A). Since the lower molecular weight band was detected by the anti-Myc antibody, it is unlikely that this shift represents a cleavage product of Myc-JunB at aspartic acid 31. We also observed the appearance of a ~24 kDa anti-Myc immunoreactive doublet in Myc-JunB–expressing cells treated with staurosporine (Figure 3.8A). Furthermore, anti-JunB blots of these lysates demonstrated an increase in the amount of the ~28 kDa JunB fragment in the Myc-JunB–expressing cells compared to the vector alone–transfected cells (Figure 3.8A). The simplest interpretation of this latter observation is that increased levels of the ~28kDa fragment in the Myc-JunB expressing cells is due to cleavage of both endogenous and Myc-tagged JunB. Importantly, the electrophoretic mobility shift of Myc-JunB in response to staurosporine treatment was also dependent on caspase activity (Figure 3.8A).

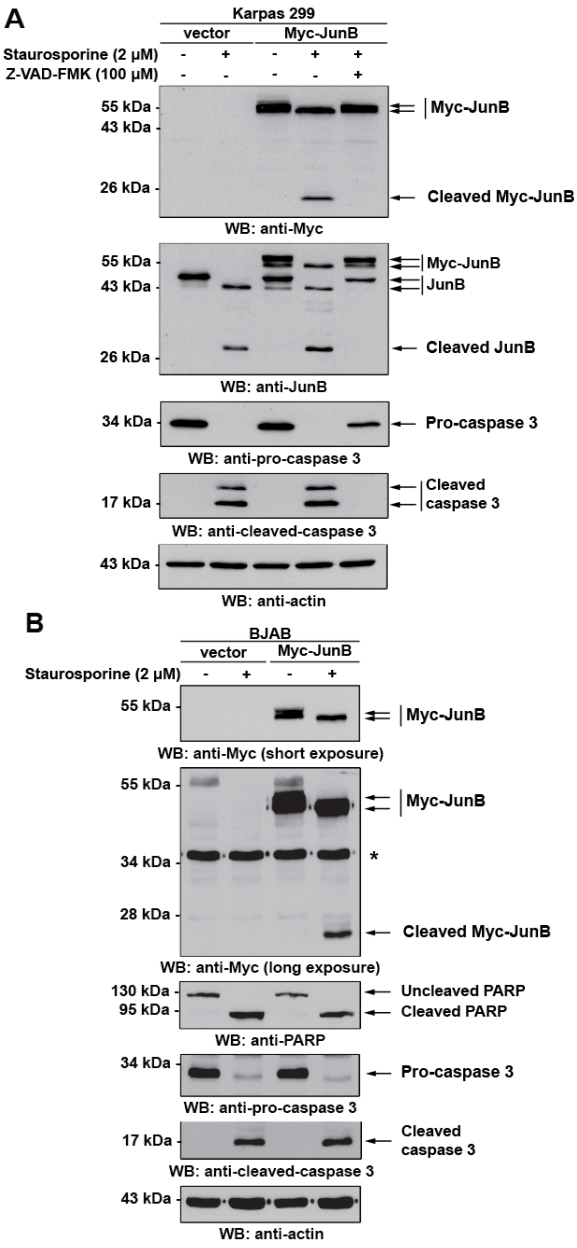

Figure 3.8: The electrophoretic mobility of Myc-tagged JunB is changed in apoptotic ALK+ ALCL and Burkitt lymphoma cell lines.

Karpas 299 **(A)** or BJAB **(B)** cells transfected with either vector alone or a Myc-JunB cDNA construct were left untreated, treated with staurosporine, or treated with staurosporine and Z-VAD-FMK as indicated. Lysates were then western blotted (WB) with an anti-Myc and/or JunB antibody. The band marked by an asterisk **(*)** in B. is a non-specific band. Note: the anti-Myc blots are different exposures of the same membrane. The efficacy of apoptosis induction in all panels was determined by the disappearance of pro-caspase 3 and/or the appearance of cleaved, active caspase 3. In panel B, PARP cleavage also demonstrates the induction of apoptosis and activation of caspases. Anti-actin blots are included to demonstrate protein loading. The electrophoretic mobility of molecular weight standards are indicated to the left of blots.

To examine whether an exogenous Myc-JunB protein could undergo similar changes in electrophoretic mobility following staurosporine treatment, we transfected the BJAB Burkitt lymphoma cell line, a cell line that expresses little to no endogenous JunB, with a myc-tagged JunB protein. Treatment of these cells with staurosporine resulted in a similar collapse of the Myc-JunB doublet and the appearance of the ~24kDa anti-Myc immunoreactive band (Figure 3.8B) as observed in the Myc-JunB expressing Karpas 299 cells. Therefore, the alteration of JunB electrophoretic mobility in response to apoptosis–inducing drugs is not restricted to ALK+ ALCL cell lines.

3.1.6: The D137A mutation protects JunB from cleavage in apoptotic ALK+ ALCL cells

The generation of Myc-JunB constructs allowed us to identify possible cleavage sites. To narrow down the potential cleavage sites, we first performed *in silico* caspase cleavage site prediction using the Cascleave webserver (337), which predicted 3 possible cleavage sites at aspartic acid residues 31, 137, and 145. The size of the lower molecular weight bands observed after anti-JunB (~28kDa) and anti-Myc (~24kDa) immunoblotting of lysates from apoptotic cells (Figure 3.8A), suggested that JunB is cleaved at one or more sites in the middle of the protein, which would be consistent with cleavage at aspartic acid 137 and/or 145 identified by Cascleave (Figure 3.9A).

To investigate whether these residues were cleavage sites, we generated a number of mutant JunB constructs, including constructs where aspartic acid 31 or 137 were mutated to alanine (Myc-JunB D31A, Myc-JunB D137A). Because aspartic acid 145 is immediately preceded by another aspartic acid residue, we mutated both these residues to alanine (Myc-JunB D144A/D145A). We also generated a mutant where all three of the central aspartic acid residues (D137/144/145) were mutated to alanine

(Myc-JunB 3A). In staurosporine–treated Karpas 299 cells we observed a collapse of the JunB doublet with all of these JunB mutant proteins (Figure 3.9B). However, while we observed the ~24kDa Myc cleavage fragment in cells expressing the Myc-JunB D31A and D144A/D145A constructs, we did not observe this band in cells expressing the Myc-JunB D137A or Myc-JunB 3A constructs (Figure 3.9B). These results demonstrate that cleavage of JunB at aspartic acid 137 is responsible for generating the anti-Myc reactive ~24kDa cleavage product.

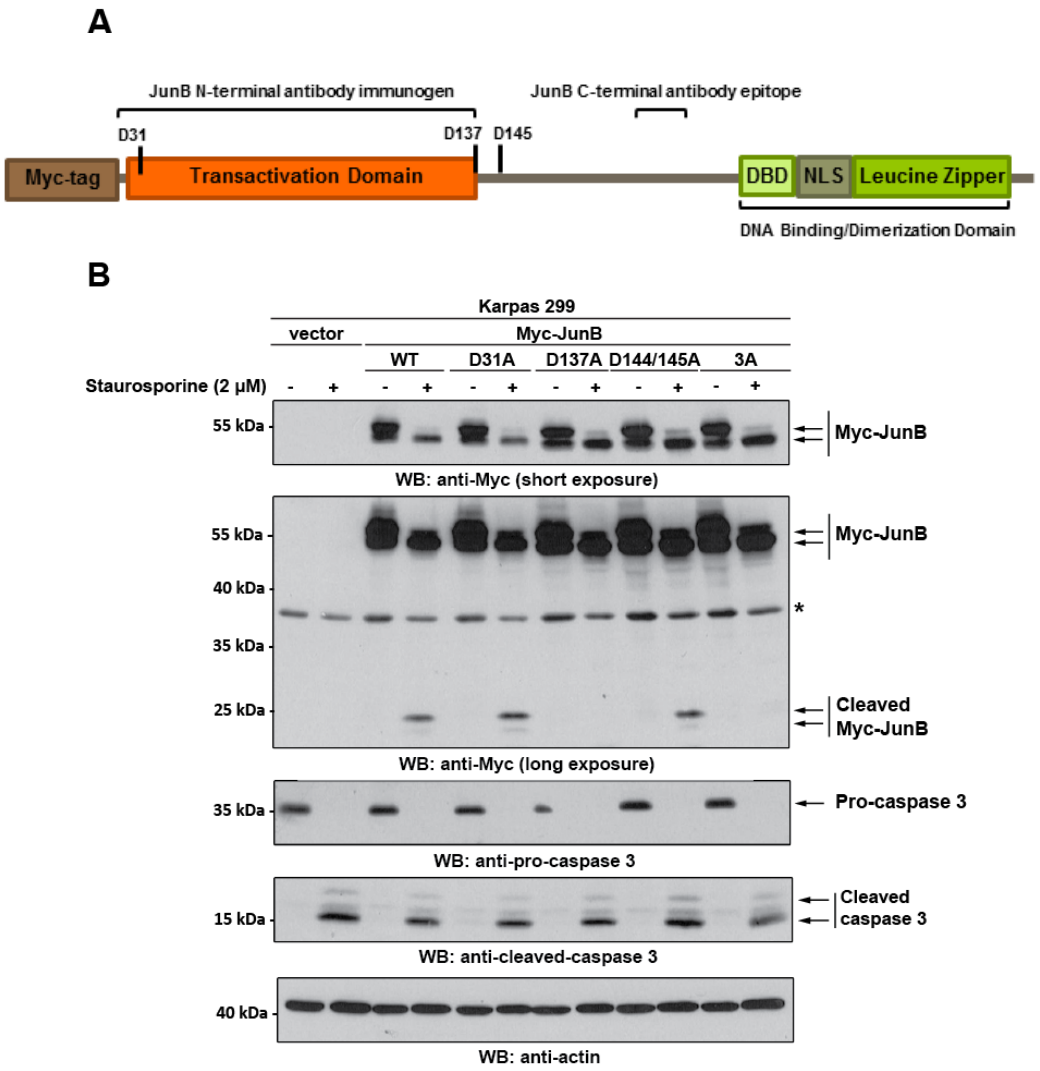

Figure 3.9: Mutation of aspartic acid 137 blocks the appearance of the lower molecular weight JunB cleavage product.

A. Cartoon of JunB showing the location of putative caspase cleavage sites (D31, D137, D145) in JunB, and the approximate locations of the transactivation domain, DNA binding domain, nuclear localization signal (NLS), and dimerization domain (Leucine zipper; Leu. Zipper) are shown. Also indicated is the location of the epitope recognized by the anti-JunB antibodies used for western blotting. **B.** Karpas 299 cells transfected with the indicated constructs were left untreated or treated with staurosporine. Lysates from these cells were then probed with an anti-Myc antibody. Note: the anti-Myc blots are different exposures of the same membrane. The band marked with an asterisk **(*)** is a non-specific band detected by the anti-Myc antibody. The efficacy of apoptosis induction in all panels was determined by the disappearance of pro-caspase 3 and/or the appearance of cleaved, active caspase 3. Anti-actin blots are included to demonstrate protein loading. The electrophoretic mobility of molecular weight standards are indicated to the left of blots.

3.2: CLEAVAGE OF JUNB BY CASPASES

3.2.1: JunB is cleaved directly by caspase 3

Since our time course experiments showed that JunB cleavage roughly correlated with caspase 3 activation (Figure 3.3), we examined whether JunB could be directly cleaved by caspase 3. We set up an in-vitro caspase cleavage assay using in-vitro transcribed/translated Myc-JunB proteins as substrates for recombinant caspase 3. We observed a time–dependent increase in the ~24kDa Myc reactive cleavage product when Myc-JunB protein was incubated with caspase 3 (Figure 3.10A). The electrophoretic mobility of the higher molecular weight Myc-JunB immunoreactive band generated in the in-vitro transcription/translation reaction was unchanged by caspase treatment, and had the same electrophoretic mobility as the lower molecular weight protein in the JunB doublet and the ~40kDa band evident after staurosporine treatment (Fig 3.10A).

3.2.2: The D137A mutation prevents JunB cleavage by recombinant caspase 3

We also investigated whether purified caspase 3 could cleave the aspartic acid mutant JunB constructs in the in-vitro cleavage assay. Consistent with our results in Karpas 299 cells (Figure 3.9B), we found that Myc-JunB D144A/D145A was cleaved by recombinant caspase 3, but the Myc-JunB D137A and Myc-JunB 3A constructs were not (Figure 3.10B). Therefore, these findings demonstrate that JunB is directly cleaved by caspase 3, and confirm our previous observations that aspartic acid 137 is the site of cleavage.

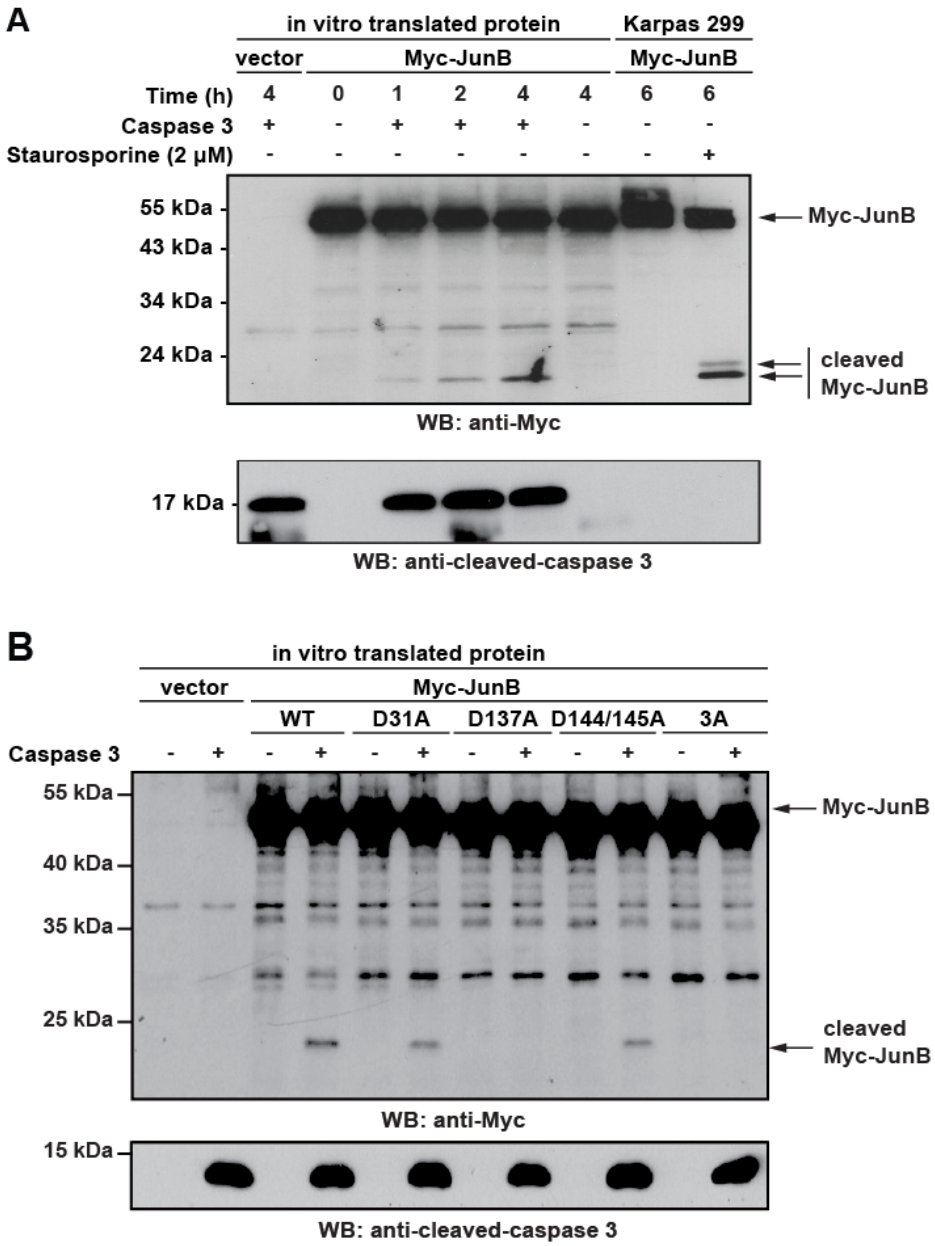

Figure 3.10: In-vitro cleavage of JunB at aspartic acid 137 by caspase 3.

A. In-vitro transcribed and translated Myc-JunB was incubated with (+) or without (-) 134 or 268 pM of purified, active recombinant caspase 3 for the indicated times. Reactions were then western blotted (WB) with an anti-Myc or anti-cleaved caspase 3 antibody. Lysates from Myc-JunB–expressing Karpas 299 cells were included to compare the electrophoretic mobility of cleaved Myc-JunB in cells with that in the in-vitro cleavage assay. **B.** The indicated in-vitro transcribed and translated Myc-JunB proteins were incubated with or without 256ng of purified, active recombinant caspase 3 for 4 h. Reactions were then western blotted with an anti-Myc or anti-cleaved caspase 3 antibody. The electrophoretic mobility of molecular weight standards are indicated to the left of blots.

3.2.3: In-vitro cleavage of JunB by other caspases

Other caspases are known to play important roles in processes other than apoptosis, and we were interested in whether JunB could be directly cleaved by other caspases. Similar to the caspase 3 cleavage experiments, we set up an additional in-vitro caspase cleavage assay using in-vitro transcribed/translated Myc-JunB proteins as substrates for recombinant caspases 1, 6, and 8. We observed the appearance of the ~24 kDa Myc reactive cleavage product matching the expected size of the JunB cleavage products when Myc-JunB protein was incubated with recombinant active caspases following the incubation with caspases (Figure 3.11). Additionally, we did not observe the ~24 kDa cleavage product when the cells were transfected with the D137A mutant (Figure 3.11), demonstrating that these other caspases are also cleaving Myc-JunB at the aspartic acid 137 residue. Although we observed a number of additional cleavage products and non-specific bands in these experiments (Figure 3.11), none of these bands were observed in the lysate of apoptotic ALK+ ALCL cells. These bands may be an artifact of the in vitro cleavage assay and may not be relevant in apoptosis, although it may be relevant in a non-apoptotic context. Therefore, these findings demonstrate that JunB can be directly cleaved at the aspartic acid 137 residue by a number of different caspases.

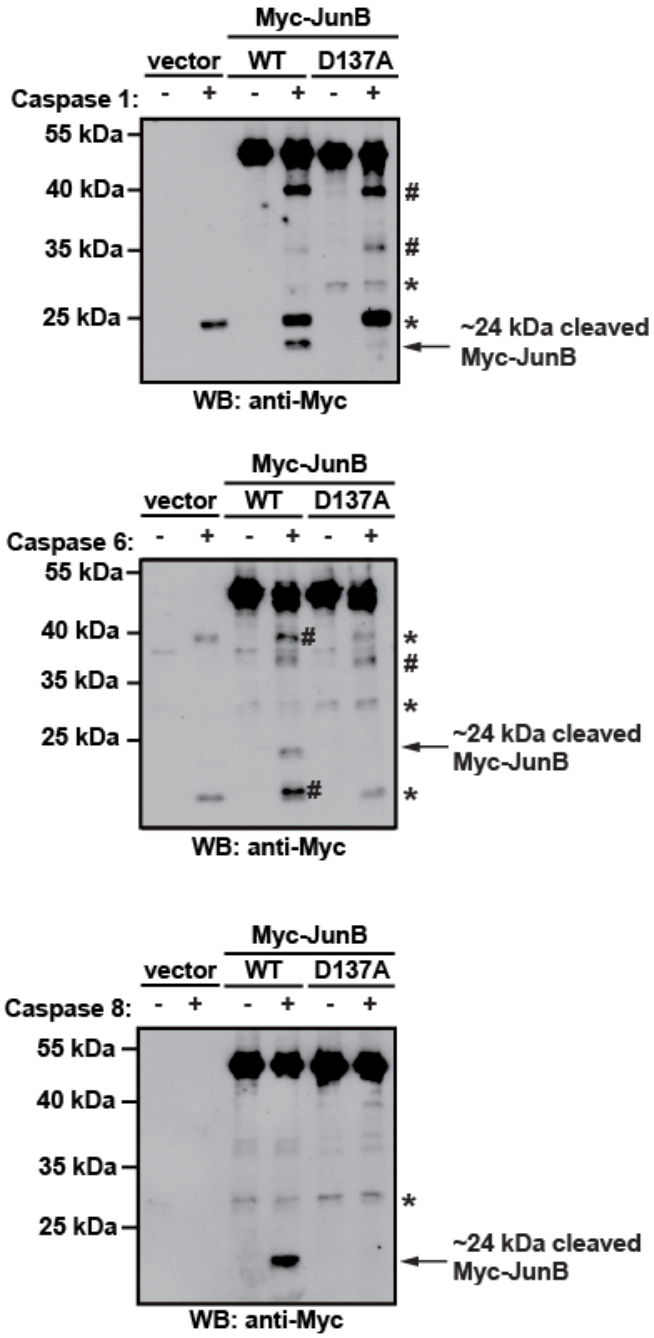

Figure 3.11: In-vitro cleavage of JunB by other caspases.

2U of Purified, active recombinant caspases 1, 6, and 8 was incubated with (+) or without (-) in-vitro transcribed and translated wild-type (WT) or mutant (D137A) Myc-JunB for 4 h. Reactions were then western blotted (WB) with an anti-Myc antibody. The ~24 kDa cleaved Myc-JunB bands are indicated by the arrow in the anti-Myc blot. Non-specific bands **(*)** and other potential cleavage products **(#)** are also indicated. The electrophoretic mobility of molecular weight standards are indicated to the left of blots.

3.2.4: Sequence analysis of the JunB cleavage site

Having identified the caspase cleavage site of JunB, we performed sequence analyses using bioinformatics to determine whether the cleavage site was evolutionarily conserved in other Jun family proteins, and in JunB proteins of other animals. In the human Jun family members JunB, c-Jun and JunD, the sequence around the cleavage site is well conserved, however, the aspartic residue present in JunB is a glutamic acid residue in both c-Jun and JunD (Figure 3.12A), possibly explaining our observation that they were not cleaved in apoptotic ALK+ ALCL cells (Figure 3.6 and Figure 3.7), although glutamic acid residues are sometimes cleaved by caspases in rare situations (274,275).

The JunB transcription factor is found in all vertebrates, and the protein sequence is well conserved in non-human JunB proteins (345), ranging from a sequence identity of approximately 50% in fish and amphibian species to 99% sequence identity in primates. However, the protein sequence adjacent to the cleavage site is very well conserved (Figure 3.12B), regardless of overall JunB sequence identity. The aspartic residue of the JunB cleavage site is conserved in mammalian, avian, reptilian, amphibian and most fish species (Figure 3.12B). This observation may suggest a potentially important role of this site, which may account for its conservation across different species.

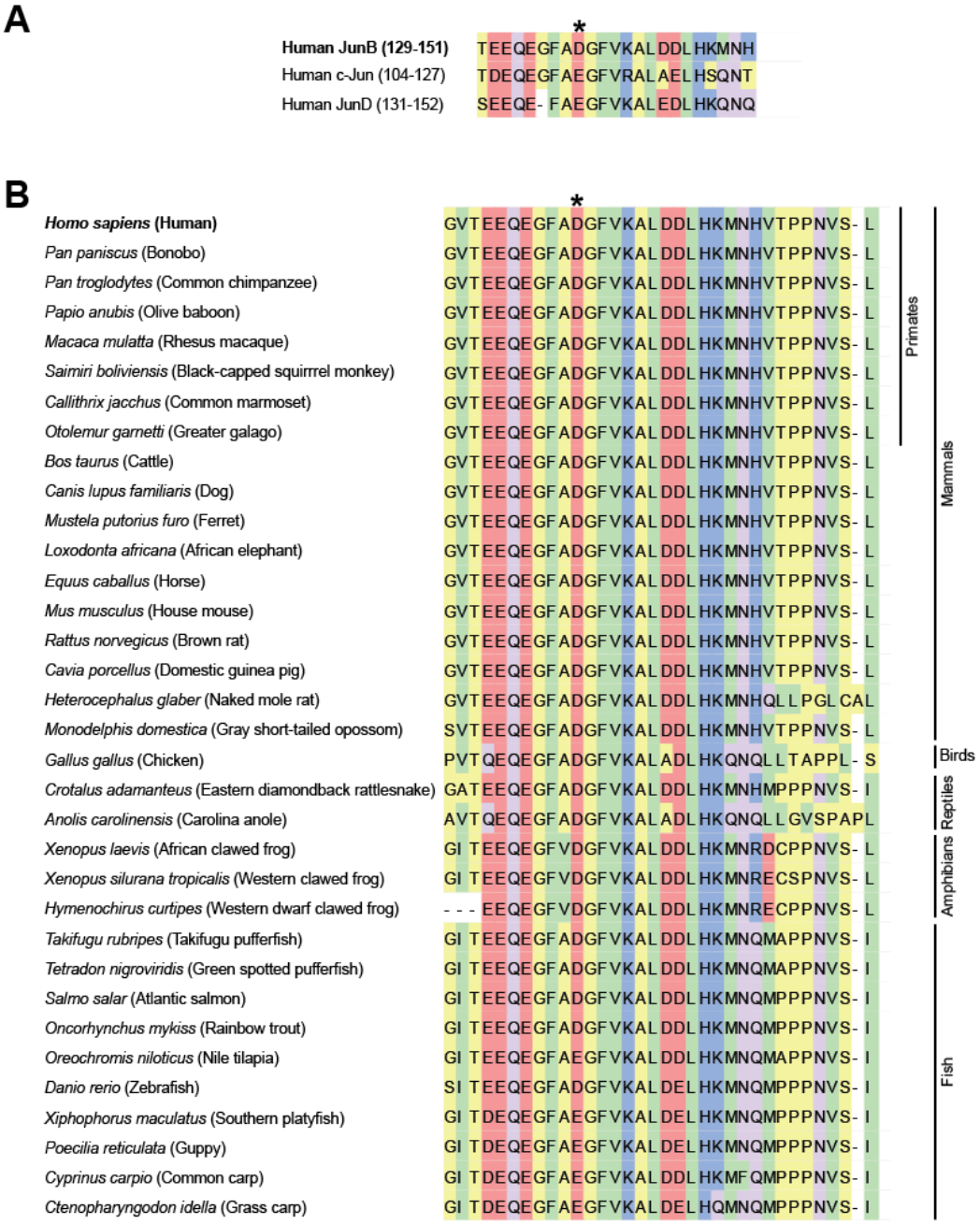

Figure 3.12: Conservation of the JunB cleavage site.

A. Amino acid sequence alignment of the JunB caspase cleavage site of human Jun-family members, **(*)** indicates the D137 residue of human JunB. **B.** Amino acid sequence alignment of select sequences near the JunB caspase cleavage site of human and vertebrates. Sequences were collected using the NCBI protein database, **(*)** indicates the D137 residue of human JunB. Protein sequences were aligned using the MAFFT alignment tool, and the sequence alignment data prepared using Pfaat software (332,333).

3.3: DEPHOSPHORYLATION OF JUNB IN APOPTOTIC ALK+ ALCL CELL LINES

3.3.1: The shift in the electrophoretic mobility of the JunB doublet following dephosphorylation is similar to the shift of the JunB doublet in apoptotic ALK+ ALCL cell lines

Our results do not support the idea that the change in electrophoretic mobility of the ~43 kDa JunB immunoreactive band observed in staurosporine- or doxorubicin-treated cells is due to caspase–mediated cleavage of JunB, as we did not observe differences in the electrophoretic mobility of the JunB doublet in any of the Myc-JunB site mutants following staurosporine treatment (Figure 3.9). Therefore, we examined whether this alteration in JunB electrophoretic mobility could be due to a change in another post-translational modification. Western blotting of lysates from untreated or staurosporine–treated Karpas 299 and SUP-M2 cells with an antibody that recognizes phosphorylated serine 259 (S259) of JunB, demonstrated that JunB is phosphorylated on this site in untreated cells but not in staurosporine–treated cells (Figure 3.13A). The phosphorylation of JunB at this residue appears to be restricted to the higher molecular protein in the JunB doublet in the untreated samples, and phosphorylation of JunB at this site could be partially restored by co-treatment of cells with Z-VAD-FMK (Figure 3.13A).

3.3.2: Phosphorylation of JunB in ALK+ ALCL cell lines

JunB is phosphorylated on a number of serine and threonine residues (132,141-143,145,346,347), and phosphorylation regulates JunB levels and transcriptional activity (132,141-143,145,346).To further investigate whether the collapse of the JunB doublet represents dephosphorylation of JunB, we immunoprecipitated JunB from untreated Karpas 299 or SUP-M2 cell lysates, and treated the immunoprecipitates with alkaline

phosphatase. Western blotting these immunoprecipitates with an anti-JunB antibody demonstrated that phosphatase treatment of JunB collapses the doublet to the lower molecular weight form, and also results in the decreased phosphorylation of JunB on S259 (Figure 3.13B and C).

The shift in the electrophoretic mobility of the JunB doublet following dephosphorylation was similar to the shift observed in the doublet after staurosporine treatment (Figure 3.14A). Furthermore, the immunoprecipitation of JunB from lysates of staurosporine–treated cells followed by phosphatase treatment did not result in a further shift in JunB electrophoretic mobility over staurosporine treatment alone (Figure 3.14B), suggesting that the changes in JunB electrophoretic mobility is likely due to dephosphorylation. Taken together, these findings argue that the higher molecular weight JunB species observed in apoptotic ALK+ ALCL cell lines is a dephosphorylated JunB species, and that this dephosphorylation is caspase dependent.

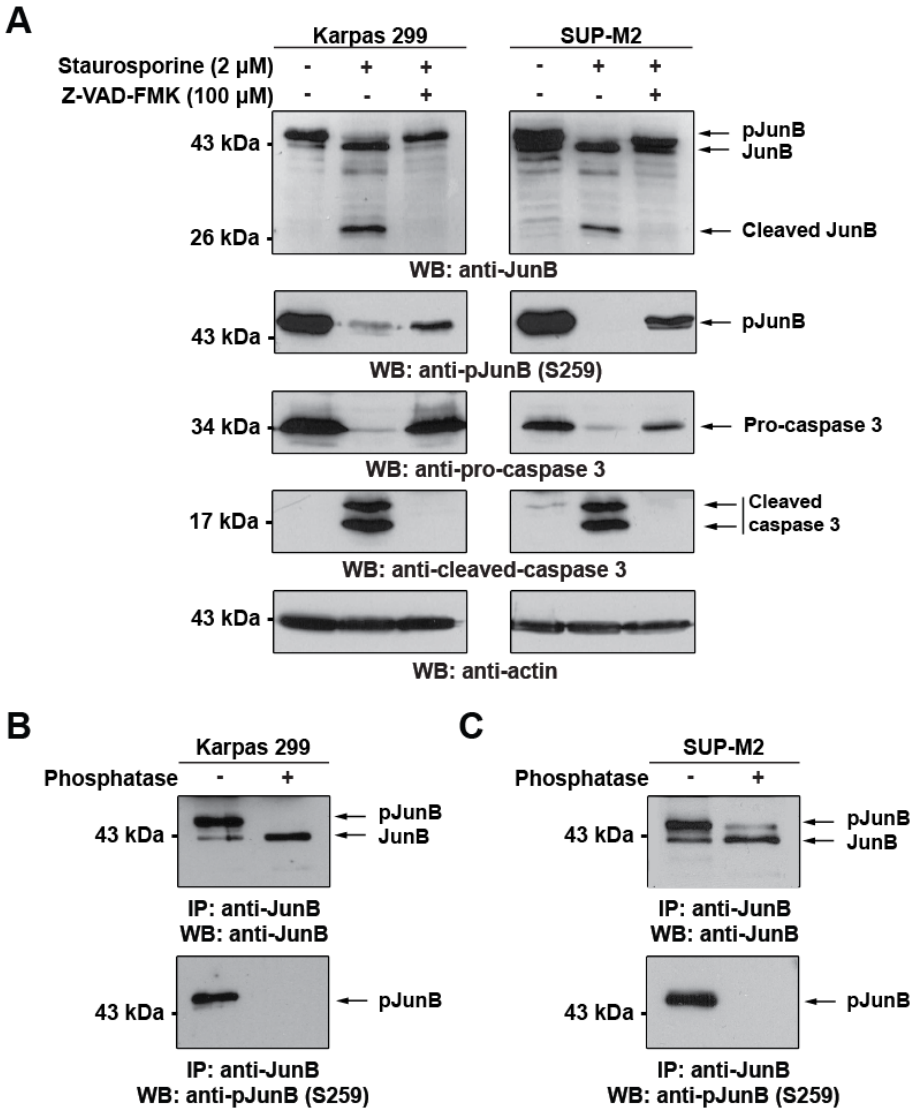

Figure 3.13: JunB is phosphorylated in ALK+ ALCL cell lines, and phosphorylated JunB levels are reduced in apoptotic ALK+ ALCL cells.

A. Lysates from Karpas 299 (left) or SUP-M2 (right) cells either untreated, treated with staurosporine, or treated with staurosporine and Z-VAD-FMK were western blotted (WB) with antibodies that recognize JunB when phosphorylated at serine 259 (anti-pJunB (S259)) or total JunB (anti-JunB). Anti-pro-caspase 3 and anti-cleaved caspase 3 blots demonstrate the induction of apoptosis, whereas the anti-actin blot demonstrates protein loading. Lysates from Karpas 299 **(B)** or SUP-M2 **(C)** cells were immunoprecipitated (IP) with an anti-JunB antibody, and immunoprecipitates were either left untreated or treated with alkaline phosphatase. Immunoprecipitates were then western blotted with an anti-JunB or anti-pJunB S259 antibody. The electrophoretic mobility of molecular weight standards are indicated to the sides of blots.

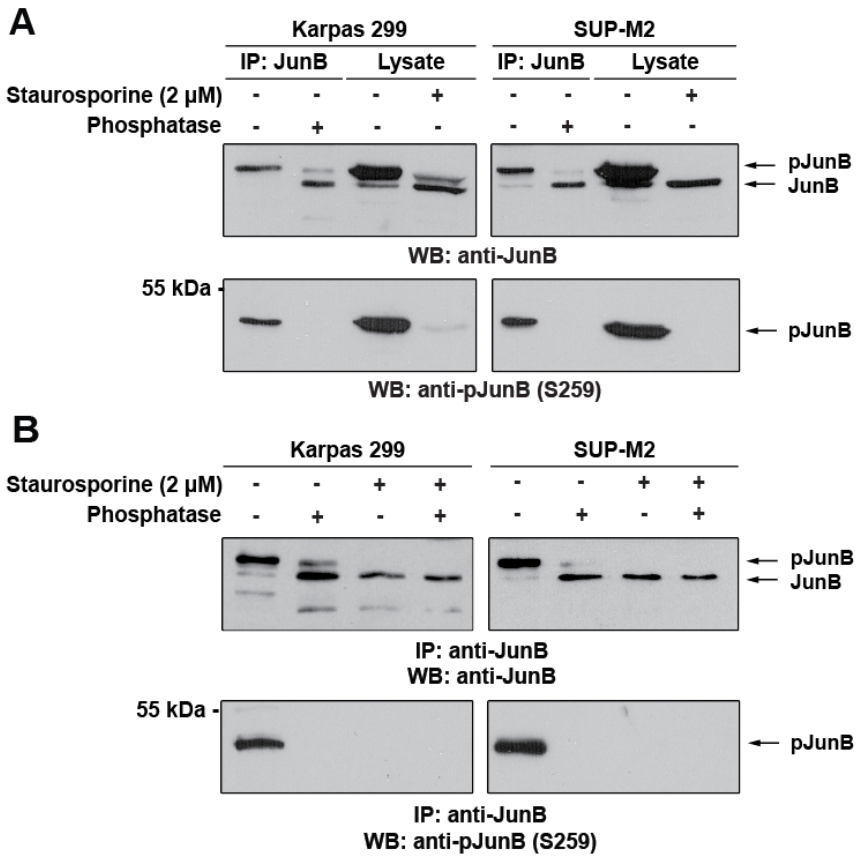

Figure 3.14: The change of JunB electrophoretic mobility in apoptotic cells is similar to the dephosphorylation of JunB.

A. Karpas 299 (left) or SUP-M2 (right) lysates were immunoprecipitated (IP) with an anti-JunB antibody, and immunoprecipitates were either left untreated or treated with alkaline phosphatase. Immunoprecipitates were then western blotted with an anti-JunB or anti-pJunB S259 antibody. Cell lysates from untreated or staurosporine–treated cells were also western blotted on the same membranes. **B.** Lysates from untreated (-) or staurosporine–treated (+) cells were immunoprecipitated, treated with (+) or without (-) phosphatase, and western blotted as described in **A**. The electrophoretic mobility of molecular weight standards are indicated to the sides of blots.

3.4: BIOLOGICAL ROLES OF THE JUNB CLEAVAGE FRAGMENTS

3.4.1: The C-terminal JunB cleavage product inhibits AP-1 dependent transcription

The cleavage of JunB at aspartic acid 137 separates the N-terminal transactivation domain from the C-terminal dimerization and DNA binding domains (see Figure 3.9A). Thus, while this cleavage would be predicted to inactivate the protein, the cleavage products may retain some biological activity. For example, the C-terminal fragment may be able to interfere with the ability of full-length JunB or other AP-1 family proteins from binding DNA (348,349). Previous studies conducted by the Birrer group on c-Jun function used a dominant-negative mutant that is similar to the C-terminal JunB cleavage fragment we have identified. The dominant negative c-Jun mutant, named TAM67, was made by deleting the N-terminal transactivation domain (amino acids 3-122) of c-Jun (348). The His-122 residue of c-Jun is analogous to the His-147 residue of JunB, and as such the TAM67 mutant is quite similar to the JunB C-terminal fragment (Δ2-137) structurally (Figure 3.15).

To examine whether the C-terminal JunB cleavage product affected AP-1–dependent transcription, we examined its ability to regulate transcription from an AP-1–responsive luciferase reporter construct. We found that expression of full-length JunB in Karpas 299 cells resulted in an approximate 2.5-fold increase in luciferase activity compared to vector alone–transfected cells (Figure 3.16). In cells transfected with the N-terminal cleavage fragment, there was no significant difference in luciferase activity over cells transfected with vector alone; however, in cells transfected with the C-terminal JunB fragment, luciferase activity was significantly reduced compared to vector alone–transfected cells (Figure 3.16).

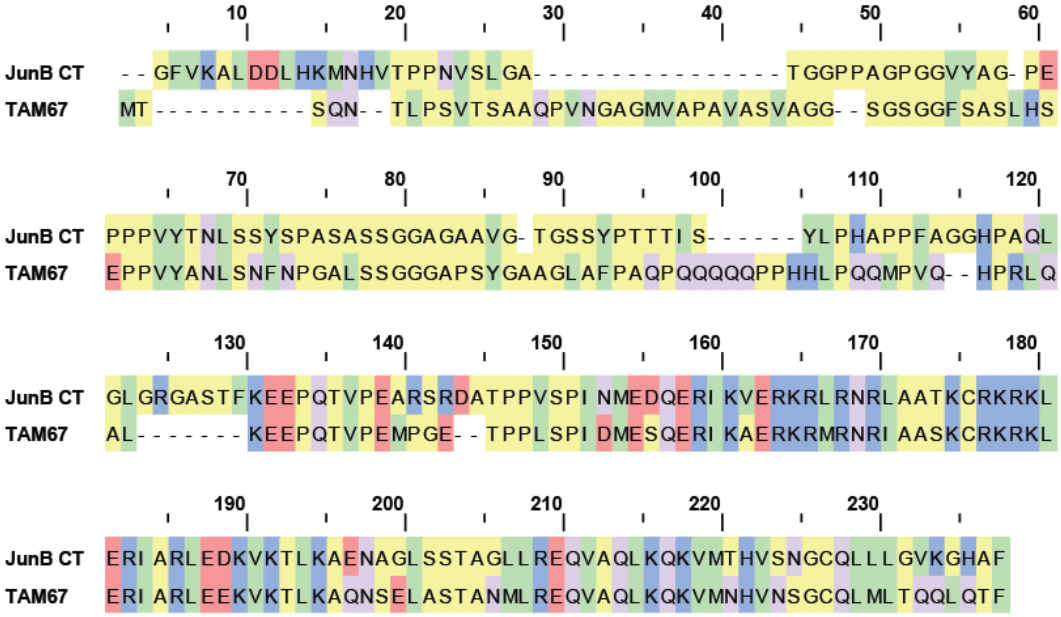

Figure 3.15: Sequence alignment of the JunB C-terminal cleavage fragment and the c-Jun TAM67 mutant.

Amino acid sequence alignment of the TAM67 c-Jun (Δ3-122) truncation mutant and the JunB C-terminal cleavage fragment (AA138-347). Sequences were collected using the NCBI protein database, and protein sequences were aligned using the MAFFT alignment tool, and the sequence alignment data prepared using Pfaat software (332,333).

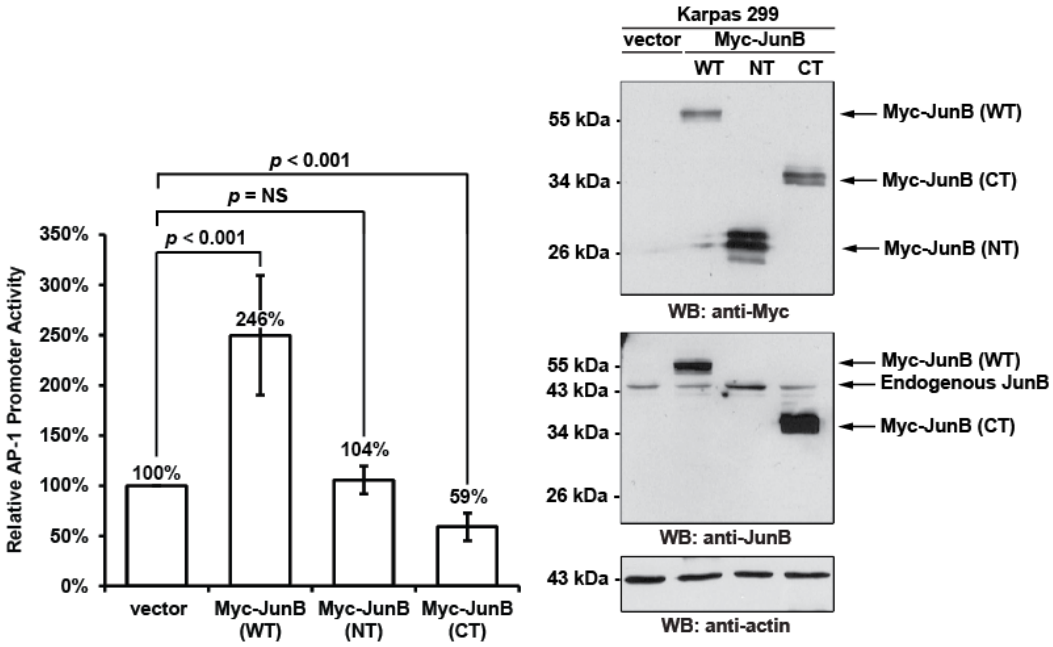

Figure 3.16: The C-terminal JunB cleavage fragment inhibits AP-1–dependent luciferase activity.

Karpas 299 cells were transfected with 5 µg of vector alone, or cDNAs encoding for Myc-tagged JunB (WT), Myc-tagged N-terminal JunB cleavage fragment (NT), or Myc-tagged C-terminal JunB cleavage fragment (CT) along with an AP-1 firefly luciferase reporter construct and a constitutively expressed *Renilla* luciferase vector. Cells were lysed and luciferase activity was measured as described in the Experimental Procedures. The results shown represent the mean and standard deviation of twelve independent experiments. *p* values were calculated by performing paired, one-tailed *t* tests. NS indicates no significant difference. The anti-Myc western blot (WB; to the right) indicates the expression of the respective Myc-tagged constructs (anti-Myc blot), whereas the anti-JunB blot illustrates the level of the over-expressed protein relative to endogenous JunB. Note: the epitope recognized by the anti-JunB antibody is not present in the N-terminal JunB protein. Anti-Myc western blots are included to illustrate the expression level of the Myc-JunB proteins, and anti-actin western blots are included to demonstrate protein loading. The electrophoretic mobility of molecular weight standards are indicated to the left of western blots.

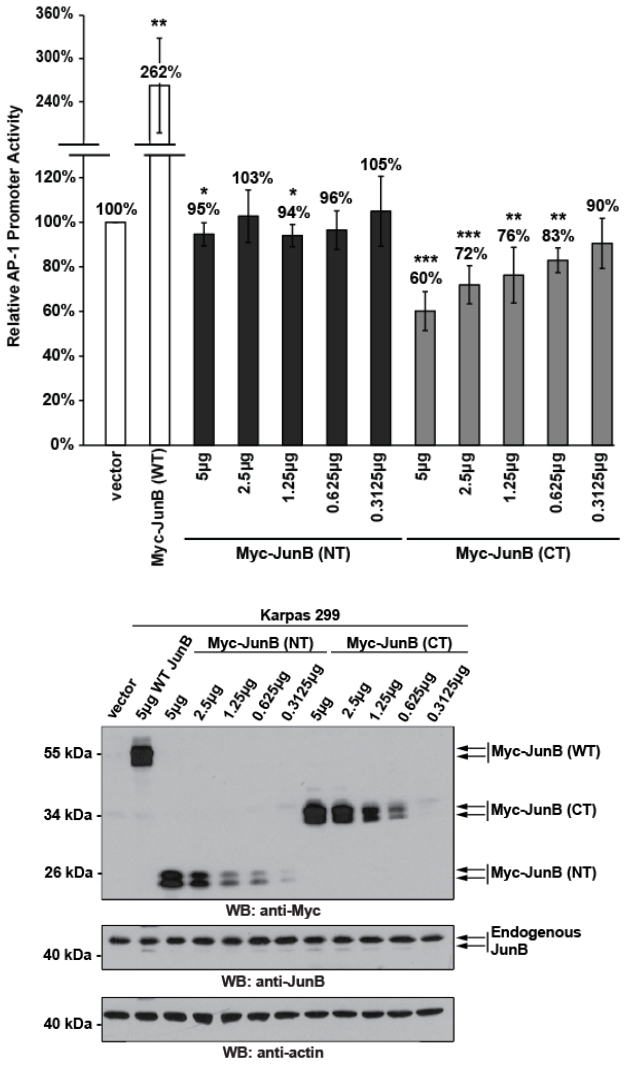

Figure 3.17: The C-terminal JunB cleavage fragment inhibits AP-1–dependent luciferase activity.

Karpas 299 cells were transfected with 5 µg of vector alone, or cDNAs encoding for Myc-tagged JunB (WT), Myc-tagged N-terminal JunB cleavage fragment (NT), or Myc-tagged C-terminal JunB cleavage fragment (CT) along with an AP-1 firefly luciferase reporter construct and a constitutively expressed *Renilla* luciferase vector. Empty vector was added to some samples to ensure equal amounts of transfected DNA in all samples. Cells were lysed and luciferase activity was measured as described in the Experimental Procedures. The results shown represent the mean and standard deviation of five independent experiments. *p* values were calculated by performing paired, one-tailed *t* tests (* $p < 0.05$; ** $p < 0.01$, *** $p < 0.001$). Anti-Myc western blots are included to show the expression level of the Myc-JunB proteins. Anti-Myc western blots are included to illustrate the expression level of the Myc-JunB proteins, and anti-actin western blots are included to demonstrate protein loading. The electrophoretic mobility of molecular weight standards are indicated to the left of western blots.

We further found that the C-terminal JunB fragment functioned as a dose–dependent inhibitor of AP-1 transcriptional activity in Karpas 299 cells, whereas in these same experiments we found that the N-terminal fragment had a minor effect on AP-1 luciferase activity at two points where the N-terminal fragment was expressed at high levels (Figure 3.17). Similar to the full length Myc-JunB, we also observed that the N- and C-terminal fragments can appear as a doublet (see western blot in Figure 3.17), possibly due to the phosphorylation of these proteins.

To determine if the C-terminal JunB fragment can also inhibit AP-1 transcription in a non-ALK+ ALCL cell line, we performed the same luciferase assay as Figure 3.16 in the DG75 Burkitt lymphoma cell line, a cell line that expresses low levels of endogenous JunB. Although the overexpression of full-length Myc-JunB was able to increase the AP-1 luciferase activity to a greater extent than observed in the ALK+ ALCL cell line (Figure 3.18), we found that the C-terminal fragment inhibited AP-1 luciferase activity in DG75 cells in a similar manner as in the Karpas 299 cells (Figure 3.18). Taken together, the results from both the Karpas 299 and DG75 cell lines demonstrate that neither of the JunB cleavage products is able to promote transcription from an AP-1 reporter, and the C-terminal fragment can inhibit AP-1–dependent transcription.

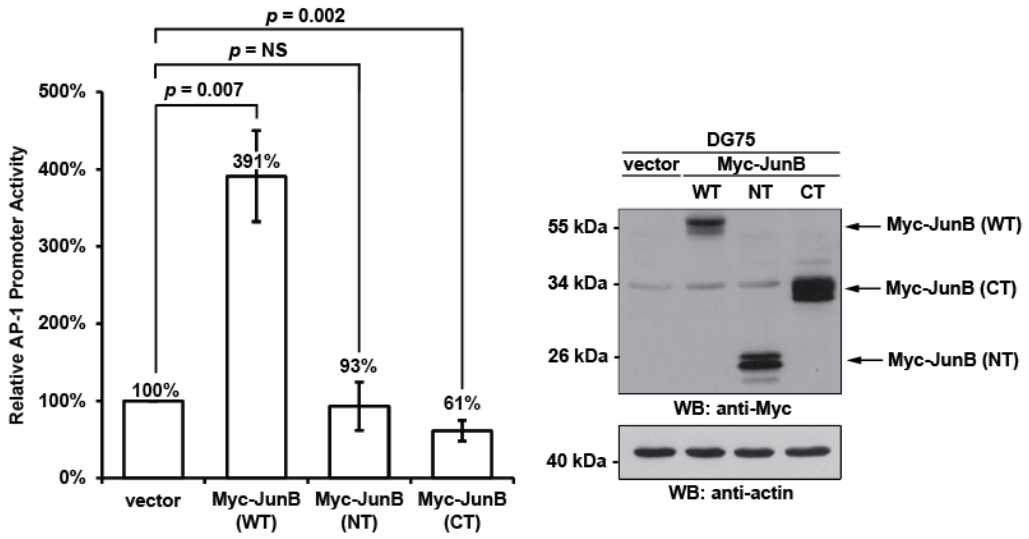

Figure 3.18: The C-terminal JunB cleavage fragment inhibits AP-1–dependent luciferase activity in DG75 cells.

DG75 B cells were transfected with 5 µg of vector alone, or cDNAs encoding for Myc-tagged JunB (WT), Myc-tagged N-terminal JunB cleavage fragment (NT), or Myc-tagged C-terminal JunB cleavage fragment (CT) along with an AP-1 firefly luciferase reporter construct and a constitutively expressed *Renilla* luciferase vector. Cells were lysed and luciferase activity was measured as described in the Experimental Procedures. The results shown represent the mean and standard deviation of three independent experiments. *p* values were calculated by performing paired, one-tailed *t* tests. NS indicates no significance difference. Anti-Myc western blots are included to illustrate the expression level of the Myc-JunB proteins, and anti-actin western blots are included to demonstrate protein loading. The electrophoretic mobility of molecular weight standards are indicated to the left of western blots.

3.4.2: Subcellular localization of the JunB cleavage fragments

We next explored the mechanism by which the C-terminal fragment could be inhibiting AP-1–dependent transcription. We postulated that because this fragment contains the dimerization and DNA binding domains, but lacks the transcriptional activation domain, it may bind AP-1 DNA binding sites as a homodimer or a transcriptionally inactive/impaired heterodimer, and prevent transcriptionally competent AP-1 dimers from binding. To test these possibilities, we first examined whether the C-terminal fragment was present in the nucleus. Nuclear and cytoplasmic fractionation experiments demonstrated that Myc-JunB was predominantly found in the nuclear fraction (Figure 3.19). The C-terminal fragment was also enriched in the nuclear fraction likely due to the fact that this fragment possesses the JunB nuclear localization signal (Figure 3.9A). In contrast, the N-terminal fragment was exclusively found in the cytoplasmic fraction.

3.4.3: Wild-type JunB and the C-terminal JunB fragment bind other AP-1 family transcription factors.

Because AP-1 transcription factors form dimers with other AP-1 proteins to promote transcription, we examined whether the C-terminal fragment could associate with other AP-1 family proteins. Co-immunoprecipitation experiments using an anti-Myc antibody demonstrated that full-length JunB and the C-terminal fragment, but not the N-terminal fragment, could co-precipitate with endogenous c-Fos and Fra2 in Karpas 299 cells (Figure 3.20). Moreover, performing the reverse co-immunoprecipitation experiments using anti-c-Fos or anti-Fra2 antibodies also co-precipitated the full length and C-terminal JunB, but not the N-terminal fragment (Figure 3.21A and B). Thus, the C-terminal JunB cleavage fragment retains its ability to dimerize with AP-1 family proteins.

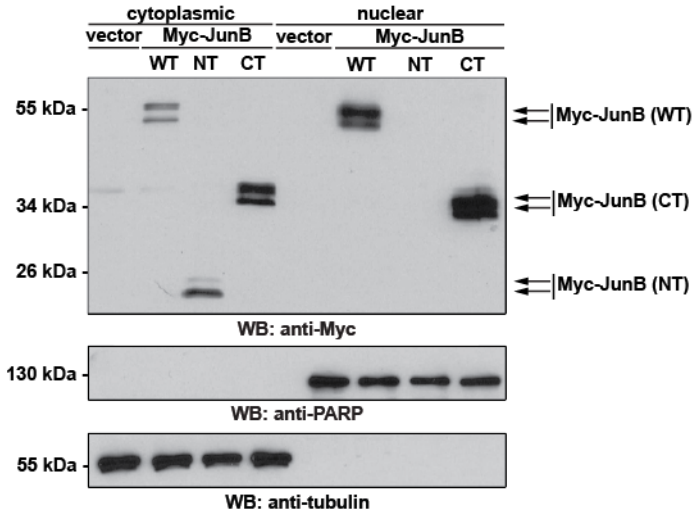

Figure 3.19: Subcellular localization of wild-type JunB and JunB truncation mutants.

Nuclear and cytoplasmic fractions of Karpas 299 cells expressing vector alone, Myc-JunB, Myc-JunB N-terminal fragment (NT), or Myc-JunB C-terminal fragment (CT) were western blotted (WB) with an anti-Myc antibody. Anti-PARP and anti-tubulin blots were performed to validate the fractionation of the nuclear and cytoplasmic fractions, respectively. The electrophoretic mobility of molecular weight standards are indicated to the left of western blots.

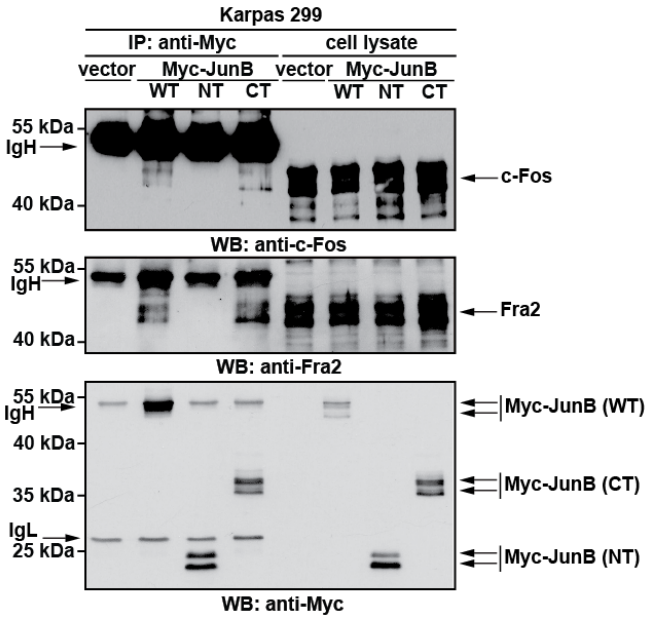

Figure 3.20: Wild-type JunB and the C-terminal JunB fragment interacts with the c-Fos and Fra2 transcription factors.

Karpas 299 cells were transfected with 20 µg of vector alone, or cDNAs encoding for Myc-tagged JunB (WT), Myc-tagged N-terminal JunB cleavage fragment (NT), or Myc-tagged C-terminal JunB cleavage fragment (CT). Cells were lysed after 24 h and lysates were immunoprecipitated (IP) with an anti-Myc antibody, and western blotted with an anti-c-Fos, Fra2 or Myc antibody. Note: IgH and IgL indicate the location of the immunoglobulin heavy and light chains respectively. Whole-cell lysates were also western blotted to illustrate the expression level of the Myc-JunB proteins. The electrophoretic mobility of molecular weight standards are indicated to the sides of blots.

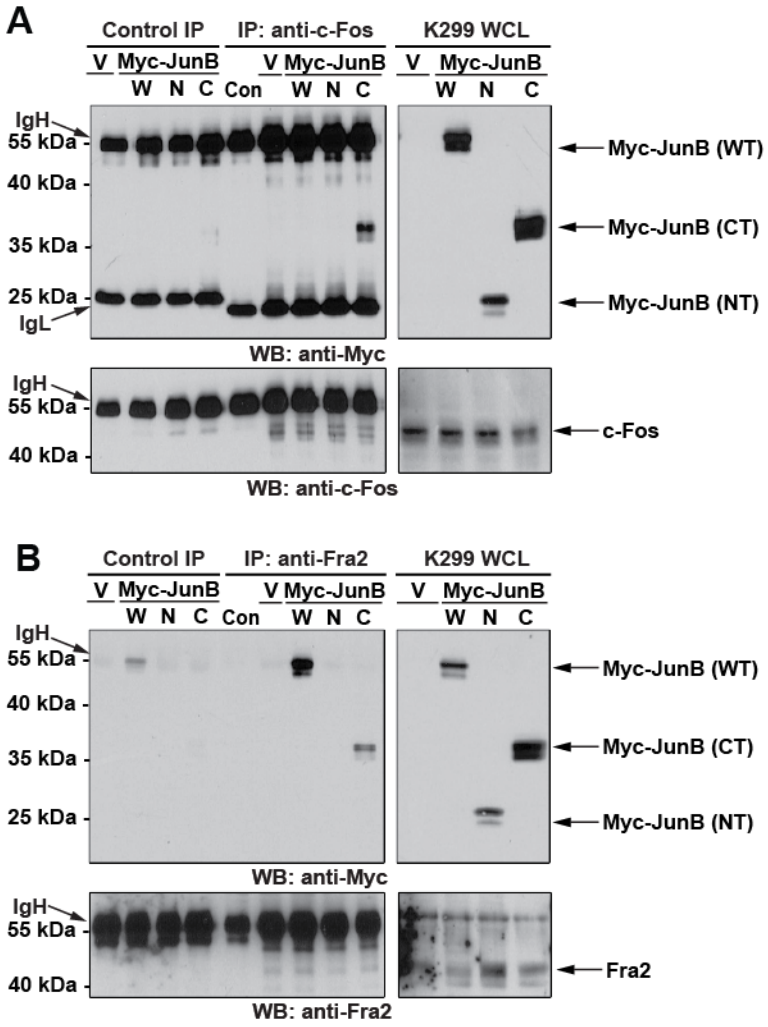

Figure 3.21: Wild-type JunB and the C-terminal JunB fragment interacts with the c-Fos and Fra2 transcription factors.

A. Karpas 299 cells were transfected with 20 µg of vector alone (V), or cDNAs encoding for Myc-tagged JunB (WT), Myc-tagged N-terminal JunB cleavage fragment (NT), or Myc-tagged C-terminal JunB cleavage fragment (CT). Cells were lysed after 24 h and lysates were immunoprecipitated (IP) with an anti-c-Fos antibody, and western blotted with an anti-c-Fos or Myc antibody. A control IP without lysate was also performed. Note: IgH and IgL indicate the location of the immunoglobulin heavy and light chains respectively. Whole-cell lysates of transfected cells were also western blotted to illustrate the expression level of the Myc-JunB proteins. The electrophoretic mobility of molecular weight standards are indicated to the sides of blots.

3.4.4: The C-terminal JunB cleavage product is able to bind DNA

Since the C-terminal JunB fragment was present in the nucleus, we used EMSA to examine whether this fragment could bind DNA. We found that a biotinylated AP-1 probe was able to bind a protein(s) in Karpas 299 cell nuclear extract (Figure 3.22; lane 2), and the electrophoretic mobility of these complexes was altered when the probe was incubated with extracts from cells expressing the Myc-tagged JunB C-terminal fragment compared to when incubated with extracts from vector alone–transfected cells (compare Figure 3.22; lanes 2 and 8; compare Figure 3.22; lanes 2 and 3). Moreover, the addition of an anti-JunB antibody to these probe-protein complexes resulted in a super-shift in the complex, demonstrating that JunB is present in these probe-protein complexes (Figure 3.22; lane 3). These probe-protein complexes could also be shifted with an anti-Myc antibody when incubated with nuclear extracts from Myc-tagged JunB (Figure 3.22; lane 7) or Myc-tagged JunB C-terminal fragment expressing cells (Figure 3.22; lane 10), but not vector alone–transfected cells (Figure 3.22; lane 4). Importantly, this latter result demonstrated that the C-terminal JunB cleavage fragment can bind DNA.

3.4.5: The C-terminal JunB cleavage product prevents endogenous AP-1 family proteins from binding DNA

We next examined whether the C-terminal fragment could compete with endogenous JunB for binding to this AP-1 probe. We again performed EMSA, this time using an anti-JunB antibody for super-shift that recognizes an epitope in the N-terminus of JunB, which is not present in the C-terminal fragment. This N-terminal JunB antibody allowed us to distinguish the endogenous full-length JunB from the exogenous C-terminal JunB fragment. In these experiments, we observed super-shifting with the C-

terminal anti-JunB antibody that recognizes both endogenous JunB and the C-terminal fragment (Figure 3.23 lanes 10 through 13). These findings are consistent with the notion that the C-terminal JunB caspase cleavage product binds AP-1 sites and prevents endogenous AP-1 family proteins from binding these sites.

We also examined whether in-vitro transcribed/translated Myc-JunB C-terminal cleavage fragment could bind this AP-1 probe independent of other factors present in Karpas 299 nuclear extract. Intriguingly, neither extracts of in-vitro transcribed/translated Myc-JunB or the C-terminal cleavage fragment alone were able to shift the AP-1 probe (Figure 3.24; lanes 3 and 5). However, we observed shifting of this probe when extracts containing Myc-JunB (lane 8) and the C-terminal fragment (lane 10) were incubated with extract containing FLAG-c-Fos. This suggests that the in-vitro transcribed/translated wild-type and C-terminal Myc-JunB can dimerize with the in-vitro transcribed/translated FLAG-c-Fos to bind the AP-1 probe. Taken together, our EMSA results are consistent with the notion that the C-terminal JunB caspase cleavage product binds AP-1 sites, prevents endogenous JunB from binding these sites, and at least with this synthetic AP-1 probe, binds as a heterodimer.

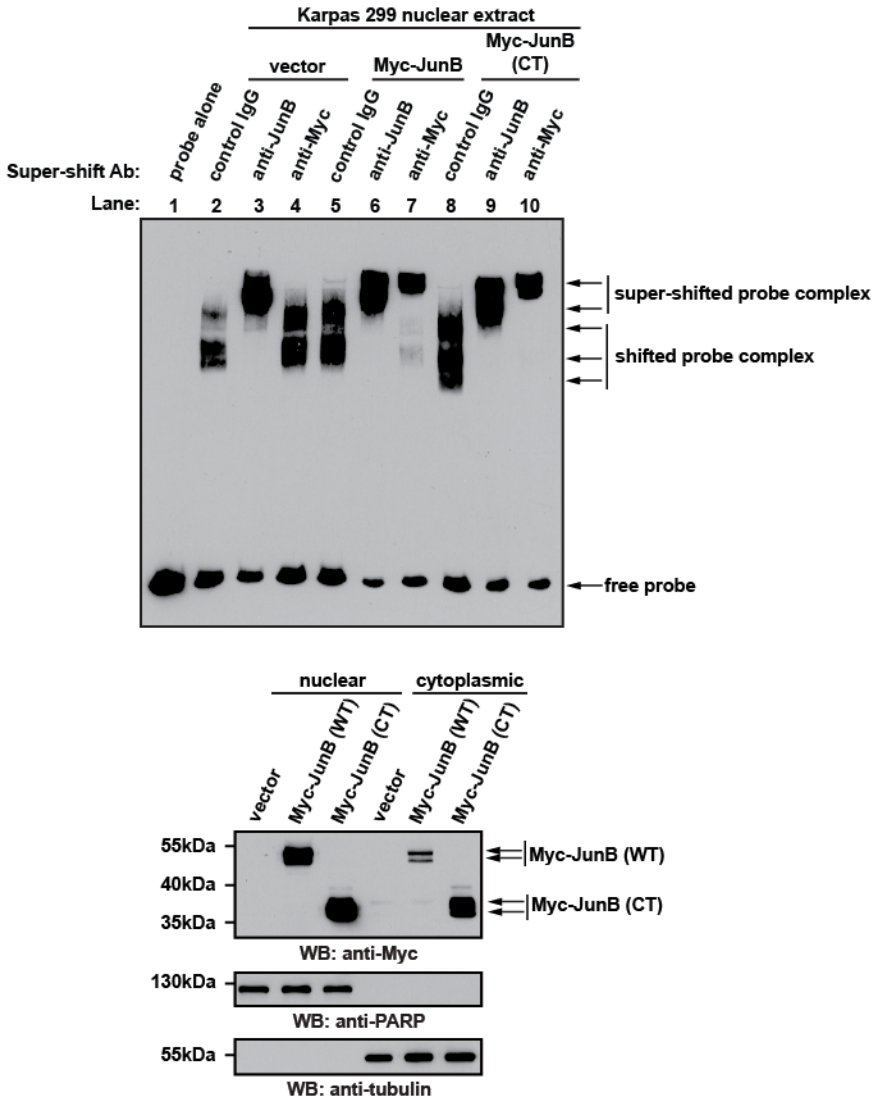

Figure 3.22: The C-terminal JunB cleavage fragment binds DNA.

EMSAs were performed by incubating nuclear extracts prepared from Karpas 299 cells transfected with the indicated cDNAs with a biotinylated AP-1 probe. The indicated antibodies were also included to test for super-shifting of probe-protein complexes. "Control IgG" is an irrelevant, isotype control antibody that serves as a negative control for super-shifting. In the lane labeled "probe alone", no nuclear extract or antibody was included in the reaction. The western blot below is included to demonstrate the expression of the Myc-tagged proteins in the nuclear fractions used for EMSA. The electrophoretic mobility of molecular weight standards are indicated to the left of western blots.

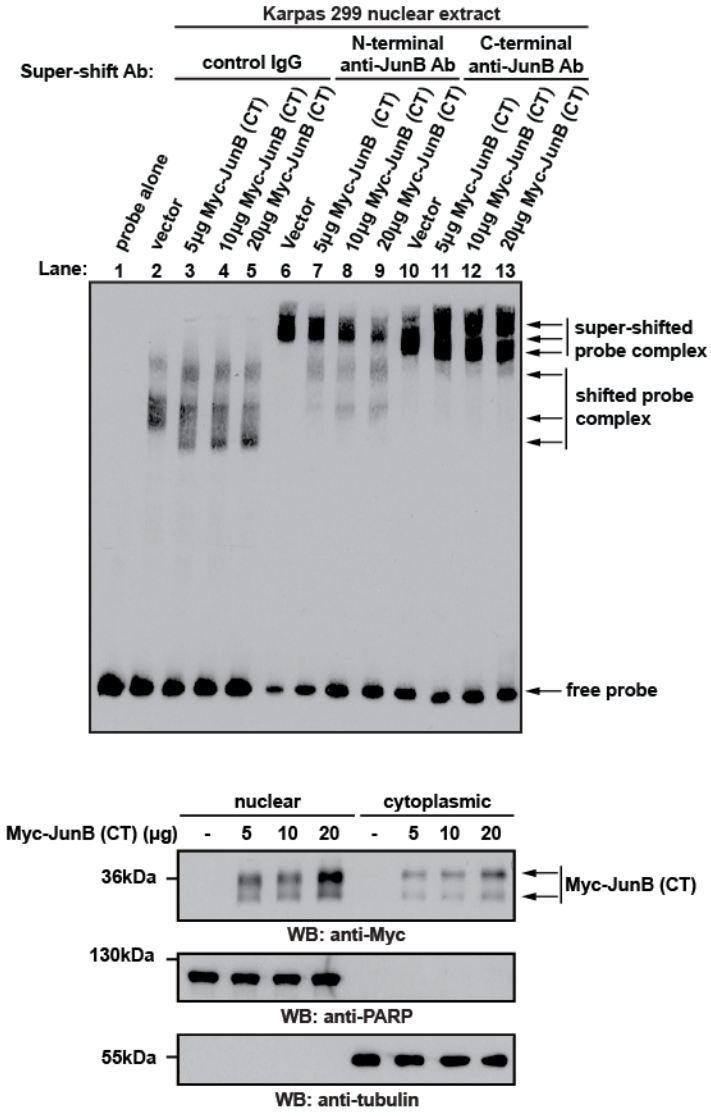

Figure 3.23: The C-terminal JunB cleavage fragment binds DNA, and competitively inhibits full-length JunB from binding DNA.

EMSAs were performed by incubating nuclear extracts prepared from Karpas 299 cells transfected with the indicated amounts of the Myc-JunB C-terminal (CT) fragment with a biotinylated AP-1 probe. Super-shifts were performed using the indicated antibodies. In the lane labeled "probe alone", no nuclear extract or antibody was included in the reaction. The western blot to the right indicates the expression level of the Myc-JunB (CT) fragment in the different nuclear fractions. The electrophoretic mobility of molecular weight standards are indicated to the left of western blots.

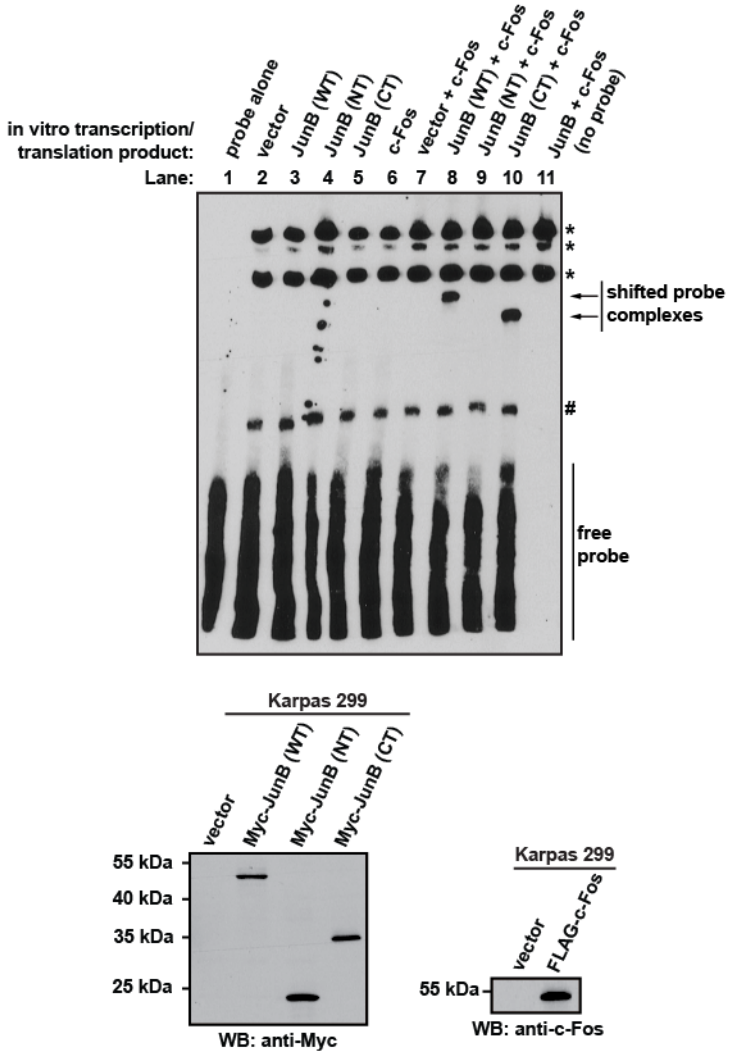

Figure 3.24: Full-length JunB and the C-terminal JunB cleavage fragment forms heterodimers with c-Fos to bind DNA.

EMSAs were performed using the indicated in-vitro transcribed/translated Myc-JunB and/or FLAG-c-Fos proteins as well as a biotinylated AP-1 probe. Bands indicated with an asterisk (*) are biotinylated proteins in the wheat germ extract, whereas the band mark with the number sign (#) is a complex between the probe and a wheat germ extract protein. The western blot to the right of the EMSA demonstrates the production of the indicated proteins using the in-vitro transcription/translation system. The electrophoretic mobility of molecular weight standards are indicated to the left of western blots.

3.4.6: The C-terminal JunB cleavage fragment reduces proliferation and enhances apoptosis when ectopically expressed in Karpas 299 cells

Both JunB and c-Jun have been shown to promote the proliferation of Karpas 299 cells (34,54). Since the C-terminal JunB fragment interfered with AP-1–dependent transcription, we examined whether this fragment had any effect on the viability of Karpas 299 cells. Using a resazurin–based cell viability assay, we noted a time–dependent decrease in the number of viable cells when Karpas 299 cells were transfected with a cDNA encoding for the C-terminal JunB fragment, but not cDNAs encoding for full-length JunB or the N-terminal cleavage product (Figure 3.25).

We next investigated whether the reduced viability was due to decreased proliferation, increased apoptosis, or both these processes. BrdU labeling of Karpas 299 cells expressing the C-terminal cleavage fragment was significantly reduced compared to vector alone–transfected cells and cells expressing Myc-JunB or the N-terminal cleavage fragment (Figure 3.26A and B). In addition, we observed a modest increase in apoptosis in Karpas 299 cells expressing the C-terminal JunB cleavage fragment (Figure 3.27). Thus, a decrease in proliferation and an increase in apoptosis are likely accounting for the reduced viability observed in cells expressing the C-terminal cleavage fragment.

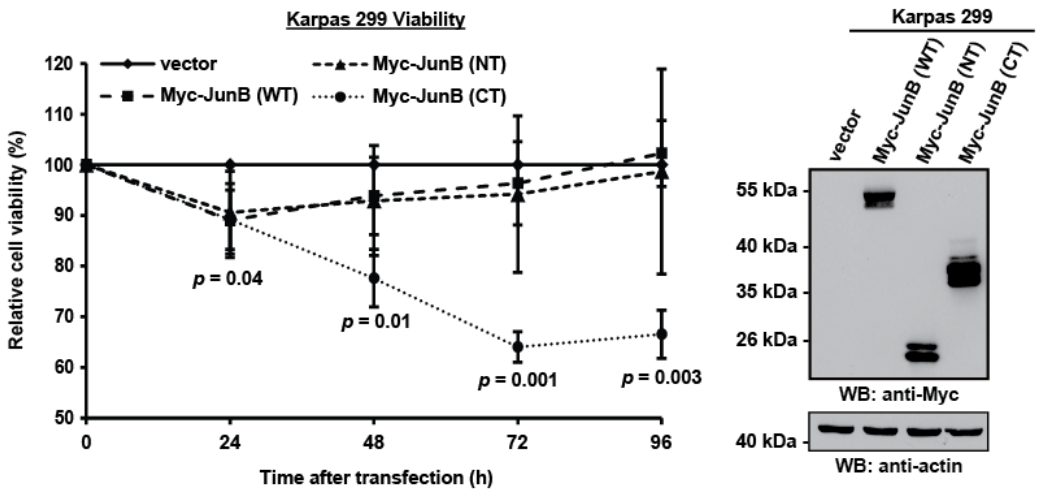

Figure 3.25: The C-terminal JunB cleavage fragment reduces the viability of Karpas 299 cells.

Karpas 299 cells were transfected with vector alone or cDNAs encoding for Myc-JunB (WT), the Myc-JunB N-terminal (NT) fragment, or the Myc-JunB C-terminal (CT) fragment. The viability of cells was then measured at the indicated times post-transfection using a resazurin–based viability assay. The results represent the average and standard deviation of three independent experiments. *p* values were calculated by performing paired, one-tailed t tests. The anti-Myc western blot (WB) to the right indicates the expression of the indicated Myc-tagged JunB proteins 24 h post-transfection, and the anti-actin blot demonstrates equivalent protein loading. The electrophoretic mobility of molecular weight standards are indicated to the left of western blots.

A

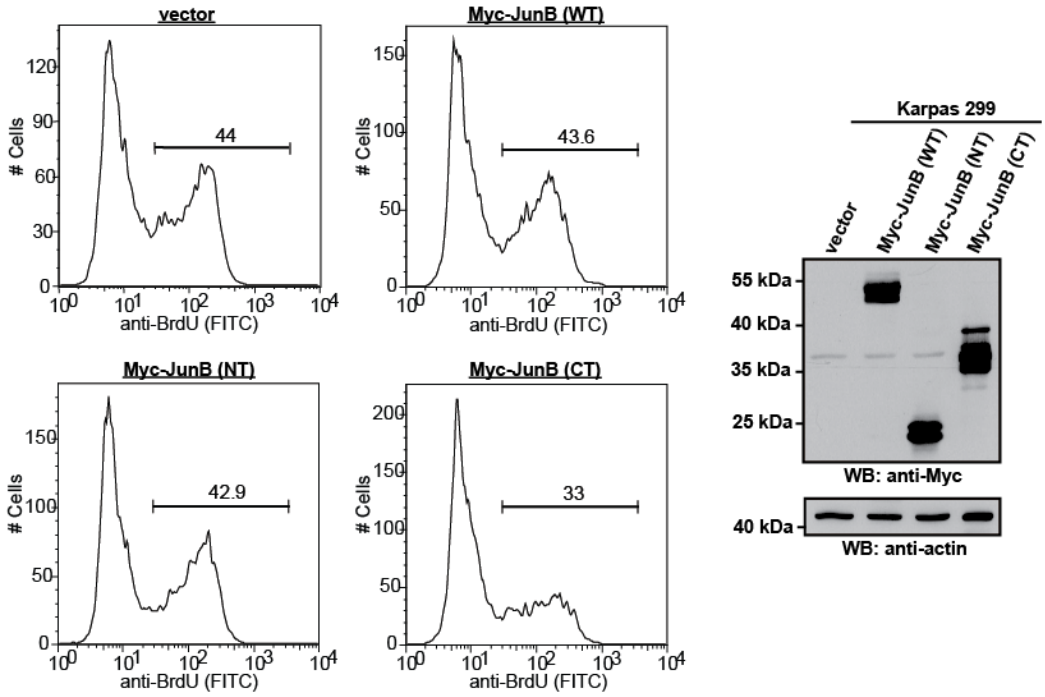

B

	Average % of BrdU+ cell	± SD	*p* value
vector	45.02	7.21	-
Myc-JunB (WT)	42.22	3.34	0.178
Myc-JunB (NT)	44.49	5.91	0.337
Myc-JunB (CT)	34.69	4.25	0.006

Figure 3.26: Expression of the C-terminal JunB cleavage fragment impairs proliferation in Karpas 299 cells.

A. Karpas 299 cells were transfected with vector alone or cDNAs encoding for the indicated Myc-tagged JunB proteins. Forty-eight hours post-transfection, cells were pulsed with BrdU for 4 h and analyzed for BrdU incorporation by flow cytometry. The western blot to the right indicates the expression of the indicated Myc-tagged JunB proteins 48 h post-transfection, and the anti-actin blot demonstrates protein loading. **B.** The values presented represent the mean and standard deviation of four independent experiments as described in **A**. *p* values were calculated by performing paired, one-tailed *t* tests.

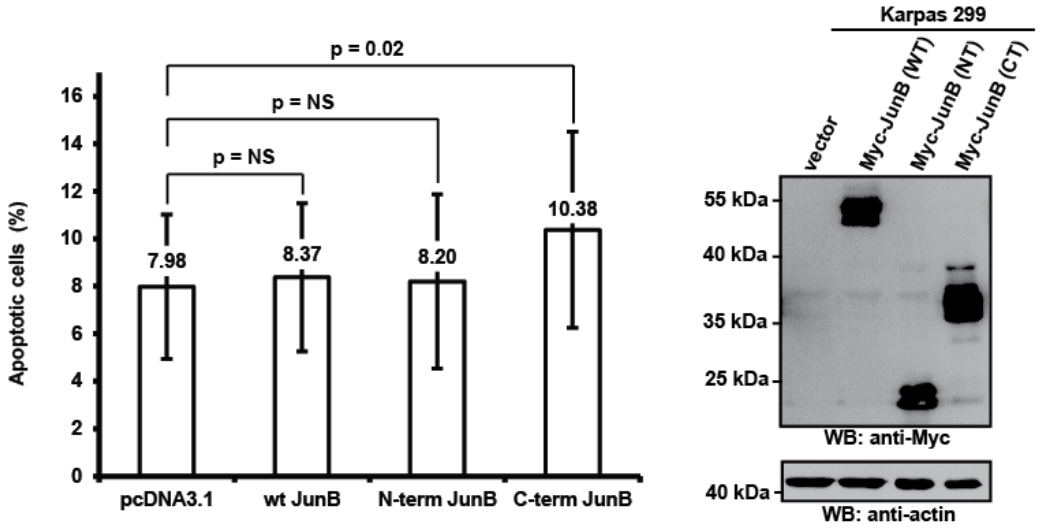

Figure 3.27: Expression of the C-terminal JunB cleavage fragment in Karpas 299 cells increases spontaneous apoptosis.

A. Karpas 299 cells were transfected with vector alone or cDNAs encoding for the indicated Myc-tagged JunB proteins, and the percentage of Annexin V–positive/propidium iodide–negative cells (early apoptotic) was determined 48 h post-transfection. The values presented represent the mean and standard deviation of four independent experiments. *p* values were calculated by performing paired, two-tailed *t* tests. NS indicates no significance difference. The western blot (WB) to the right indicates the expression of the indicated Myc-tagged JunB proteins 48 h post-transfection, and the anti-actin blot demonstrates protein loading. The electrophoretic mobility of molecular weight standards are indicated to the left of western blots.

CHAPTER 4: DISCUSSION

A portion of this chapter has been submitted for publication:

Lee JK, Pearson JD, Maser BM, and Ingham RJ. 2013. Cleavage of the JunB transcription factor by caspases generates a carboxy-terminal fragment that inhibits activator protein-1 transcriptional activity. *Journal of Biological Chemistry.* [undergoing revision]. The original manuscript was written by J. Lee, J. Pearson, and Dr. R. Ingham.

4.1: SUMMARY OF RESULTS

Activated caspases are associated with the alteration of the architecture and function of the cell during apoptotic cell death, and plays important roles in cell proliferation, cell differentiation and the immune response. In this study, we make the novel observation that the JunB transcription factor is a caspase substrate in apoptotic cells, and that cleavage of JunB generates a C-terminal fragment that inhibits AP-1-dependent transcription. We identified aspartic acid 137 as the JunB caspase cleavage site both in vivo and in-vitro. This site is conserved in all mammalian JunB proteins, and cleavage of JunB at this site separates the N-terminal transactivation domain from the C-terminal DNA binding and dimerization domains. Not only does cleavage inactivate the protein, but it generates a C-terminal fragment that inhibits AP-1–dependent transcription. Our results are consistent with a model (Figure 4.1) whereby the C-terminal JunB cleavage fragment binds AP-1 sites either as a homodimer, or as a heterodimer with c-Fos or other AP-1 family proteins. These C-terminal JunB fragment containing dimers can then prevent transcriptionally–competent AP-1 dimers from binding these sites and promoting transcription. The importance of this inhibition is demonstrated by our finding that the C-terminal cleavage fragment interferes with AP-1 function to the extent that there is impaired cell proliferation and survival when the C-terminal cleavage fragment is overexpressed in an ALK+ ALCL cell line.

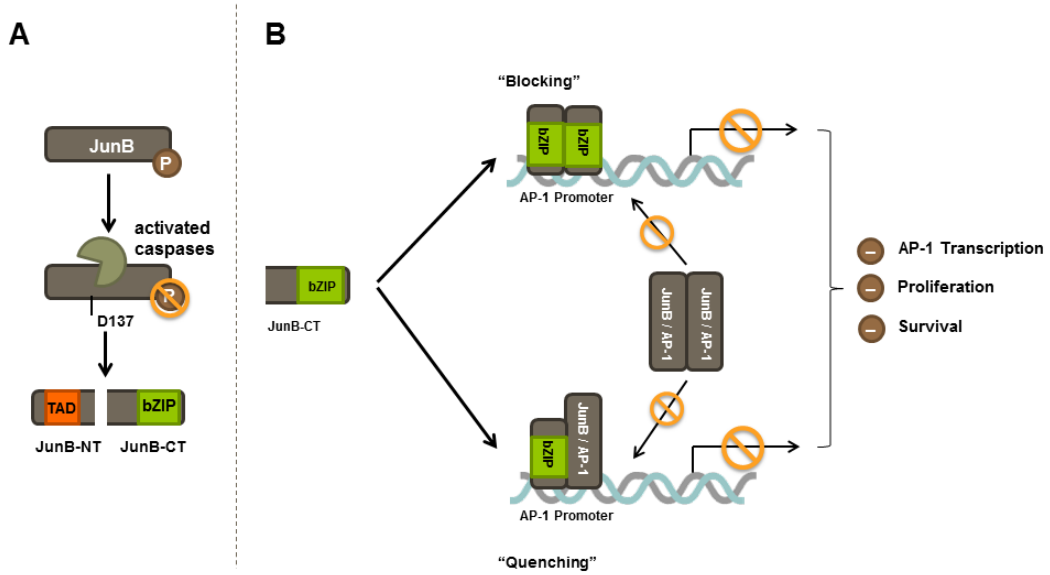

Figure 4.1: Overview of caspase-mediated JunB cleavage and its consequences.

A. Activated caspases cleaves the JunB transcription factor at aspartic acid residue 137 to generate an N-terminal fragment containing the transactivating domain (TAD) and a C-terminal fragment containing the DNA binding and dimerization domains (bZIP). JunB was also observed to be dephosphorylated during apoptosis. **B.** When expressed in ALK+ ALCL cells, the C-terminal JunB truncation mutant functions as an inhibitor of AP-1 transcription by either homodimerizing to "block" AP-1 promoter access, or heterodimerizes with other AP-1 proteins to form non-functional dimers that "quench" the AP-1 proteins in the cell. In both scenarios, functional wild-type AP-1 dimers are unable to bind to AP-1 promoter sites. The decreased AP-1 activity from both mechanisms results in impaired proliferation and survival of ALK+ ALCL cells. Figure adapted from (349).

4.2: CASPASE-MEDIATED CLEAVAGE OF JUNB

4.2.1: Consequences of caspase cleavage

The C-terminal JunB cleavage fragment we have characterized is structurally and functional reminiscent of TAM67, a dominant-negative c-Jun construct generated by the Birrer group (348). TAM67 lacks amino acids 3-122 of c-Jun, which comprises the majority of the transcriptional activation domain, but retains the DNA binding and dimerization domains (348). Because the H122 residue of c-Jun is analogous to the H147 residue of JunB, the two truncated proteins are very similar structurally as JunB is cleaved at the D137 residue (Figure 3.15). Indeed, similar to our findings, TAM67 was shown to bind AP-1 sites and interfere with AP-1–dependent transcription (348,349). As an inhibitor of AP-1 dependent transcription, the TAM67 mutant has been used in a number of different cell types as a tool to study AP-1 function. The expression of TAM67 has been shown to alter the expression of cell cycle proteins to negatively affect cell growth in lung cancer (349), breast cancer (350) and nasopharyngeal carcinoma models (351,352). Moreover it was found to block the proliferation of a fibrosarcoma cell line (353). The expression of TAM67 was also found to sensitize neuroblastoma cells for apoptosis induced by oxidative stress and blocked neuronal differentiation (354), and TAM67 was shown to block the differentiation of melanoma cells by inhibiting the transcription of the melanoma differentiation associated genes (355). There have also been many studies using TAM67 to examine the role of AP-1 transcription factors in keratinocytes, and TAM67 has been shown to inhibit keratinocyte differentiation and the expression of terminal differentiation markers (356-359).

In light of their observation that TAM67 interferes with AP-1 activity, the Birrer group proposed 2 mechanisms by which TAM67 was interfering with AP-1 signalling.

They hypothesized that TAM67 was either present at high enough levels to form TAM67 homodimers that bound to AP-1 sites to "block" AP-1 transcription, or was able to form defective heterodimers with endogenous AP-1 proteins to "quench" the AP-1 population in the cell to block transcription (Figure 4.1B)(348). Because TAM67 is able to form stable dimers with other AP-1 proteins to bind DNA, the authors concluded that TAM67 primarily inhibits transcription via a "quenching" mechanism (349). In this model, transcriptionally impaired TAM67/c-Fos or TAM67/c-Jun heterodimers bind AP-1 sites in place of more transcriptionally active c-Jun homodimers or c-Jun/c-Fos heterodimers (349). Our findings are consistent with their findings as the C-terminal JunB cleavage fragment functions in a similar manner. We demonstrated that the C-terminal JunB cleavage fragment is also able to bind other AP-1 transcription factors, and when over-expressed, out-compete wild-type AP-1 proteins for binding to AP-1 promoter sequences, suggesting that the C-terminal JunB fragment can also function to "block" or "quench" AP-1 transcription.

4.2.2: The caspase cleavage site of JunB

In this study, we identified that JunB can be cleaved by caspases at the aspartic acid 137 residue, with the sequence of the cleavage site being GFAD↓G (↓ indicating the cleaved peptide bond). The identified cleavage site appears to be a suitable caspase cleavage site, as it contains an aspartic acid residue at the P1 position. Although the P4-P2 sequence of the JunB cleavage site does not match canonical sites for either apical, executioner, or inflammatory caspases, the P1' residue of the JunB caspase cleavage site, which is a glycine, satisfies the preference of caspases for a small residue at the P1' position (276,277). Nevertheless, the idea that caspases have stringent substrate specificities and only cleave substrates containing canonical cleavage sites may be an

oversimplification of how caspases cleave protein substrates (268). This notion, stemming from the early experiments using the cleavage of synthetic peptides by caspases to characterize caspase cleavage sites (236,278) – neglects to take into consideration additional factors that influence caspase activity such as protein structure (172). Additionally, natural caspase substrate cleavage sites often deviate from the consensus sequence, made evident by the observation that the apparent consensus sequence for caspase 3 (DEVD) makes up less than 1% of known caspase substrate cleavage sites, while the more general DXXD motif only made up 22% of substrates in apoptotic Jurkat cells (276). Therefore, it appears that the presence of the consensus sequence is not sufficient nor is it necessarily required for caspase cleavage. When we take into account other determinants of caspase cleavage, such as secondary, tertiary, and quaternary protein structure (reviewed in (172)), the actual specificities for caspase substrate cleavage sites may be more variable than previously thought.

In this study, our in-vitro caspase cleavage data demonstrated that recombinant caspase 3 was able to cleave in-vitro transcribed and translated Myc-JunB protein at aspartic acid 137. Although the cleavage of Myc-JunB by caspase 3 was not very efficient, as indicated by a significant amount of full-length Myc-JunB that was left uncleaved, it corresponded to our observations that a large amount of the full-length endogenous JunB was left uncleaved as well. The low efficiency of the in-vitro cleavage of Myc-JunB may have been due to technical reasons such as the in-vitro reaction conditions, or it may be due to JunB may be cleaved by other caspases in vivo. While we were unable to determine whether or not JunB is primarily cleaved by caspase 3 in apoptotic cells, the kinetics of our time course experiments seemed to suggest that it occurred later in apoptosis, roughly correlating with the activation of caspase 3 and the cleavage of the

caspase 3 substrate PARP. These observations suggests that JunB may be cleaved by an executioner caspase. We found that other caspases were able to cleave JunB, including caspases 1, 6, and 8. This suggested that other caspases may be responsible for the cleavage of JunB in apoptotic cells or in other non-apoptotic situations.

4.2.3: JunB cleavage in other cell types

We observed the caspase-mediated cleavage of endogenous JunB in 2 ALK+ ALCL cell lines, as well as cleavage of exogenous JunB in the Burkitt lymphoma cell line BJAB. We were intrigued by the possibility that the cleavage of JunB may be a more universal mechanism of regulating JunB in other cell types, although there were a number of factors that affected the ability to observe JunB cleavage in other cell types.

The two main factors that contributed to our observation of JunB cleavage in ALK+ ALCL cells were the high levels of JunB expressed by ALK+ ALCL cells relative to other lymphoma cells, and the relative ease of inducing apoptosis in ALK+ ALCL with apoptosis-inducing drugs. We performed experiments to try to look for endogenous JunB cleavage in other cell types that express high levels of JunB, such as Hodgkin lymphoma cell lines, but were unable to observe JunB cleavage, despite observing some caspase 3 activation and PARP cleavage. It may be possible that a smaller proportion of cells were undergoing apoptosis which may affect the ability to observe the JunB cleavage. It is also likely that these cancers have acquired mechanisms to block apoptosis or enhance the efflux of the apoptosis inducing agents (360,361), resulting in decreased caspase activation and subsequent cleavage of JunB. Moreover, as transcription and translational processes are often affected during apoptosis (362), JunB protein levels itself may also decrease, and affect the ability to detect JunB by western blotting. Therefore, while the cleavage by caspases may be a regulation mechanism of

JunB in other cell types, it may require more sensitive methods to detect the low levels of JunB cleavage in other cells types.

In addition to drug treatment, we also attempted to use other methods of inducing apoptosis in the ALK+ ALCL cells. Experiments performed by Drs. Ingham and Barry using a vaccinia virus (Copenhagen) with a deletion in the antiapoptotic viral protein F1L (VV(Cop)ΔF1L), which has previously been shown to initiate apoptosis upon infection (363). Upon infection of ALK+ ALCL cells with the virus, we observed that while apoptosis was induced in cells, there was not much, if any, JunB cleavage (M Barry and RJ Ingham, unpublished data). Additionally, we also did not observe any dephosphorylation of JunB (M Barry and RJ Ingham, unpublished data). This may have to do with the different method of inducing apoptotis, and the virus may also regulate the phosphatase/kinase involved in the JunB dephosphorylation in a different way.

4.3: CASPASE-MEDIATED DEPHOSPHORYLATION OF JUNB

In addition to its cleavage by caspases, we also observed what was likely a dephosphorylation of the JunB to result in the apparent collapse of the JunB doublet into a lower molecular weight form. Although it is possible that staurosporine, a kinase inhibitor, may be responsible for some of the dephosphorylation we have observed, the fact that JunB was dephosphorylated similarly following doxorubicin treatment, and that JunB was not dephosphorylated to as large of an extent in cells treated with staurosporine and Z-VAD-FMK seems to indicate that at least a part of the dephosphorylation of JunB was caspase-dependent. We were intrigued by this observation, as a number of studies have implicated phosphorylation as an important mechanism of regulating JunB activity. As JunB and AP-1 transcription factors are heavily regulated by phosphorylation, the dephosphorylation of JunB can either positively or negatively regulate the transcriptional activity of JunB, or target it for proteasomal degradation (132,141-143,145,346).

Both kinases and phosphatases have been observed to be caspase substrates (reviewed in(364)). The cleavage of kinases typically results in increased apoptotic signaling through a number of mechanisms. For example, the cleavage of pro-apoptotic kinases such as PKCδ (365), ROCK1 (366,367), and MEKK1 (368-371) results in their activation to amplify pro-apoptotic signaling. Alternatively, the cleavage of pro-survival kinases such as Akt (372,373) and FAK (374,375) results in their inactivation and the subsequent termination of pro-survival signaling in the cell. Phosphatases are also known to be cleaved by caspases. For example, protein phosphatase 2A (PP2A) is activated following cleavage of its regulatory subunit Aα by caspase 3 (376). Additionally, the phosphatase PP1 is also known to be activated by caspases, as caspase

3 was found to cleave its inhibitor PP1 inhibitor-3 to activate the PP1α and PP1γ1 phosphatases (377). Thus, during apoptosis, caspases can activate or inactivate kinases and phosphatases by cleavage, and it is likely that the caspase-dependent dephosphorylation of JunB may be due to the activation of a phosphatase(s), inactivation of a kinase(s), or both these processes. However, to begin to address these questions we first need to identify the sites of JunB phosphorylation in ALK+ ALCL, and the kinases and phosphatases that regulate these sites.

Whether there is a relationship between JunB dephosphorylation and caspase cleavage is also an important question, as several studies have demonstrated that phosphorylation can regulate the caspase-mediated cleavage of substrates. For example, cleavage of the Max transcription factor at glutamic acid 10 residue by caspase 5 was found to be is inhibited by phosphorylation of Max at serine 11 (275), while the phosphorylation of the threonine 59 residue of Bid blocked its cleavage by caspase 8 at the aspartic acid 60 residue (378). In contrast, cleavage of PKC-δ by caspase 3 at aspartic acid 327 was promoted by phosphorylation of the adjacent tyrosine residue (379). Additionally, it has been suggested that the phosphorylation of the P3 residue on the caspase substrate can enhance its cleavage by caspase 8 (380). Nevertheless, the nearest potential phosphorylation site to aspartic acid 137 in JunB is threonine 129, 8 AA residues away, and there are no reports indicating this residue is phosphorylated, although it is likely too distant from aspartic acid 137 to affect caspase cleavage even if it were phosphorylated. Although we are not aware of any published reports of a distal phosphorylation site on the substrate protein that regulates caspase cleavage, we can't exclude the possibility of a phosphorylation site that can affect the cleavage of JunB by caspases. It is possible that the phosphorylation of JunB at a distal site can change the

conformation of JunB to expose the caspase site for enhanced cleavage, or expose an exosite that may interact with caspases. Nevertheless, we have found that the phosphorylation of some sites of JunB does not appear to be required for its cleavage, as a phosphorylation mutant of JunB generated in our laboratory, where the serines 251, 259, and threonine 255 were mutated to alanine, was still found to be cleaved in apoptotic ALK+ ALCL cell lines (JD Pearson, unpublished data). Moreover, the fact that the in-vitro transcribed and translated JunB used in our in-vitro cleavage assay appears not be phosphorylated, but was still cleaved by caspases, suggested that the phosphorylation of JunB is likely not a requirement for caspase cleavage.

4.4: CASPASE-DEPENDENT CLEAVAGE OF TRANSCRIPTION FACTORS

The destruction of the nucleus is a key event during apoptotic cell death, and caspases play an important role in this through the cleavage of a large number of substrates. Caspases cleave nuclear proteins such as nuclear lamins to result in the disassembly of the nuclear lamina, nuclear pore proteins to block nuclear transport, DNA repair and synthesis proteins, chromatin binding proteins, and also transcription factors (reviewed in (282,293)). The cleavage of these nuclear proteins contribute to the apoptotic phenotype, and has been suggested to play important functions including the breakdown of the nucleus, chromatin condensation and DNA cleavage, and also limiting the spread of viral DNA in infected cells undergoing apoptotic cell death (281,282). Of the many nuclear proteins that are caspase substrates in apoptotic cells (282), many transcription factors such as the NF-κB subunits, p65/RelA, p50, and (381,382), as well as c-Rel (383), STAT1 (384), STAT3 (385), FOXO3a (386), and GATA-1 (387) are cleaved during apoptosis.

4.4.1: Separation of transactivating and DNA binding domains

During the caspase mediated cleavage of JunB, we noted that the cleavage at aspartic acid 137 resulted in the generation of cleaved fragments that separated the transcriptional activation domain from the DNA binding/dimerization domain of JunB. Interestingly, the separation of the transactivation domain from the DNA binding domain is also a consequence of the caspase–mediated cleavage of other transcription factors. These include p65/RelA (382), FOXO3a (386), Ying Yang 1 (YY1) (388), as well as PU.1 (389).

The separation of the transactivating domain from the DNA binding/dimerization domains of some transcription factors by caspase cleavage has

also been demonstrated to generate an inhibitory fragment of transcription, similar to what we had observed for JunB. One such transcription factor is the NF-κB p65/RelA subunit, which has been shown to be cleaved by caspases during apoptosis (381). This discovery, made by Levkau *et al* following an interesting observation that NF-κB was activated during growth factor deprivation in a number of cell types (382). They found that despite NF-κB being a generally pro-survival transcription factor, most cells underwent apoptosis and lost NF-κB activity. Nevertheless, cells that did survive growth factor deprivation maintained NF-κB activity. This unusual observation was reconciled by the discovery that during apoptosis, the cleavage of p65/RelA by executioner caspases generates cleavage products that interferes with NF-κB activity. Cleavage of p65/RelA by caspases generates an N-terminal fragment where the transcriptional activation domains have been disrupted, but the fragment still retains the DNA binding domain (382). This fragment was demonstrated to inhibit overexpressed full-length p65/RelA from promoting transcription, and as a result also blocked cell survival. Additionally, a non-cleavable p65/RelA mutant was found to protect HUVEC cells from apoptosis induced by growth factor withdrawal, suggesting a role for the N-terminal cleavage product in apoptosis induction (382).

Similarly, cleavage of the yin yang 1 (YY1) transcription factor at aspartic acid 119 generates a transcriptionally–inactive fragment that retains DNA binding and is able to inhibit transcription mediated by full-length YY1 (388). YY1, a zinc finger transcription factor, is involved in regulating genes that regulate a number of genes involved in cellular processes such as proliferation, differentiation, and embryogenesis (reviewed in (390)). During apoptosis, YY1 localizes rapidly to the nucleus, and was found to be cleaved at multiple sites in its transactivation domain. As a result of the caspase

cleavage, the YY1 cleavage fragment – which contains the DNA binding domain but not the transactivation domain – acts as a dominant negative protein as it loses the ability to recruit cofactors required for the transcriptional activation of its target genes. Additionally, the expression of the YY1 cleavage product also sensitized HeLa cells to Fas–mediated apoptosis (388).

Our results demonstrating that the overexpression of the C-terminal JunB cleavage fragment resulted in a modest increase of apoptotic cells, represents another example of caspase–mediated cleavage of a transcription factor promoting apoptosis. However, unlike what was observed with p65/RelA, we found that the overexpression of non-cleavable D137A JunB mutant did not protect cells from undergoing apoptosis (JD Pearson and RJ Ingham, unpublished data). Thus, it is possible that the caspase–mediated cleavage of some transcription factors can inactivate their transcriptional activity, and in some cases this cleavage may generate fragments which inhibit transcription, although the cleavage of JunB does not appear to play a major role in the apoptosis of ALK+ ALCL cells.

4.5: ROLE OF JUNB CLEAVAGE DURING APOPTOSIS

In both JunB and other caspase substrates, it is difficult to conclude definitively whether a protein cleaved during apoptosis is a caspase substrate that plays an important role in apoptosis, or is simply cleaved as a bystander. It is also possible that the caspase cleavage of that protein may only be required for certain processes, making its cleavage during apoptosis appear to be redundant. Nevertheless, unless the cleavage of a bystander protein results in a significant blockage of apoptotic signalling or execution, there is little selection pressure to limit the cleavage of these bystander proteins by caspases (172). Indeed, as apoptosis is the cumulative effect of the cleavage of many caspase substrates, and the cleavage of a single caspase substrate is likely not sufficient to result in apoptosis, or block the induction of apoptosis (282). For example, even mice lacking the well characterized caspase substrate PARP show no overt phenotypes that would be indicative of either impaired apoptosis nor resistance to Fas or TNFR mediated apoptosis (391). Moreover, as the expression of an non-cleavable PARP mutant only resulted in the temporary delay of apoptosis (392), demonstrating that the cleavage of PARP is neither sufficient nor necessary for apoptosis.

Nonetheless, it is still interesting to ponder the reason that JunB is cleaved by caspases during apoptosis. A role of caspases during apoptosis is to cleave proteins that function in energy intensive processes to conserve the cell's energy consumption during apoptosis. For example, uncontrolled PARP-mediated DNA repair during apoptosis can result in the depletion of cellular stores of ATP and lead to necrosis instead of apoptosis (393-395). One of the processes interrupted by caspases' cleavage of protein substrates during apoptosis is the energy intensive process of protein translation. Proteins involved in translation initiation, such as eukaryotic initiation factors are cleaved during apoptosis

to block transcription initiation (reviewed in (362)). A recent study by Rajani *et al* demonstrated that in addition to these eukaryotic initiation factors, RNA processing proteins such as anti-silencing factor 1 (ASF1) and heterogeneous nuclear ribonucleoproteins (hnRNPs) are cleaved by granzyme A during immune cell mediated apoptosis affected RNA processing, and interfered with the export of mRNA transcripts which required splicing, such as c-*fos and c-myc*, while leaving intron-less mRNA such as c-*jun* unaffected (396).

These findings are interesting as it suggests that the inhibition of mRNA processing during apoptosis may be an important step of apoptosis, and that it may be possible that the caspase cleavage of the intron-less JunB may be a mechanism of eliminating proteins translated from intron-less mRNA that escape this mechanism of translation inhibition during apoptosis. The requirement to conserve the cell's energy stores in order to complete apoptotic cell death necessitates the shutdown of energy intensive processes. While genes that require mRNA processing can be targeted by the process described by Rajani *et al*, caspase cleavage may be how proteins translated from intron-less genes are shut down. Although it is not known whether caspases cleave other proteins derived from intron-less genes during apoptosis, it is an interesting theory that could potentially explain the importance of the cleavage of JunB during apoptosis, and why it occurs.

4.6: NON-APOPTOTIC ROLES OF JUNB CLEAVAGE BY CASPASES

Although we make the novel discovery in this study that JunB is a caspase substrate in apoptotic cells, whether or not it is cleaved to perform a biologically relevant role during apoptosis, or is cleaved merely as a bystander protein remains to be determined. Indeed, the caspase cleavage of a transcription factor such as JunB late in apoptosis is unlikely to affect the outcome of apoptosis in a major way. Nevertheless, cleavage of substrate proteins by caspases do not occur solely during apoptosis, and in fact plays important roles in a number of different processes. These non-death processes may be relevant to JunB's cleavage by caspases and may be a way of regulating JunB function.

4.6.1: Caspases in lymphocyte activation

Both caspases and AP-1 transcription factors play important roles in the activation of lymphocytes. Caspase 8 has been shown to play a role in T, B, and natural killer cell activation (397,398), and caspase 8 mutations in humans that produce an inactive caspase 8 results in immunodeficiency due to defects in lymphocyte apoptosis and homeostasis (reviewed in (399)). Caspase 8 mutations have also been shown to impair the activation of T and B lymphocytes and NK cells, suggesting a role in immunity in addition to its pro-apoptotic role (397). During T-cell activation, caspase 8, but not caspase 3, was found to be activated. In addition, the addition of caspase inhibitors during T-cell activation was found to reduce cell proliferation and the production of IL-2 (400,401). It is thought that caspase 8, along with its inhibitory homologue c-FLIP, play an important role in modulating NF-κB signalling (402,403). Caspase 8 and c-FLIP can either homodimerize with itself or heterodimerize with each other (402,404,405). Whereas the formation of caspase 8 homodimers can lead to the formation of DISC and

the induction of apoptosis, the formation of caspase 8 and c-FLIP heterodimers or c-FLIP homodimers can result in NF-κB activation (405-408). Experiments performed by Su *et al* described impaired NF-κB activation in caspase 8 deficient cells following TCR stimulation (409). Additionally, it is thought that during the limited activation of caspase 8 in these caspase 8/c-FLIP heterodimers, caspase 8 can be sequestered onto lipid rafts where only select substrates are cleaved to promote the activation of NF-κB (410).

JunB, which can function as a c-Jun antagonist to inhibit AP-1 transcription, may be inactivated by caspase cleavage in a similar mechanism. Whether JunB is cleaved by caspases during T-cell activation warrants further investigation. We have found that JunB can be cleaved in-vitro by caspases including caspase 8. The cleavage of JunB by caspase 8 suggests that JunB cleavage may be important in lymphocyte activation in addition to apoptosis.

4.6.2: Caspases in cell cycle

Caspases have also been shown to directly influence cell proliferation through the modulation of the cell cycle. While the expression levels of cell cycle proteins through cell cycle progression are often regulated by ubiquitin ligases (411), recent studies have shown that caspases may also play a role in regulating cell cycle progression. Active caspase 3 was found to be expressed in proliferating rat brain cells (412), and caspase 3 was specifically found to be upregulated prior to mitosis in HeLa cells (413). Additionally, treatment of HeLa cells with caspase 3 inhibitors resulted in cell death at late mitosis (414). Other caspases, such as caspase 7, have also been shown to regulate cell cycle (415,416), although the specific substrate proteins cleaved by caspases to modulate the cell cycle has not been identified.

The cleavage of JunB may be relevant in the context of cell cycle, as JunB can reduce the proliferation and promote the differentiation of a number of cell types including erythrocytes and keratinocytes (417,418). As JunB can be cleaved by multiple caspases in vitro, it may be possible that JunB is cleaved in progenitor cell types to prevent differentiation into more specialized cell types.

4.6.3: Caspases in cell differentiation

Caspase activity has been found to be required for certain cell types to reach a terminally differentiated state, usually through the removal of specific organelles. Examples of caspases playing a role in the differentiation of cells include the differentiation of macrophages, erythrocytes and keratinocytes. For example, the maturation of red blood cells during erythropoiesis is a process that involves the extrusion of the erythrocyte nucleus to be digested by macrophages, and significant remodelling of the cells cytoskeleton to form the distinctive shape of the mature erythrocyte (419-422). During erythrocyte differentiation, activated caspases are responsible for the morphological changes during erythrocyte maturation, such as chromatin condensation, loss of organelles, and extrusion of the nucleus to be broken down by macrophages (423,424). Similarly, activated caspases 3 and 14 function in keratinocytes to remove organelles during the terminal differentiation of keratinocytes into corneocytes, and are also required for the removal of the nucleus, or enucleation of these cells (425,426).

Caspases are involved in the differentiation of cells that do not reach a terminal differentiated state as well. The differentiation of monocytes to activated macrophages, for example, involves the activation of caspases. In response to macrophage colony-stimulating factor (M-CSF), caspases 8, 9, and 3 become activated and cleave a number

of protein substrates to mediate macrophage differentiation (427). Cells lacking caspase 8 or treated with caspase inhibitors failed to differentiate into macrophages. It is thought that the cleavage of RIP1 by caspase 8 blocked the activation of NF-κB to favour the differentiation into macrophages (428). A number of cytoskeletal proteins have also been identified to be caspase substrates, and its cleavage is thought to facilitate the cytoskeletal changes involved in macrophage differentiation (429).

JunB is also involved in the differentiation of a number of different cell types, and its cleavage by caspases may influence this process. In erythrocytes, the erythropoietin (EPO) induced expression of JunB is required for the differentiation of primary erythroid cells (417). Also key to erythrocyte differentiation are the transcription factors GATA-1 and Tal1, which are also activated by EPO. Interestingly, these transcription factors are protected from caspase cleavage in the presence of EPO, which protects the cell from undergoing apoptosis completely. In the absence of EPO however, both GATA-1 and Tal1 are cleaved by caspases, and the erythrocyte undergoes apoptosis (424,430). As we have observed that JunB can be cleaved by caspases including caspase 8, it may be possible that JunB is protected by a similar mechanism in differentiating cells, or that the caspase cleavage of JunB may be a way of limiting cell differentiation.

4.6.4: Caspases in inflammation

Caspases are also important in the innate immune response as caspase 1 is a major component of the inflammasome complex, and plays a major role in activating pro-inflammatory cytokines (296,431). However, in addition to cytokine processing, caspases can modulate inflammatory signalling through the cleavage of protein substrates. Work performed by Rajput *et al* described a mechanism by which caspase 8

can suppress inflammatory signalling. It was found that caspase 8 is recruited to the retinoic acid-inducible gene I (RIG-I) signalling complex, a cytoplasmic RNA sensor that activates the proinflammatory transcription factor interferon regulatory factor 3 (IRF3)(432). Caspase 8 cleaves polyubiquitylated kinase RIP-1 within the RIG-I complex to downregulate IRF3 signalling to downregulate the inflammatory response (432). Caspase 8 appears to play an important role in suppressing inflammation as caspase 8 deficient mice develop chronic inflammatory diseases (433,434), demonstrating a non-apoptotic role for a caspase traditionally associated with apoptosis. JunB, which is known to be able to promote pro-inflammatory signalling by inducing the expression of proinflammatory cytokines such as TNF-α, IL-6, and IL-12 (435), may also be regulated by caspase 1 cleavage to downregulate the inflammatory response. Whether JunB is cleaved by caspases under non-apoptotic conditions, and whether this cleavage is biologically important, warrants further investigation. Nevertheless, we have observed that JunB can be cleaved in-vitro by caspase 1. The potential cleavage of JunB by caspase 1 suggests that JunB cleavage may be relevant in inflammation as well.

4.7: FUTURE WORK

In this study we identified and characterized a mechanism by which JunB was cleaved by caspases to generate an inhibitory fragment. Whether or not the cleavage of JunB plays a role in apoptosis or in another non-apoptotic situation remains to be determined. The identification of the situation where JunB is cleaved, and the cellular caspase that cleaves JunB may help further narrow down the context in which JunB is cleaved naturally. Current experiments being performed in the Ingham lab is looking at whether JunB can be cleaved in cells following the activation of the inflammasome. Further experiments using either siRNAs or specific caspase inhibitors may help determine the caspase(s) that cleave JunB in cells.

Another aspect of JunB cleavage that also warrants further investigation is the dephosphorylation of JunB during apoptosis, whether or not it affects JunB cleavage or activity, and which phosphatase or kinase is responsible for the dephosphorylation. Experiments to study this aspect of JunB cleavage would involve determining the phosphorylation site(s) of JunB affected during apoptosis, which phosphatases/kinases usually phosphorylate/dephosphorylate those residues, and how they are affected by caspases. It would also be interesting to determine how changes in phosphorylation affect the cleavage of JunB.

The overexpression of the C-terminal JunB cleavage fragment resulted in decreased viability of the Karpas 299 ALK+ ALCL cell line through a combination of reduced proliferation survival. The identification of the gene targets that are affected by the overexpression of the C-terminal JunB cleavage fragment is important in determining the mechanism by which this occurs. Recent work in our laboratory made use of an mRNA microarray to identify differentially regulated genes in cells expressing

either the C-terminal JunB fragment, or vector alone (JD Pearson and RJ Ingham, unpublished data). Work is currently underway to validate the microarray results and identifying possible gene targets. As the reduced proliferation and survival of ALK+ ALCL cells following the expression of the C-terminal JunB fragment likely involves a number of different genes, it would be interesting to see the other proteins that are involved in this phenotype.

Finally, it would be interesting to determine the physiological role(s) of JunB cleavage. The generation of transgenic mice expressing the non-cleavable D137A JunB mutant can be used to identify any biological differences, and can be used to determine whether the cleavage of JunB plays important roles in any biological processes such as cell proliferation, differentiation, or in inflammation.

4.8: CONCLUSIONS

The cleavage of transcription factors by caspases during apoptosis has been shown to be a way of modulating their activity during programmed cell death and other processes such as cell proliferation and differentiation. This project has identified and characterized the cleavage of a novel caspase substrate – the JunB transcription factor – by caspases in apoptotic cells. We demonstrated that JunB is cleaved directly by caspases at aspartic acid 137 and that the cleavage of JunB generates a C-terminal cleavage fragment that can bind to DNA and other AP-1 proteins to interfere with their function. The C-terminal cleavage fragment that we have identified may also be useful in determining both JunB and AP-1 protein function – similar to how the dominant negative c-Jun mutant TAM67 was used to study c-Jun and AP-1 function. As we have shown that the overexpression of the JunB fragment can interfere with AP-1 function, it is possible that the truncated JunB mutant can be used as a similar tool to study JunB function, especially in tumours or other diseases that result in the elevated expression of JunB or other AP-1 proteins. In conclusion, our observations reveal a novel mechanism of modulating JunB function during apoptosis, and due to the many non-apoptotic roles of caspases, JunB cleavage may well be relevant in other processes regulated by caspases.

CHAPTER 5: BIBLIOGRAPHY

1. Howlader, N., Noone, A. M., Krapcho, M., Neyman, N., Aminou, R., Altekruse, S. F., Kosary, C. L., Ruhl, J., Tatalovich, Z., Cho, H., Mariotto, A., Eisner, M. P., Lewis, D. R., Chen, H. S., Feuer, E. J., and Cronin, K. A. (2012) SEER Cancer Statistics Review, 1975-2009 (Vintage 2009 Populations). National Cancer Institute, Bethesda, MD
2. Delsol, G., Falini, B., Muller-Hermelink, H.K., Campo, E., Jaffe, E.S., Gascoyne, R.D., Stein, H., Kinney, M.C. (2008) *Anaplastic large cell lymphoma (ALCL), ALK-positive*, 4th ed., International Agency for Research on Cancer (IARC), Lyon
3. Stein, H., Foss, H. D., Durkop, H., Marafioti, T., Delsol, G., Pulford, K., Pileri, S., and Falini, B. (2000) CD30(+) anaplastic large cell lymphoma: a review of its histopathologic, genetic, and clinical features. *Blood* **96**, 3681-3695
4. Stein, H., Mason, D. Y., Gerdes, J., O'Connor, N., Wainscoat, J., Pallesen, G., Gatter, K., Falini, B., Delsol, G., Lemke, H., and et al. (1985) The expression of the Hodgkin's disease associated antigen Ki-1 in reactive and neoplastic lymphoid tissue: evidence that Reed-Sternberg cells and histiocytic malignancies are derived from activated lymphoid cells. *Blood* **66**, 848-858
5. Gruss, H. J., DaSilva, N., Hu, Z. B., Uphoff, C. C., Goodwin, R. G., and Drexler, H. G. (1994) Expression and regulation of CD30 ligand and CD30 in human leukemia-lymphoma cell lines. *Leukemia* **8**, 2083-2094
6. Horie, R., and Watanabe, T. (1998) CD30: expression and function in health and disease. *Seminars in immunology* **10**, 457-470
7. Falini, B., Pileri, S., Pizzolo, G., Durkop, H., Flenghi, L., Stirpe, F., Martelli, M., and Stein, H. (1995) CD30 (Ki-1) molecule: a new cytokine receptor of the tumor necrosis factor receptor superfamily as a tool for diagnosis and immunotherapy. *Blood* **85**, 1-14
8. Hubinger, G., Muller, E., Scheffrahn, I., Schneider, C., Hildt, E., Singer, B. B., Sigg, I., Graf, J., and Bergmann, L. (2001) CD30-mediated cell cycle arrest associated with induced expression of p21(CIP1/WAF1) in the anaplastic large cell lymphoma cell line Karpas 299. *Oncogene* **20**, 590-598
9. Mir, S. S., Richter, B. W., and Duckett, C. S. (2000) Differential effects of CD30 activation in anaplastic large cell lymphoma and Hodgkin disease cells. *Blood* **96**, 4307-4312
10. Hubinger, G., Scheffrahn, I., Muller, E., Bai, R., Duyster, J., Morris, S. W., Schrezenmeier, H., and Bergmann, L. (1999) The tyrosine kinase NPM-ALK, associated with anaplastic large cell lymphoma, binds the intracellular domain of the surface receptor CD30 but is not activated by CD30 stimulation. *Experimental hematology* **27**, 1796-1805
11. Levi, E., Pfeifer, W. M., and Kadin, M. E. (2001) CD30-activation-mediated growth inhibition of anaplastic large-cell lymphoma cell lines: apoptosis or cell-cycle arrest? *Blood* **98**, 1630-1632
12. Kaneko, Y., Frizzera, G., Edamura, S., Maseki, N., Sakurai, M., Komada, Y., Tanaka, H., Sasaki, M., Suchi, T., and et al. (1989) A novel translocation, t(2;5)(p23;q35), in childhood phagocytic large T-cell lymphoma mimicking malignant histiocytosis. *Blood* **73**, 806-813
13. Rimokh, R., Magaud, J. P., Berger, F., Samarut, J., Coiffier, B., Germain, D., and Mason, D. Y. (1989) A translocation involving a specific breakpoint (q35) on chromosome 5 is characteristic of anaplastic large cell lymphoma ('Ki-1 lymphoma'). *British journal of haematology* **71**, 31-36

14. Bitter, M. A., Franklin, W. A., Larson, R. A., McKeithan, T. W., Rubin, C. M., Le Beau, M. M., Stephens, J. K., and Vardiman, J. W. (1990) Morphology in Ki-1(CD30)-positive non-Hodgkin's lymphoma is correlated with clinical features and the presence of a unique chromosomal abnormality, t(2;5)(p23;q35). *The American journal of surgical pathology* **14**, 305-316
15. Le Beau, M. M., Bitter, M. A., Larson, R. A., Doane, L. A., Ellis, E. D., Franklin, W. A., Rubin, C. M., Kadin, M. E., and Vardiman, J. W. (1989) The t(2;5)(p23;q35): a recurring chromosomal abnormality in Ki-1-positive anaplastic large cell lymphoma. *Leukemia* **3**, 866-870
16. Morris, S. W., Kirstein, M. N., Valentine, M. B., Dittmer, K. G., Shapiro, D. N., Saltman, D. L., and Look, A. T. (1994) Fusion of a kinase gene, ALK, to a nucleolar protein gene, NPM, in non-Hodgkin's lymphoma. *Science* **263**, 1281-1284
17. Fornari, A., Piva, R., Chiarle, R., Novero, D., and Inghirami, G. (2009) Anaplastic large cell lymphoma: one or more entities among T-cell lymphoma? *Hematological oncology* **27**, 161-170
18. Fraga, M., Brousset, P., Schlaifer, D., Payen, C., Robert, A., Rubie, H., Huguet-Rigal, F., and Delsol, G. (1995) Bone marrow involvement in anaplastic large cell lymphoma. Immunohistochemical detection of minimal disease and its prognostic significance. *American journal of clinical pathology* **103**, 82-89
19. Sato, N., Sato, K., Yagi, E., and Tomita, Y. (1995) Primary cutaneous Ki-1+ anaplastic large cell lymphoma: a morphologic, immunohistochemical and genetic study of an indolent case. *The Journal of dermatology* **22**, 441-449
20. Bonzheim, I., Geissinger, E., Roth, S., Zettl, A., Marx, A., Rosenwald, A., Muller-Hermelink, H. K., and Rudiger, T. (2004) Anaplastic large cell lymphomas lack the expression of T-cell receptor molecules or molecules of proximal T-cell receptor signaling. *Blood* **104**, 3358-3360
21. Eckerle, S., Brune, V., Doring, C., Tiacci, E., Bohle, V., Sundstrom, C., Kodet, R., Paulli, M., Falini, B., Klapper, W., Chaubert, A. B., Willenbrock, K., Metzler, D., Brauninger, A., Kuppers, R., and Hansmann, M. L. (2009) Gene expression profiling of isolated tumour cells from anaplastic large cell lymphomas: insights into its cellular origin, pathogenesis and relation to Hodgkin lymphoma. *Leukemia* **23**, 2129-2138
22. Krenacs, L., Wellmann, A., Sorbara, L., Himmelmann, A. W., Bagdi, E., Jaffe, E. S., and Raffeld, M. (1997) Cytotoxic cell antigen expression in anaplastic large cell lymphomas of T- and null-cell type and Hodgkin's disease: evidence for distinct cellular origin. *Blood* **89**, 980-989
23. Medeiros, L. J., and Elenitoba-Johnson, K. S. (2007) Anaplastic Large Cell Lymphoma. *American journal of clinical pathology* **127**, 707-722
24. Kinney, M. C., Higgins, R. A., and Medina, E. A. (2011) Anaplastic large cell lymphoma: twenty-five years of discovery. *Archives of pathology & laboratory medicine* **135**, 19-43
25. Pulford, K., Lamant, L., Morris, S. W., Butler, L. H., Wood, K. M., Stroud, D., Delsol, G., and Mason, D. Y. (1997) Detection of anaplastic lymphoma kinase (ALK) and nucleolar protein nucleophosmin (NPM)-ALK proteins in normal and neoplastic cells with the monoclonal antibody ALK1. *Blood* **89**, 1394-1404
26. Jaffe, E. S. (2004) Mature T-cell and NK-cell lymphomas in the pediatric age group. *American journal of clinical pathology* **122 Suppl**, S110-121

27. Inghirami, G., and Pileri, S. A. (2011) Anaplastic large-cell lymphoma. *Seminars in diagnostic pathology* **28**, 190-201
28. Burkhardt, B., Zimmermann, M., Oschlies, I., Niggli, F., Mann, G., Parwaresch, R., Riehm, H., Schrappe, M., and Reiter, A. (2005) The impact of age and gender on biology, clinical features and treatment outcome of non-Hodgkin lymphoma in childhood and adolescence. *British journal of haematology* **131**, 39-49
29. Le Deley, M. C., Reiter, A., Williams, D., Delsol, G., Oschlies, I., McCarthy, K., Zimmermann, M., and Brugieres, L. (2008) Prognostic factors in childhood anaplastic large cell lymphoma: results of a large European intergroup study. *Blood* **111**, 1560-1566
30. Hochberg, J., Waxman, I. M., Kelly, K. M., Morris, E., and Cairo, M. S. (2009) Adolescent non-Hodgkin lymphoma and Hodgkin lymphoma: state of the science. *British journal of haematology* **144**, 24-40
31. Gascoyne, R. D., Aoun, P., Wu, D., Chhanabhai, M., Skinnider, B. F., Greiner, T. C., Morris, S. W., Connors, J. M., Vose, J. M., Viswanatha, D. S., Coldman, A., and Weisenburger, D. D. (1999) Prognostic significance of anaplastic lymphoma kinase (ALK) protein expression in adults with anaplastic large cell lymphoma. *Blood* **93**, 3913-3921
32. FDA approves Adcetris to treat two types of lymphoma. in *FDA News Release*, U.S. Food and Drug Administration, Silver Spring, MD
33. (2011) FDA approves Xalkori with companion diagnostic for a type of late-stage lung cancer. . in *FDA News Release*, U.S. Food and Drug Administration, Silver Spring, MD
34. Pfizer. (2007) A Study Of Oral PF-02341066, A c-Met/Hepatocyte Growth Factor Tyrosine Kinase Inhibitor, In Patients With Advanced Cancer. National Library of Medicine (US), Bethesda, MD
35. National Cancer Institute (NCI), and (COG)., C. s. O. G. (2009) Crizotinib in Treating Young Patients With Relapsed or Refractory Solid Tumors or Anaplastic Large Cell Lymphoma. National Library of Medicine (US), Bethesda, MD
36. Iwahara, T., Fujimoto, J., Wen, D., Cupples, R., Bucay, N., Arakawa, T., Mori, S., Ratzkin, B., and Yamamoto, T. (1997) Molecular characterization of ALK, a receptor tyrosine kinase expressed specifically in the nervous system. *Oncogene* **14**, 439-449
37. Morris, S. W., Naeve, C., Mathew, P., James, P. L., Kirstein, M. N., Cui, X., and Witte, D. P. (1997) ALK, the chromosome 2 gene locus altered by the t(2;5) in non-Hodgkin's lymphoma, encodes a novel neural receptor tyrosine kinase that is highly related to leukocyte tyrosine kinase (LTK). *Oncogene* **14**, 2175-2188
38. Vernersson, E., Khoo, N. K., Henriksson, M. L., Roos, G., Palmer, R. H., and Hallberg, B. (2006) Characterization of the expression of the ALK receptor tyrosine kinase in mice. *Gene expression patterns : GEP* **6**, 448-461
39. Palmer, R. H., Vernersson, E., Grabbe, C., and Hallberg, B. (2009) Anaplastic lymphoma kinase: signalling in development and disease. *The Biochemical journal* **420**, 345-361
40. Weiss, J. B., Xue, C., Benice, T., Xue, L., Morris, S. W., and Raber, J. (2012) Anaplastic lymphoma kinase and leukocyte tyrosine kinase: functions and genetic interactions in learning, memory and adult neurogenesis. *Pharmacology, biochemistry, and behavior* **100**, 566-574

41. Bilsland, J. G., Wheeldon, A., Mead, A., Znamenskiy, P., Almond, S., Waters, K. A., Thakur, M., Beaumont, V., Bonnert, T. P., Heavens, R., Whiting, P., McAllister, G., and Munoz-Sanjuan, I. (2008) Behavioral and neurochemical alterations in mice deficient in anaplastic lymphoma kinase suggest therapeutic potential for psychiatric indications. *Neuropsychopharmacology : official publication of the American College of Neuropsychopharmacology* **33**, 685-700
42. Lasek, A. W., Lim, J., Kliethermes, C. L., Berger, K. H., Joslyn, G., Brush, G., Xue, L., Robertson, M., Moore, M. S., Vranizan, K., Morris, S. W., Schuckit, M. A., White, R. L., and Heberlein, U. (2011) An evolutionary conserved role for anaplastic lymphoma kinase in behavioral responses to ethanol. *PloS one* **6**, e22636
43. Englund, C., Loren, C. E., Grabbe, C., Varshney, G. K., Deleuil, F., Hallberg, B., and Palmer, R. H. (2003) Jeb signals through the Alk receptor tyrosine kinase to drive visceral muscle fusion. *Nature* **425**, 512-516
44. Lee, H. H., Norris, A., Weiss, J. B., and Frasch, M. (2003) Jelly belly protein activates the receptor tyrosine kinase Alk to specify visceral muscle pioneers. *Nature* **425**, 507-512
45. Stute, C., Schimmelpfeng, K., Renkawitz-Pohl, R., Palmer, R. H., and Holz, A. (2004) Myoblast determination in the somatic and visceral mesoderm depends on Notch signalling as well as on milliways(mili(Alk)) as receptor for Jeb signalling. *Development* **131**, 743-754
46. Stoica, G. E., Kuo, A., Aigner, A., Sunitha, I., Souttou, B., Malerczyk, C., Caughey, D. J., Wen, D., Karavanov, A., Riegel, A. T., and Wellstein, A. (2001) Identification of anaplastic lymphoma kinase as a receptor for the growth factor pleiotrophin. *The Journal of biological chemistry* **276**, 16772-16779
47. Stoica, G. E., Kuo, A., Powers, C., Bowden, E. T., Sale, E. B., Riegel, A. T., and Wellstein, A. (2002) Midkine binds to anaplastic lymphoma kinase (ALK) and acts as a growth factor for different cell types. *The Journal of biological chemistry* **277**, 35990-35998
48. Perez-Pinera, P., Zhang, W., Chang, Y., Vega, J. A., and Deuel, T. F. (2007) Anaplastic lymphoma kinase is activated through the pleiotrophin/receptor protein-tyrosine phosphatase beta/zeta signaling pathway: an alternative mechanism of receptor tyrosine kinase activation. *The Journal of biological chemistry* **282**, 28683-28690
49. Mourali, J., Benard, A., Lourenco, F. C., Monnet, C., Greenland, C., Moog-Lutz, C., Racaud-Sultan, C., Gonzalez-Dunia, D., Vigny, M., Mehlen, P., Delsol, G., and Allouche, M. (2006) Anaplastic lymphoma kinase is a dependence receptor whose proapoptotic functions are activated by caspase cleavage. *Mol Cell Biol* **26**, 6209-6222
50. Mehlen, P., and Bredesen, D. E. (2004) The dependence receptor hypothesis. *Apoptosis* **9**, 37-49
51. Soda, M., Choi, Y. L., Enomoto, M., Takada, S., Yamashita, Y., Ishikawa, S., Fujiwara, S., Watanabe, H., Kurashina, K., Hatanaka, H., Bando, M., Ohno, S., Ishikawa, Y., Aburatani, H., Niki, T., Sohara, Y., Sugiyama, Y., and Mano, H. (2007) Identification of the transforming EML4-ALK fusion gene in non-small-cell lung cancer. *Nature* **448**, 561-566
52. Rikova, K., Guo, A., Zeng, Q., Possemato, A., Yu, J., Haack, H., Nardone, J., Lee, K., Reeves, C., Li, Y., Hu, Y., Tan, Z., Stokes, M., Sullivan, L., Mitchell, J., Wetzel, R., Macneill, J., Ren, J. M., Yuan, J., Bakalarski, C. E., Villen, J., Kornhauser, J. M.,

Smith, B., Li, D., Zhou, X., Gygi, S. P., Gu, T. L., Polakiewicz, R. D., Rush, J., and Comb, M. J. (2007) Global survey of phosphotyrosine signaling identifies oncogenic kinases in lung cancer. *Cell* **131**, 1190-1203

53. Takeuchi, K., Choi, Y. L., Togashi, Y., Soda, M., Hatano, S., Inamura, K., Takada, S., Ueno, T., Yamashita, Y., Satoh, Y., Okumura, S., Nakagawa, K., Ishikawa, Y., and Mano, H. (2009) KIF5B-ALK, a novel fusion oncokinase identified by an immunohistochemistry-based diagnostic system for ALK-positive lung cancer. *Clinical cancer research : an official journal of the American Association for Cancer Research* **15**, 3143-3149
54. Togashi, Y., Soda, M., Sakata, S., Sugawara, E., Hatano, S., Asaka, R., Nakajima, T., Mano, H., and Takeuchi, K. (2012) KLC1-ALK: A Novel Fusion in Lung Cancer Identified Using a Formalin-Fixed Paraffin-Embedded Tissue Only. *PloS one* **7**, e31323
55. Griffin, C. A., Hawkins, A. L., Dvorak, C., Henkle, C., Ellingham, T., and Perlman, E. J. (1999) Recurrent involvement of 2p23 in inflammatory myofibroblastic tumors. *Cancer research* **59**, 2776-2780
56. Lawrence, B., Perez-Atayde, A., Hibbard, M. K., Rubin, B. P., Dal Cin, P., Pinkus, J. L., Pinkus, G. S., Xiao, S., Yi, E. S., Fletcher, C. D., and Fletcher, J. A. (2000) TPM3-ALK and TPM4-ALK oncogenes in inflammatory myofibroblastic tumors. *Am J Pathol* **157**, 377-384
57. Debiec-Rychter, M., Marynen, P., Hagemeijer, A., and Pauwels, P. (2003) ALK-ATIC fusion in urinary bladder inflammatory myofibroblastic tumor. *Genes, chromosomes & cancer* **38**, 187-190
58. Bridge, J. A., Kanamori, M., Ma, Z., Pickering, D., Hill, D. A., Lydiatt, W., Lui, M. Y., Colleoni, G. W., Antonescu, C. R., Ladanyi, M., and Morris, S. W. (2001) Fusion of the ALK gene to the clathrin heavy chain gene, CLTC, in inflammatory myofibroblastic tumor. *Am J Pathol* **159**, 411-415
59. Cools, J., Wlodarska, I., Somers, R., Mentens, N., Pedeutour, F., Maes, B., De Wolf-Peeters, C., Pauwels, P., Hagemeijer, A., and Marynen, P. (2002) Identification of novel fusion partners of ALK, the anaplastic lymphoma kinase, in anaplastic large-cell lymphoma and inflammatory myofibroblastic tumor. *Genes, chromosomes & cancer* **34**, 354-362
60. Ma, Z., Hill, D. A., Collins, M. H., Morris, S. W., Sumegi, J., Zhou, M., Zuppan, C., and Bridge, J. A. (2003) Fusion of ALK to the Ran-binding protein 2 (RANBP2) gene in inflammatory myofibroblastic tumor. *Genes, chromosomes & cancer* **37**, 98-105
61. Panagopoulos, I., Nilsson, T., Domanski, H. A., Isaksson, M., Lindblom, P., Mertens, F., and Mandahl, N. (2006) Fusion of the SEC31L1 and ALK genes in an inflammatory myofibroblastic tumor. *International journal of cancer. Journal international du cancer* **118**, 1181-1186
62. Takeuchi, K., Soda, M., Togashi, Y., Sugawara, E., Hatano, S., Asaka, R., Okumura, S., Nakagawa, K., Mano, H., and Ishikawa, Y. (2011) Pulmonary inflammatory myofibroblastic tumor expressing a novel fusion, PPFIBP1-ALK: reappraisal of anti-ALK immunohistochemistry as a tool for novel ALK fusion identification. *Clinical cancer research : an official journal of the American Association for Cancer Research* **17**, 3341-3348

63. Lamant, L., Dastugue, N., Pulford, K., Delsol, G., and Mariame, B. (1999) A new fusion gene TPM3-ALK in anaplastic large cell lymphoma created by a (1;2)(q25;p23) translocation. *Blood* **93**, 3088-3095
64. Lamant, L., Pulford, K., Bischof, D., Morris, S. W., Mason, D. Y., Delsol, G., and Mariame, B. (2000) Expression of the ALK tyrosine kinase gene in neuroblastoma. *Am J Pathol* **156**, 1711-1721
65. Janoueix-Lerosey, I., Lequin, D., Brugieres, L., Ribeiro, A., de Pontual, L., Combaret, V., Raynal, V., Puisieux, A., Schleiermacher, G., Pierron, G., Valteau-Couanet, D., Frebourg, T., Michon, J., Lyonnet, S., Amiel, J., and Delattre, O. (2008) Somatic and germline activating mutations of the ALK kinase receptor in neuroblastoma. *Nature* **455**, 967-970
66. Chen, Y., Takita, J., Choi, Y. L., Kato, M., Ohira, M., Sanada, M., Wang, L., Soda, M., Kikuchi, A., Igarashi, T., Nakagawara, A., Hayashi, Y., Mano, H., and Ogawa, S. (2008) Oncogenic mutations of ALK kinase in neuroblastoma. *Nature* **455**, 971-974
67. George, R. E., Sanda, T., Hanna, M., Frohling, S., Luther, W., 2nd, Zhang, J., Ahn, Y., Zhou, W., London, W. B., McGrady, P., Xue, L., Zozulya, S., Gregor, V. E., Webb, T. R., Gray, N. S., Gilliland, D. G., Diller, L., Greulich, H., Morris, S. W., Meyerson, M., and Look, A. T. (2008) Activating mutations in ALK provide a therapeutic target in neuroblastoma. *Nature* **455**, 975-978
68. Caren, H., Abel, F., Kogner, P., and Martinsson, T. (2008) High incidence of DNA mutations and gene amplifications of the ALK gene in advanced sporadic neuroblastoma tumours. *The Biochemical journal* **416**, 153-159
69. Mosse, Y. P., Laudenslager, M., Longo, L., Cole, K. A., Wood, A., Attiyeh, E. F., Laquaglia, M. J., Sennett, R., Lynch, J. E., Perri, P., Laureys, G., Speleman, F., Kim, C., Hou, C., Hakonarson, H., Torkamani, A., Schork, N. J., Brodeur, G. M., Tonini, G. P., Rappaport, E., Devoto, M., and Maris, J. M. (2008) Identification of ALK as a major familial neuroblastoma predisposition gene. *Nature* **455**, 930-935
70. Drexler, H. G., Gignac, S. M., von Wasielewski, R., Werner, M., and Dirks, W. G. (2000) Pathobiology of NPM-ALK and variant fusion genes in anaplastic large cell lymphoma and other lymphomas. *Leukemia* **14**, 1533-1559
71. Morris, S. W., Xue, L., Ma, Z., and Kinney, M. C. (2001) Alk+ CD30+ lymphomas: a distinct molecular genetic subtype of non-Hodgkin's lymphoma. *British journal of haematology* **113**, 275-295
72. Liu, Q. R., and Chan, P. K. (1991) Formation of nucleophosmin/B23 oligomers requires both the amino- and the carboxyl-terminal domains of the protein. *European journal of biochemistry / FEBS* **200**, 715-721
73. Adachi, Y., Copeland, T. D., Hatanaka, M., and Oroszlan, S. (1993) Nucleolar targeting signal of Rex protein of human T-cell leukemia virus type I specifically binds to nucleolar shuttle protein B-23. *The Journal of biological chemistry* **268**, 13930-13934
74. Lindstrom, M. S. (2011) NPM1/B23: A Multifunctional Chaperone in Ribosome Biogenesis and Chromatin Remodeling. *Biochemistry research international* **2011**, 195209
75. Chiarle, R., Voena, C., Ambrogio, C., Piva, R., and Inghirami, G. (2008) The anaplastic lymphoma kinase in the pathogenesis of cancer. *Nat Rev Cancer* **8**, 11-23

76. Barreca, A., Lasorsa, E., Riera, L., Machiorlatti, R., Piva, R., Ponzoni, M., Kwee, I., Bertoni, F., Piccaluga, P. P., and Pileri, S. A. (2011) Anaplastic lymphoma kinase in human cancer. *Journal of molecular endocrinology* **47**, R11-R23
77. Pearson, J. D., Lee, J. K., Bacani, J. T., Lai, R., and Ingham, R. J. (2012) NPM-ALK: The Prototypic Member of a Family of Oncogenic Fusion Tyrosine Kinases. *Journal of signal transduction* **2012**, 123253
78. Leventaki, V., Drakos, E., Medeiros, L. J., Lim, M. S., Elenitoba-Johnson, K. S., Claret, F. X., and Rassidakis, G. Z. (2007) NPM-ALK oncogenic kinase promotes cell-cycle progression through activation of JNK/cJun signaling in anaplastic large-cell lymphoma. *Blood* **110**, 1621-1630
79. Staber, P. B., Vesely, P., Haq, N., Ott, R. G., Funato, K., Bambach, I., Fuchs, C., Schauer, S., Linkesch, W., Hrzenjak, A., Dirks, W. G., Sexl, V., Bergler, H., Kadin, M. E., Sternberg, D. W., Kenner, L., and Hoefler, G. (2007) The oncoprotein NPM-ALK of anaplastic large-cell lymphoma induces JUNB transcription via ERK1/2 and JunB translation via mTOR signaling. *Blood* **110**, 3374-3383
80. Eferl, R., and Wagner, E. F. (2003) AP-1: a double-edged sword in tumorigenesis. *Nat Rev Cancer* **3**, 859-868
81. Shaulian, E. (2010) AP-1--The Jun proteins: Oncogenes or tumor suppressors in disguise? *Cell Signal* **22**, 894-899
82. Shaulian, E., and Karin, M. (2002) AP-1 as a regulator of cell life and death. *Nature cell biology* **4**, E131-136
83. Angel, P., Imagawa, M., Chiu, R., Stein, B., Imbra, R. J., Rahmsdorf, H. J., Jonat, C., Herrlich, P., and Karin, M. (1987) Phorbol ester-inducible genes contain a common cis element recognized by a TPA-modulated trans-acting factor. *Cell* **49**, 729-739
84. Bohmann, D., Bos, T. J., Admon, A., Nishimura, T., Vogt, P. K., and Tjian, R. (1987) Human proto-oncogene c-jun encodes a DNA binding protein with structural and functional properties of transcription factor AP-1. *Science* **238**, 1386-1392
85. Curran, T., and Franza Jr, B. R. (1988) Fos and jun: the AP-1 connection. *Cell* **55**, 395-397
86. Kouzarides, T., and Ziff, E. (1988) The role of the leucine zipper in the fos-jun interaction. *Nature* **336**, 646-651
87. Nakabeppu, Y., Ryder, K., and Nathans, D. (1988) DNA binding activities of three murine Jun proteins: Stimulation by Fos. *Cell* **55**, 907-915
88. Sassone-Corsi, P., Der, C. J., and Verma, I. M. (1989) ras-induced neuronal differentiation of PC12 cells: possible involvement of fos and jun. *Molecular and cellular biology* **9**, 3174-3183
89. Schuermann, M., Neuberg, M., Hunter, J. B., Jenuwein, T., Ryseck, R. P., Bravo, R., and Müller, R. (1989) The leucine repeat motif in Fos protein mediates complex formation with Jun/AP-1 and is required for transformation. *Cell* **56**, 507-516
90. Turner, R., and Tjian, R. (1989) Leucine repeats and an adjacent DNA binding domain mediate the formation of functional cFos-cJun heterodimers. *Science* **243**, 1689-1694
91. Halazonetis, T. D., Georgopoulos, K., Greenberg, M. E., and Leder, P. (1988) C-Jun dimerizes with itself and with c-Fos, forming complexes of different DNA binding affinities. *Cell* **55**, 917-924

92. Piette, J., Hirai, S., and Yaniv, M. (1988) Constitutive synthesis of activator protein 1 transcription factor after viral transformation of mouse fibroblasts. *Proceedings of the National Academy of Sciences of the United States of America* **85**, 3401-3405
93. Angel, P., and Karin, M. (1991) The role of Jun, Fos and the AP-1 complex in cell-proliferation and transformation. *Biochimica et biophysica acta* **1072**, 129-157
94. Hai, T. W., Liu, F., Coukos, W. J., and Green, M. R. (1989) Transcription factor ATF cDNA clones: an extensive family of leucine zipper proteins able to selectively form DNA-binding heterodimers. *Genes & development* **3**, 2083-2090
95. Chanda, S. K., White, S., Orth, A. P., Reisdorph, R., Miraglia, L., Thomas, R. S., DeJesus, P., Mason, D. E., Huang, Q., Vega, R., Yu, D. H., Nelson, C. G., Smith, B. M., Terry, R., Linford, A. S., Yu, Y., Chirn, G. W., Song, C., Labow, M. A., Cohen, D., King, F. J., Peters, E. C., Schultz, P. G., Vogt, P. K., Hogenesch, J. B., and Caldwell, J. S. (2003) Genome-scale functional profiling of the mammalian AP-1 signaling pathway. *Proceedings of the National Academy of Sciences of the United States of America* **100**, 12153-12158
96. O'Shea, E. K., Rutkowski, R., and Kim, P. S. (1989) Evidence that the leucine zipper is a coiled coil. *Science* **243**, 538-542
97. Glover, J. N., and Harrison, S. C. (1995) Crystal structure of the heterodimeric bZIP transcription factor c-Fos-c-Jun bound to DNA. *Nature* **373**, 257-261
98. Prendergast, G. C., and Ziff, E. B. (1989) DNA-binding motif. *Nature* **341**, 392
99. Landschulz, W. H., Johnson, P. F., and McKnight, S. L. (1988) The leucine zipper: a hypothetical structure common to a new class of DNA binding proteins. *Science* **240**, 1759-1764
100. Gentz, R., Rauscher, F. J., 3rd, Abate, C., and Curran, T. (1989) Parallel association of Fos and Jun leucine zippers juxtaposes DNA binding domains. *Science* **243**, 1695-1699
101. Chida, K., and Vogt, P. K. (1992) Nuclear translocation of viral Jun but not of cellular Jun is cell cycle dependent. *Proceedings of the National Academy of Sciences of the United States of America* **89**, 4290-4294
102. Alani, R., Brown, P., Binetruy, B., Dosaka, H., Rosenberg, R. K., Angel, P., Karin, M., and Birrer, M. J. (1991) The transactivating domain of the c-Jun proto-oncoprotein is required for cotransformation of rat embryo cells. *Molecular and cellular biology* **11**, 6286-6295
103. Deng, T., and Karin, M. (1993) JunB differs from c-Jun in its DNA-binding and dimerization domains, and represses c-Jun by formation of inactive heterodimers. *Genes & development* **7**, 479-490
104. Jooss, K. U., Funk, M., and Muller, R. (1994) An autonomous N-terminal transactivation domain in Fos protein plays a crucial role in transformation. *EMBO J* **13**, 1467-1475
105. McBride, K., and Nemer, M. (1998) The C-terminal domain of c-fos is required for activation of an AP-1 site specific for jun-fos heterodimers. *Molecular and cellular biology* **18**, 5073-5081
106. Metz, R., Kouzarides, T., and Bravo, R. (1994) A C-terminal domain in FosB, absent in FosB/SF and Fra-1, which is able to interact with the TATA binding protein, is required for altered cell growth. *The EMBO journal* **13**, 3832-3842
107. Wisdon, R., and Verma, I. M. (1993) Transformation by Fos proteins requires a C-terminal transactivation domain. *Molecular and cellular biology* **13**, 7429-7438

108. Schiffer, M., and Edmundson, A. B. (1967) Use of helical wheels to represent the structures of proteins and to identify segments with helical potential. *Biophysical journal* **7**, 121-135
109. Schrodinger, LLC. (2010) The PyMOL Molecular Graphics System, Version 1.3r1.
110. Ryder, K., Lau, L. F., and Nathans, D. (1988) A gene activated by growth factors is related to the oncogene v-jun. *Proceedings of the National Academy of Sciences of the United States of America* **85**, 1487-1491
111. Schutte, J., Viallet, J., Nau, M., Segal, S., Fedorko, J., and Minna, J. (1989) jun-B inhibits and c-fos stimulates the transforming and trans-activating activities of c-jun. *Cell* **59**, 987-997
112. Chiu, R., Angel, P., and Karin, M. (1989) Jun-B differs in its biological properties from, and is a negative regulator of, c-Jun. *Cell* **59**, 979-986
113. Passegue, E., and Wagner, E. F. (2000) JunB suppresses cell proliferation by transcriptional activation of p16(INK4a) expression. *Embo J* **19**, 2969-2979
114. Andrecht, S., Kolbus, A., Hartenstein, B., Angel, P., and Schorpp-Kistner, M. (2002) Cell cycle promoting activity of JunB through cyclin A activation. *The Journal of biological chemistry* **277**, 35961-35968
115. Kovary, K., and Bravo, R. (1991) The jun and fos protein families are both required for cell cycle progression in fibroblasts. *Molecular and cellular biology* **11**, 4466-4472
116. Schorpp-Kistner, M., Wang, Z. Q., Angel, P., and Wagner, E. F. (1999) JunB is essential for mammalian placentation. *Embo J* **18**, 934-948
117. Passegue, E., Jochum, W., Behrens, A., Ricci, R., and Wagner, E. F. (2002) JunB can substitute for Jun in mouse development and cell proliferation. *Nature genetics* **30**, 158-166
118. Passegue, E., Jochum, W., Schorpp-Kistner, M., Mohle-Steinlein, U., and Wagner, E. F. (2001) Chronic myeloid leukemia with increased granulocyte progenitors in mice lacking junB expression in the myeloid lineage. *Cell* **104**, 21-32
119. Kenner, L., Hoebertz, A., Beil, F. T., Keon, N., Karreth, F., Eferl, R., Scheuch, H., Szremska, A., Amling, M., Schorpp-Kistner, M., Angel, P., and Wagner, E. F. (2004) Mice lacking JunB are osteopenic due to cell-autonomous osteoblast and osteoclast defects. *The Journal of cell biology* **164**, 613-623
120. Smith-Garvin, J. E., Koretzky, G. A., and Jordan, M. S. (2009) T Cell Activation. *Annual review of immunology* **27**, 591-619
121. Savignac, M., Mellstrom, B., and Naranjo, J. R. (2007) Calcium-dependent transcription of cytokine genes in T lymphocytes. *Pflugers Archiv : European journal of physiology* **454**, 523-533
122. Rao, A., Luo, C., and Hogan, P. G. (1997) Transcription factors of the NFAT family: regulation and function. *Annual review of immunology* **15**, 707-747
123. Zhu, J., and Paul, W. E. (2008) CD4 T cells: fates, functions, and faults. *Blood* **112**, 1557-1569
124. Carding, S. R., West, J., Woods, A., and Bottomly, K. (1989) Differential activation of cytokine genes in normal CD4-bearing T cells is stimulus dependent. *European journal of immunology* **19**, 231-238
125. Firestein, G. S., Roeder, W. D., Laxer, J. A., Townsend, K. S., Weaver, C. T., Hom, J. T., Linton, J., Torbett, B. E., and Glasebrook, A. L. (1989) A new murine CD4+ T cell subset with an unrestricted cytokine profile. *J Immunol* **143**, 518-525

126. Openshaw, P., Murphy, E. E., Hosken, N. A., Maino, V., Davis, K., Murphy, K., and O'Garra, A. (1995) Heterogeneity of intracellular cytokine synthesis at the single-cell level in polarized T helper 1 and T helper 2 populations. *The Journal of experimental medicine* **182**, 1357-1367
127. Paliard, X., de Waal Malefijt, R., Yssel, H., Blanchard, D., Chretien, I., Abrams, J., de Vries, J., and Spits, H. (1988) Simultaneous production of IL-2, IL-4, and IFN-gamma by activated human CD4+ and CD8+ T cell clones. *J Immunol* **141**, 849-855
128. Mowen, K. A., and Glimcher, L. H. (2004) Signaling pathways in Th2 development. *Immunological reviews* **202**, 203-222
129. Murphy, K. M., and Reiner, S. L. (2002) The lineage decisions of helper T cells. *Nature reviews. Immunology* **2**, 933-944
130. Hsieh, C. S., Heimberger, A. B., Gold, J. S., O'Garra, A., and Murphy, K. M. (1992) Differential regulation of T helper phenotype development by interleukins 4 and 10 in an alpha beta T-cell-receptor transgenic system. *Proceedings of the National Academy of Sciences of the United States of America* **89**, 6065-6069
131. Le Gros, G., Ben-Sasson, S. Z., Seder, R., Finkelman, F. D., and Paul, W. E. (1990) Generation of interleukin 4 (IL-4)-producing cells in vivo and in vitro: IL-2 and IL-4 are required for in vitro generation of IL-4-producing cells. *The Journal of experimental medicine* **172**, 921-929
132. Li, B., Tournier, C., Davis, R. J., and Flavell, R. A. (1999) Regulation of IL-4 expression by the transcription factor JunB during T helper cell differentiation. *Embo J* **18**, 420-432
133. Seder, R. A., Gazzinelli, R., Sher, A., and Paul, W. E. (1993) Interleukin 12 acts directly on CD4+ T cells to enhance priming for interferon gamma production and diminishes interleukin 4 inhibition of such priming. *Proceedings of the National Academy of Sciences of the United States of America* **90**, 10188-10192
134. Seder, R. A., Paul, W. E., Davis, M. M., and Fazekas de St Groth, B. (1992) The presence of interleukin 4 during in vitro priming determines the lymphokine-producing potential of CD4+ T cells from T cell receptor transgenic mice. *The Journal of experimental medicine* **176**, 1091-1098
135. Rincon, M., Derijard, B., Chow, C. W., Davis, R. J., and Flavell, R. A. (1997) Reprogramming the signalling requirement for AP-1 (activator protein-1) activation during differentiation of precursor CD4+ T-cells into effector Th1 and Th2 cells. *Genes and function* **1**, 51-68
136. Rincon, M., and Flavell, R. A. (1997) T-cell subsets: transcriptional control in the Th1/Th2 decision. *Current biology : CB* **7**, R729-732
137. Rincon, M., and Flavell, R. A. (1997) Regulation of the activity of the transcription factors AP-1 and NFAT during differentiation of precursor CD4+ T-cells into effector cells. *Biochemical Society transactions* **25**, 347-354
138. Kovary, K., and Bravo, R. (1991) Expression of different Jun and Fos proteins during the G0-to-G1 transition in mouse fibroblasts: in vitro and in vivo associations. *Molecular and cellular biology* **11**, 2451-2459
139. Franklin, C. C., Sanchez, V., Wagner, F., Woodgett, J. R., and Kraft, A. S. (1992) Phorbol ester-induced amino-terminal phosphorylation of human JUN but not JUNB regulates transcriptional activation. *Proceedings of the National Academy of Sciences of the United States of America* **89**, 7247-7251

140. Kallunki, T., Deng, T., Hibi, M., and Karin, M. (1996) c-Jun can recruit JNK to phosphorylate dimerization partners via specific docking interactions. *Cell* **87**, 929-939
141. Narayanan, K., Srinivas, R., Peterson, M. C., Ramachandran, A., Hao, J., Thimmapaya, B., Scherer, P. E., and George, A. (2004) Transcriptional regulation of dentin matrix protein 1 by JunB and p300 during osteoblast differentiation. *The Journal of biological chemistry* **279**, 44294-44302
142. Farras, R., Baldin, V., Gallach, S., Acquaviva, C., Bossis, G., Jariel-Encontre, I., and Piechaczyk, M. (2008) JunB breakdown in mid-/late G2 is required for down-regulation of cyclin A2 levels and proper mitosis. *Molecular and cellular biology* **28**, 4173-4187
143. Bakiri, L., Lallemand, D., Bossy-Wetzel, E., and Yaniv, M. (2000) Cell cycle-dependent variations in c-Jun and JunB phosphorylation: a role in the control of cyclin D1 expression. *Embo J* **19**, 2056-2068
144. Welcker, M., and Clurman, B. E. (2008) FBW7 ubiquitin ligase: a tumour suppressor at the crossroads of cell division, growth and differentiation. *Nat Rev Cancer* **8**, 83-93
145. Perez-Benavente, B., Garcia, J. L., Rodriguez, M. S., Pineda-Lucena, A., Piechaczyk, M., Font de Mora, J., and Farras, R. (2012) GSK3-SCF(FBXW7) targets JunB for degradation in G2 to preserve chromatid cohesion before anaphase. *Oncogene*
146. Boyle, W. J., Smeal, T., Defize, L. H., Angel, P., Woodgett, J. R., Karin, M., and Hunter, T. (1991) Activation of protein kinase C decreases phosphorylation of c-Jun at sites that negatively regulate its DNA-binding activity. *Cell* **64**, 573-584
147. Gao, M., Labuda, T., Xia, Y., Gallagher, E., Fang, D., Liu, Y. C., and Karin, M. (2004) Jun turnover is controlled through JNK-dependent phosphorylation of the E3 ligase Itch. *Science* **306**, 271-275
148. Zhao, L., Huang, J., Guo, R., Wang, Y., Chen, D., and Xing, L. (2010) Smurf1 inhibits mesenchymal stem cell proliferation and differentiation into osteoblasts through JunB degradation. *Journal of bone and mineral research : the official journal of the American Society for Bone and Mineral Research* **25**, 1246-1256
149. Migliorini, D., Bogaerts, S., Defever, D., Vyas, R., Denecker, G., Radaelli, E., Zwolinska, A., Depaepe, V., Hochepied, T., Skarnes, W. C., and Marine, J. C. (2011) Cop1 constitutively regulates c-Jun protein stability and functions as a tumor suppressor in mice. *The Journal of clinical investigation* **121**, 1329-1343
150. Wertz, I. E., O'Rourke, K. M., Zhang, Z., Dornan, D., Arnott, D., Deshaies, R. J., and Dixit, V. M. (2004) Human De-etiolated-1 regulates c-Jun by assembling a CUL4A ubiquitin ligase. *Science* **303**, 1371-1374
151. van Dam, H., Huguier, S., Kooistra, K., Baguet, J., Vial, E., van der Eb, A. J., Herrlich, P., Angel, P., and Castellazzi, M. (1998) Autocrine growth and anchorage independence: two complementing Jun-controlled genetic programs of cellular transformation. *Genes & development* **12**, 1227-1239
152. Behrens, A., Jochum, W., Sibilia, M., and Wagner, E. F. (2000) Oncogenic transformation by ras and fos is mediated by c-Jun N-terminal phosphorylation. *Oncogene* **19**, 2657-2663
153. Smith, L. M., Wise, S. C., Hendricks, D. T., Sabichi, A. L., Bos, T., Reddy, P., Brown, P. H., and Birrer, M. J. (1999) cJun overexpression in MCF-7 breast cancer cells

produces a tumorigenic, invasive and hormone resistant phenotype. *Oncogene* **18**, 6063-6070

154. Szremska, A. P., Kenner, L., Weisz, E., Ott, R. G., Passegue, E., Artwohl, M., Freissmuth, M., Stoxreiter, R., Theussl, H. C., Parzer, S. B., Moriggl, R., Wagner, E. F., and Sexl, V. (2003) JunB inhibits proliferation and transformation in B-lymphoid cells. *Blood* **102**, 4159-4165
155. Mathas, S., Hinz, M., Anagnostopoulos, I., Krappmann, D., Lietz, A., Jundt, F., Bommert, K., Mechta-Grigoriou, F., Stein, H., Dorken, B., and Scheidereit, C. (2002) Aberrantly expressed c-Jun and JunB are a hallmark of Hodgkin lymphoma cells, stimulate proliferation and synergize with NF-kappa B. *Embo J* **21**, 4104-4113
156. Rassidakis, G. Z., Thomaides, A., Atwell, C., Ford, R., Jones, D., Claret, F. X., and Medeiros, L. J. (2005) JunB expression is a common feature of CD30+ lymphomas and lymphomatoid papulosis. *Mod Pathol* **18**, 1365-1370
157. Watanabe, M., Ogawa, Y., Ito, K., Higashihara, M., Kadin, M. E., Abraham, L. J., Watanabe, T., and Horie, R. (2003) AP-1 mediated relief of repressive activity of the CD30 promoter microsatellite in Hodgkin and Reed-Sternberg cells. *Am J Pathol* **163**, 633-641
158. Watanabe, M., Itoh, K., Togano, T., Kadin, M. E., Watanabe, T., Higashihara, M., and Horie, R. (2012) Ets-1 activates overexpression of JunB and CD30 in Hodgkin's lymphoma and anaplastic large-cell lymphoma. *Am J Pathol* **180**, 831-838
159. Watanabe, M., Sasaki, M., Itoh, K., Higashihara, M., Umezawa, K., Kadin, M. E., Abraham, L. J., Watanabe, T., and Horie, R. (2005) JunB induced by constitutive CD30-extracellular signal-regulated kinase 1/2 mitogen-activated protein kinase signaling activates the CD30 promoter in anaplastic large cell lymphoma and reed-sternberg cells of Hodgkin lymphoma. *Cancer research* **65**, 7628-7634
160. Pearson, J. D., Lee, J. K., Bacani, J. T., Lai, R., and Ingham, R. J. (2011) NPM-ALK and the JunB transcription factor regulate the expression of cytotoxic molecules in ALK-positive, anaplastic large cell lymphoma. *International journal of clinical and experimental pathology* **4**, 124-133
161. Laimer, D., Dolznig, H., Kollmann, K., Vesely, P. W., Schlederer, M., Merkel, O., Schiefer, A. I., Hassler, M. R., Heider, S., Amenitsch, L., Thallinger, C., Staber, P. B., Simonitsch-Klupp, I., Artaker, M., Lagger, S., Turner, S. D., Pileri, S., Piccaluga, P. P., Valent, P., Messana, K., Landra, I., Weichhart, T., Knapp, S., Shehata, M., Todaro, M., Sexl, V., Hofler, G., Piva, R., Medico, E., Ruggeri, B. A., Cheng, M., Eferl, R., Egger, G., Penninger, J. M., Jaeger, U., Moriggl, R., Inghirami, G., and Kenner, L. (2012) PDGFR blockade is a rational and effective therapy for NPM-ALK-driven lymphomas. *Nature medicine* **18**, 1699-1704
162. Drakos, E., Leventaki, V., Schlette, E. J., Jones, D., Lin, P., Medeiros, L. J., and Rassidakis, G. Z. (2007) c-Jun expression and activation are restricted to CD30+ lymphoproliferative disorders. *The American journal of surgical pathology* **31**, 447-453
163. Arias, J., Alberts, A. S., Brindle, P., Claret, F. X., Smeal, T., Karin, M., Feramisco, J., and Montminy, M. (1994) Activation of cAMP and mitogen responsive genes relies on a common nuclear factor. *Nature* **370**, 226-229
164. Hsu, F. Y., Johnston, P. B., Burke, K. A., and Zhao, Y. (2006) The expression of CD30 in anaplastic large cell lymphoma is regulated by nucleophosmin-

anaplastic lymphoma kinase-mediated JunB level in a cell type-specific manner. *Cancer research* **66**, 9002-9008
165. Fuchs, Y., and Steller, H. (2011) Programmed cell death in animal development and disease. *Cell* **147**, 742-758
166. Friedlander, R. M. (2003) Apoptosis and caspases in neurodegenerative diseases. *The New England journal of medicine* **348**, 1365-1375
167. Hanahan, D., and Weinberg, R. A. (2011) Hallmarks of cancer: the next generation. *Cell* **144**, 646-674
168. Kelly, G. L., and Strasser, A. (2011) The essential role of evasion from cell death in cancer. *Advances in cancer research* **111**, 39-96
169. Nagata, S. (2010) Apoptosis and autoimmune diseases. *Annals of the New York Academy of Sciences* **1209**, 10-16
170. Maniati, E., Potter, P., Rogers, N. J., and Morley, B. J. (2008) Control of apoptosis in autoimmunity. *The Journal of pathology* **214**, 190-198
171. Jin, Z., and El-Deiry, W. S. (2005) Overview of cell death signaling pathways. *Cancer biology & therapy* **4**, 139-163
172. Crawford, E. D., and Wells, J. A. (2011) Caspase substrates and cellular remodeling. *Annual review of biochemistry* **80**, 1055-1087
173. Meier, P., Finch, A., and Evan, G. (2000) Apoptosis in development. *Nature* **407**, 796-801
174. Vaux, D. L., and Korsmeyer, S. J. (1999) Cell death in development. *Cell* **96**, 245-254
175. Ellis, H. M., and Horvitz, H. R. (1986) Genetic control of programmed cell death in the nematode C. elegans. *Cell* **44**, 817-829
176. Hisahara, S., Kanuka, H., Shoji, S., Yoshikawa, S., Okano, H., and Miura, M. (1998) Caenorhabditis elegans anti-apoptotic gene ced-9 prevents ced-3-induced cell death in Drosophila cells. *Journal of cell science* **111 (Pt 6)**, 667-673
177. Brison, D. R., and Schultz, R. M. (1997) Apoptosis during mouse blastocyst formation: evidence for a role for survival factors including transforming growth factor alpha. *Biology of reproduction* **56**, 1088-1096
178. Coucouvanis, E. C., Martin, G. R., and Nadeau, J. H. (1995) Genetic approaches for studying programmed cell death during development of the laboratory mouse. *Methods in cell biology* **46**, 387-440
179. Milligan, C. E., Prevette, D., Yaginuma, H., Homma, S., Cardwell, C., Fritz, L. C., Tomaselli, K. J., Oppenheim, R. W., and Schwartz, L. M. (1995) Peptide inhibitors of the ICE protease family arrest programmed cell death of motoneurons in vivo and in vitro. *Neuron* **15**, 385-393
180. Bergmann, A., and Steller, H. (2010) Apoptosis, stem cells, and tissue regeneration. *Science signaling* **3**, re8
181. Opferman, J. T., and Korsmeyer, S. J. (2003) Apoptosis in the development and maintenance of the immune system. *Nature immunology* **4**, 410-415
182. Barry, M., and Bleackley, R. C. (2002) Cytotoxic T lymphocytes: all roads lead to death. *Nature reviews. Immunology* **2**, 401-409
183. Russell, J. H., and Ley, T. J. (2002) Lymphocyte-mediated cytotoxicity. *Annual review of immunology* **20**, 323-370
184. Vandivier, R. W., Henson, P. M., and Douglas, I. S. (2006) Burying the dead: the impact of failed apoptotic cell removal (efferocytosis) on chronic inflammatory lung disease. *Chest* **129**, 1673-1682

185. Li, M. O., Sarkisian, M. R., Mehal, W. Z., Rakic, P., and Flavell, R. A. (2003) Phosphatidylserine receptor is required for clearance of apoptotic cells. *Science* **302**, 1560-1563
186. Wang, X., Wu, Y. C., Fadok, V. A., Lee, M. C., Gengyo-Ando, K., Cheng, L. C., Ledwich, D., Hsu, P. K., Chen, J. Y., Chou, B. K., Henson, P., Mitani, S., and Xue, D. (2003) Cell corpse engulfment mediated by C. elegans phosphatidylserine receptor through CED-5 and CED-12. *Science* **302**, 1563-1566
187. Hoffmann, P. R., deCathelineau, A. M., Ogden, C. A., Leverrier, Y., Bratton, D. L., Daleke, D. L., Ridley, A. J., Fadok, V. A., and Henson, P. M. (2001) Phosphatidylserine (PS) induces PS receptor-mediated macropinocytosis and promotes clearance of apoptotic cells. *The Journal of cell biology* **155**, 649-659
188. Gershov, D., Kim, S., Brot, N., and Elkon, K. B. (2000) C-Reactive protein binds to apoptotic cells, protects the cells from assembly of the terminal complement components, and sustains an antiinflammatory innate immune response: implications for systemic autoimmunity. *The Journal of experimental medicine* **192**, 1353-1364
189. Huynh, M. L., Fadok, V. A., and Henson, P. M. (2002) Phosphatidylserine-dependent ingestion of apoptotic cells promotes TGF-beta1 secretion and the resolution of inflammation. *The Journal of clinical investigation* **109**, 41-50
190. Gregory, C. D., and Devitt, A. (2004) The macrophage and the apoptotic cell: an innate immune interaction viewed simplistically? *Immunology* **113**, 1-14
191. Ashkenazi, A., and Dixit, V. M. (1998) Death receptors: signaling and modulation. *Science* **281**, 1305-1308
192. Schulze-Osthoff, K., Ferrari, D., Los, M., Wesselborg, S., and Peter, M. E. (1998) Apoptosis signaling by death receptors. *European journal of biochemistry / FEBS* **254**, 439-459
193. Tartaglia, L. A., Pennica, D., and Goeddel, D. V. (1993) Ligand passing: the 75-kDa tumor necrosis factor (TNF) receptor recruits TNF for signaling by the 55-kDa TNF receptor. *The Journal of biological chemistry* **268**, 18542-18548
194. Walczak, H., Degli-Esposti, M. A., Johnson, R. S., Smolak, P. J., Waugh, J. Y., Boiani, N., Timour, M. S., Gerhart, M. J., Schooley, K. A., Smith, C. A., Goodwin, R. G., and Rauch, C. T. (1997) TRAIL-R2: a novel apoptosis-mediating receptor for TRAIL. *Embo J* **16**, 5386-5397
195. Tartaglia, L. A., Ayres, T. M., Wong, G. H., and Goeddel, D. V. (1993) A novel domain within the 55 kd TNF receptor signals cell death. *Cell* **74**, 845-853
196. Tartaglia, L. A., Rothe, M., Hu, Y. F., and Goeddel, D. V. (1993) Tumor necrosis factor's cytotoxic activity is signaled by the p55 TNF receptor. *Cell* **73**, 213-216
197. Suda, T., Takahashi, T., Golstein, P., and Nagata, S. (1993) Molecular cloning and expression of the Fas ligand, a novel member of the tumor necrosis factor family. *Cell* **75**, 1169-1178
198. Nagata, S. (1997) Apoptosis by death factor. *Cell* **88**, 355-365
199. Wallach, D., Varfolomeev, E. E., Malinin, N. L., Goltsev, Y. V., Kovalenko, A. V., and Boldin, M. P. (1999) Tumor necrosis factor receptor and Fas signaling mechanisms. *Annual review of immunology* **17**, 331-367
200. Chinnaiyan, A. M., O'Rourke, K., Yu, G. L., Lyons, R. H., Garg, M., Duan, D. R., Xing, L., Gentz, R., Ni, J., and Dixit, V. M. (1996) Signal transduction by DR3, a death domain-containing receptor related to TNFR-1 and CD95. *Science* **274**, 990-992

201. Pan, G., O'Rourke, K., Chinnaiyan, A. M., Gentz, R., Ebner, R., Ni, J., and Dixit, V. M. (1997) The receptor for the cytotoxic ligand TRAIL. *Science* **276**, 111-113
202. Muzio, M. (1998) Signalling by proteolysis: death receptors induce apoptosis. *International journal of clinical & laboratory research* **28**, 141-147
203. Chaudhary, P. M., Eby, M., Jasmin, A., Bookwalter, A., Murray, J., and Hood, L. (1997) Death receptor 5, a new member of the TNFR family, and DR4 induce FADD-dependent apoptosis and activate the NF-kappaB pathway. *Immunity* **7**, 821-830
204. Kelley, R. F., Totpal, K., Lindstrom, S. H., Mathieu, M., Billeci, K., Deforge, L., Pai, R., Hymowitz, S. G., and Ashkenazi, A. (2005) Receptor-selective mutants of apoptosis-inducing ligand 2/tumor necrosis factor-related apoptosis-inducing ligand reveal a greater contribution of death receptor (DR) 5 than DR4 to apoptosis signaling. *The Journal of biological chemistry* **280**, 2205-2212
205. Wiley, S. R., Schooley, K., Smolak, P. J., Din, W. S., Huang, C. P., Nicholl, J. K., Sutherland, G. R., Smith, T. D., Rauch, C., Smith, C. A., and et al. (1995) Identification and characterization of a new member of the TNF family that induces apoptosis. *Immunity* **3**, 673-682
206. Ashkenazi, A. (2002) Targeting death and decoy receptors of the tumour-necrosis factor superfamily. *Nat Rev Cancer* **2**, 420-430
207. Ashkenazi, A., and Dixit, V. M. (1999) Apoptosis control by death and decoy receptors. *Current opinion in cell biology* **11**, 255-260
208. LeBlanc, H. N., and Ashkenazi, A. (2003) Apo2L/TRAIL and its death and decoy receptors. *Cell death and differentiation* **10**, 66-75
209. Wajant, H., Pfizenmaier, K., and Scheurich, P. (2003) Tumor necrosis factor signaling. *Cell death and differentiation* **10**, 45-65
210. Micheau, O., and Tschopp, J. (2003) Induction of TNF receptor I-mediated apoptosis via two sequential signaling complexes. *Cell* **114**, 181-190
211. Rothe, M., Pan, M. G., Henzel, W. J., Ayres, T. M., and Goeddel, D. V. (1995) The TNFR2-TRAF signaling complex contains two novel proteins related to baculoviral inhibitor of apoptosis proteins. *Cell* **83**, 1243-1252
212. Pop, C., Fitzgerald, P., Green, D. R., and Salvesen, G. S. (2007) Role of proteolysis in caspase-8 activation and stabilization. *Biochemistry* **46**, 4398-4407
213. Chen, G., and Goeddel, D. V. (2002) TNF-R1 Signaling: A Beautiful Pathway. *Science* **296**, 1634-1635
214. Elmore, S. (2007) Apoptosis: a review of programmed cell death. *Toxicologic pathology* **35**, 495-516
215. Levine, A. J., and Oren, M. (2009) The first 30 years of p53: growing ever more complex. *Nat Rev Cancer* **9**, 749-758
216. Haupt, Y., Maya, R., Kazaz, A., and Oren, M. (1997) Mdm2 promotes the rapid degradation of p53. *Nature* **387**, 296-299
217. Honda, R., Tanaka, H., and Yasuda, H. (1997) Oncoprotein MDM2 is a ubiquitin ligase E3 for tumor suppressor p53. *FEBS letters* **420**, 25-27
218. Momand, J., Zambetti, G. P., Olson, D. C., George, D., and Levine, A. J. (1992) The mdm-2 oncogene product forms a complex with the p53 protein and inhibits p53-mediated transactivation. *Cell* **69**, 1237-1245
219. Vogelstein, B., Lane, D., and Levine, A. J. (2000) Surfing the p53 network. *Nature* **408**, 307-310

220. Fridman, J. S., and Lowe, S. W. (2003) Control of apoptosis by p53. *Oncogene* **22**, 9030-9040
221. Cory, S., and Adams, J. M. (2002) The Bcl2 family: regulators of the cellular life-or-death switch. *Nat Rev Cancer* **2**, 647-656
222. Youle, R. J., and Strasser, A. (2008) The BCL-2 protein family: opposing activities that mediate cell death. *Nature reviews. Molecular cell biology* **9**, 47-59
223. Marsden, V. S., O'Connor, L., O'Reilly, L. A., Silke, J., Metcalf, D., Ekert, P. G., Huang, D. C., Cecconi, F., Kuida, K., Tomaselli, K. J., Roy, S., Nicholson, D. W., Vaux, D. L., Bouillet, P., Adams, J. M., and Strasser, A. (2002) Apoptosis initiated by Bcl-2-regulated caspase activation independently of the cytochrome c/Apaf-1/caspase-9 apoptosome. *Nature* **419**, 634-637
224. Willis, S. N., Fletcher, J. I., Kaufmann, T., van Delft, M. F., Chen, L., Czabotar, P. E., Ierino, H., Lee, E. F., Fairlie, W. D., Bouillet, P., Strasser, A., Kluck, R. M., Adams, J. M., and Huang, D. C. (2007) Apoptosis initiated when BH3 ligands engage multiple Bcl-2 homologs, not Bax or Bak. *Science* **315**, 856-859
225. Green, D. R., and Kroemer, G. (2004) The pathophysiology of mitochondrial cell death. *Science* **305**, 626-629
226. Wolter, K. G., Hsu, Y. T., Smith, C. L., Nechushtan, A., Xi, X. G., and Youle, R. J. (1997) Movement of Bax from the cytosol to mitochondria during apoptosis. *The Journal of cell biology* **139**, 1281-1292
227. Esposti, M. D. (2002) The roles of Bid. *Apoptosis : an international journal on programmed cell death* **7**, 433-440
228. Li, H., Zhu, H., Xu, C. J., and Yuan, J. (1998) Cleavage of BID by caspase 8 mediates the mitochondrial damage in the Fas pathway of apoptosis. *Cell* **94**, 491-501
229. Kaufmann, T., Tai, L., Ekert, P. G., Huang, D. C., Norris, F., Lindemann, R. K., Johnstone, R. W., Dixit, V. M., and Strasser, A. (2007) The BH3-only protein bid is dispensable for DNA damage- and replicative stress-induced apoptosis or cell-cycle arrest. *Cell* **129**, 423-433
230. Saelens, X., Festjens, N., Vande Walle, L., van Gurp, M., van Loo, G., and Vandenabeele, P. (2004) Toxic proteins released from mitochondria in cell death. *Oncogene* **23**, 2861-2874
231. Chinnaiyan, A. M. (1999) The apoptosome: heart and soul of the cell death machine. *Neoplasia* **1**, 5-15
232. Hill, M. M., Adrain, C., Duriez, P. J., Creagh, E. M., and Martin, S. J. (2004) Analysis of the composition, assembly kinetics and activity of native Apaf-1 apoptosomes. *EMBO J* **23**, 2134-2145
233. Acehan, D., Jiang, X., Morgan, D. G., Heuser, J. E., Wang, X., and Akey, C. W. (2002) Three-dimensional structure of the apoptosome: implications for assembly, procaspase-9 binding, and activation. *Molecular cell* **9**, 423-432
234. Yu, X., Acehan, D., Menetret, J. F., Booth, C. R., Ludtke, S. J., Riedl, S. J., Shi, Y., Wang, X., and Akey, C. W. (2005) A structure of the human apoptosome at 12.8 A resolution provides insights into this cell death platform. *Structure (London, England : 1993)* **13**, 1725-1735
235. Trapani, J. A., and Smyth, M. J. (2002) Functional significance of the perforin/granzyme cell death pathway. *Nature reviews. Immunology* **2**, 735-747
236. Thornberry, N. A., Rano, T. A., Peterson, E. P., Rasper, D. M., Timkey, T., Garcia-Calvo, M., Houtzager, V. M., Nordstrom, P. A., Roy, S., Vaillancourt, J. P.,

Chapman, K. T., and Nicholson, D. W. (1997) A combinatorial approach defines specificities of members of the caspase family and granzyme B. Functional relationships established for key mediators of apoptosis. *The Journal of biological chemistry* **272**, 17907-17911

237. Darmon, A. J., Nicholson, D. W., and Bleackley, R. C. (1995) Activation of the apoptotic protease CPP32 by cytotoxic T-cell-derived granzyme B. *Nature* **377**, 446-448
238. Quan, L. T., Tewari, M., O'Rourke, K., Dixit, V., Snipas, S. J., Poirier, G. G., Ray, C., Pickup, D. J., and Salvesen, G. S. (1996) Proteolytic activation of the cell death protease Yama/CPP32 by granzyme B. *Proceedings of the National Academy of Sciences of the United States of America* **93**, 1972-1976
239. Sutton, V. R., Davis, J. E., Cancilla, M., Johnstone, R. W., Ruefli, A. A., Sedelies, K., Browne, K. A., and Trapani, J. A. (2000) Initiation of apoptosis by granzyme B requires direct cleavage of bid, but not direct granzyme B-mediated caspase activation. *The Journal of experimental medicine* **192**, 1403-1414
240. Sutton, V. R., Wowk, M. E., Cancilla, M., and Trapani, J. A. (2003) Caspase activation by granzyme B is indirect, and caspase autoprocessing requires the release of proapoptotic mitochondrial factors. *Immunity* **18**, 319-329
241. Waterhouse, N. J., Sedelies, K. A., Browne, K. A., Wowk, M. E., Newbold, A., Sutton, V. R., Clarke, C. J., Oliaro, J., Lindemann, R. K., Bird, P. I., Johnstone, R. W., and Trapani, J. A. (2005) A central role for Bid in granzyme B-induced apoptosis. *The Journal of biological chemistry* **280**, 4476-4482
242. Eckhart, L., Ballaun, C., Hermann, M., VandeBerg, J. L., Sipos, W., Uthman, A., Fischer, H., and Tschachler, E. (2008) Identification of novel mammalian caspases reveals an important role of gene loss in shaping the human caspase repertoire. *Molecular biology and evolution* **25**, 831-841
243. Fuentes-Prior, P., and Salvesen, G. S. (2004) The protein structures that shape caspase activity, specificity, activation and inhibition. *The Biochemical journal* **384**, 201-232
244. Pop, C., and Salvesen, G. S. (2009) Human caspases: activation, specificity, and regulation. *The Journal of biological chemistry* **284**, 21777-21781
245. Denecker, G., Hoste, E., Gilbert, B., Hochepied, T., Ovaere, P., Lippens, S., Van den Broecke, C., Van Damme, P., D'Herde, K., Hachem, J. P., Borgonie, G., Presland, R. B., Schoonjans, L., Libert, C., Vandekerckhove, J., Gevaert, K., Vandenabeele, P., and Declercq, W. (2007) Caspase-14 protects against epidermal UVB photodamage and water loss. *Nature cell biology* **9**, 666-674
246. Salvesen, G. S., and Abrams, J. M. (2004) Caspase activation - stepping on the gas or releasing the brakes? Lessons from humans and flies. *Oncogene* **23**, 2774-2784
247. Boatright, K. M., Renatus, M., Scott, F. L., Sperandio, S., Shin, H., Pedersen, I. M., Ricci, J. E., Edris, W. A., Sutherlin, D. P., Green, D. R., and Salvesen, G. S. (2003) A unified model for apical caspase activation. *Molecular cell* **11**, 529-541
248. Rodriguez, J., and Lazebnik, Y. (1999) Caspase-9 and APAF-1 form an active holoenzyme. *Genes & development* **13**, 3179-3184
249. Shi, Y. (2004) Caspase activation: revisiting the induced proximity model. *Cell* **117**, 855-858

250. Shiozaki, E. N., Chai, J., and Shi, Y. (2002) Oligomerization and activation of caspase-9, induced by Apaf-1 CARD. *Proceedings of the National Academy of Sciences of the United States of America* **99**, 4197-4202
251. Pop, C., Timmer, J., Sperandio, S., and Salvesen, G. S. (2006) The apoptosome activates caspase-9 by dimerization. *Molecular cell* **22**, 269-275
252. Lassus, P., Opitz-Araya, X., and Lazebnik, Y. (2002) Requirement for caspase-2 in stress-induced apoptosis before mitochondrial permeabilization. *Science* **297**, 1352-1354
253. Troy, C. M., Rabacchi, S. A., Friedman, W. J., Frappier, T. F., Brown, K., and Shelanski, M. L. (2000) Caspase-2 mediates neuronal cell death induced by beta-amyloid. *The Journal of neuroscience : the official journal of the Society for Neuroscience* **20**, 1386-1392
254. Tinel, A., and Tschopp, J. (2004) The PIDDosome, a protein complex implicated in activation of caspase-2 in response to genotoxic stress. *Science* **304**, 843-846
255. Berube, C., Boucher, L. M., Ma, W., Wakeham, A., Salmena, L., Hakem, R., Yeh, W. C., Mak, T. W., and Benchimol, S. (2005) Apoptosis caused by p53-induced protein with death domain (PIDD) depends on the death adapter protein RAIDD. *Proceedings of the National Academy of Sciences of the United States of America* **102**, 14314-14320
256. Bouchier-Hayes, L., Oberst, A., McStay, G. P., Connell, S., Tait, S. W., Dillon, C. P., Flanagan, J. M., Beere, H. M., and Green, D. R. (2009) Characterization of cytoplasmic caspase-2 activation by induced proximity. *Molecular cell* **35**, 830-840
257. Janssens, S., Tinel, A., Lippens, S., and Tschopp, J. (2005) PIDD mediates NF-kappaB activation in response to DNA damage. *Cell* **123**, 1079-1092
258. Ando, K., Kernan, J. L., Liu, P. H., Sanda, T., Logette, E., Tschopp, J., Look, A. T., Wang, J., Bouchier-Hayes, L., and Sidi, S. (2012) PIDD death-domain phosphorylation by ATM controls prodeath versus prosurvival PIDDosome signaling. *Molecular cell* **47**, 681-693
259. Tinel, A., Janssens, S., Lippens, S., Cuenin, S., Logette, E., Jaccard, B., Quadroni, M., and Tschopp, J. (2007) Autoproteolysis of PIDD marks the bifurcation between pro-death caspase-2 and pro-survival NF-kappaB pathway. *Embo J* **26**, 197-208
260. Kumar, S. (2009) Caspase 2 in apoptosis, the DNA damage response and tumour suppression: enigma no more? *Nat Rev Cancer* **9**, 897-903
261. Yang, X., Stennicke, H. R., Wang, B., Green, D. R., Janicke, R. U., Srinivasan, A., Seth, P., Salvesen, G. S., and Froelich, C. J. (1998) Granzyme B mimics apical caspases. Description of a unified pathway for trans-activation of executioner caspase-3 and -7. *The Journal of biological chemistry* **273**, 34278-34283
262. Stennicke, H. R., Jurgensmeier, J. M., Shin, H., Deveraux, Q., Wolf, B. B., Yang, X., Zhou, Q., Ellerby, H. M., Ellerby, L. M., Bredesen, D., Green, D. R., Reed, J. C., Froelich, C. J., and Salvesen, G. S. (1998) Pro-caspase-3 is a major physiologic target of caspase-8. *The Journal of biological chemistry* **273**, 27084-27090
263. Chai, J., Wu, Q., Shiozaki, E., Srinivasula, S. M., Alnemri, E. S., and Shi, Y. (2001) Crystal structure of a procaspase-7 zymogen: mechanisms of activation and substrate binding. *Cell* **107**, 399-407
264. Riedl, S. J., Fuentes-Prior, P., Renatus, M., Kairies, N., Krapp, S., Huber, R., Salvesen, G. S., and Bode, W. (2001) Structural basis for the activation of human

procaspase-7. *Proceedings of the National Academy of Sciences of the United States of America* **98**, 14790-14795

265. Riedl, S. J., Renatus, M., Schwarzenbacher, R., Zhou, Q., Sun, C., Fesik, S. W., Liddington, R. C., and Salvesen, G. S. (2001) Structural basis for the inhibition of caspase-3 by XIAP. *Cell* **104**, 791-800
266. Riedl, S. J., Renatus, M., Snipas, S. J., and Salvesen, G. S. (2001) Mechanism-based inactivation of caspases by the apoptotic suppressor p35. *Biochemistry* **40**, 13274-13280
267. Wei, Y., Fox, T., Chambers, S. P., Sintchak, J., Coll, J. T., Golec, J. M., Swenson, L., Wilson, K. P., and Charifson, P. S. (2000) The structures of caspases-1, -3, -7 and -8 reveal the basis for substrate and inhibitor selectivity. *Chemistry & biology* **7**, 423-432
268. Timmer, J. C., and Salvesen, G. S. (2007) Caspase substrates. *Cell death and differentiation* **14**, 66-72
269. Rawlings, N. D., and Barrett, A. J. (1993) Evolutionary families of peptidases. *The Biochemical journal* **290 (Pt 1)**, 205-218
270. Datta, D., Scheer, J. M., Romanowski, M. J., and Wells, J. A. (2008) An allosteric circuit in caspase-1. *Journal of molecular biology* **381**, 1157-1167
271. Denault, J. B., Bekes, M., Scott, F. L., Sexton, K. M., Bogyo, M., and Salvesen, G. S. (2006) Engineered hybrid dimers: tracking the activation pathway of caspase-7. *Molecular cell* **23**, 523-533
272. Schechter, I., and Berger, A. (1967) On the size of the active site in proteases. I. Papain. *Biochem Biophys Res Commun* **27**, 157-162
273. Stennicke, H. R., and Salvesen, G. S. (1999) Catalytic properties of the caspases. *Cell death and differentiation* **6**, 1054-1059
274. Hawkins, C. J., Yoo, S. J., Peterson, E. P., Wang, S. L., Vernooy, S. Y., and Hay, B. A. (2000) The Drosophila caspase DRONC cleaves following glutamate or aspartate and is regulated by DIAP1, HID, and GRIM. *The Journal of biological chemistry* **275**, 27084-27093
275. Krippner-Heidenreich, A., Talanian, R. V., Sekul, R., Kraft, R., Thole, H., Ottleben, H., and Luscher, B. (2001) Targeting of the transcription factor Max during apoptosis: phosphorylation-regulated cleavage by caspase-5 at an unusual glutamic acid residue in position P1. *The Biochemical journal* **358**, 705-715
276. Mahrus, S., Trinidad, J. C., Barkan, D. T., Sali, A., Burlingame, A. L., and Wells, J. A. (2008) Global sequencing of proteolytic cleavage sites in apoptosis by specific labeling of protein N termini. *Cell* **134**, 866-876
277. Stennicke, H. R., Renatus, M., Meldal, M., and Salvesen, G. S. (2000) Internally quenched fluorescent peptide substrates disclose the subsite preferences of human caspases 1, 3, 6, 7 and 8. *The Biochemical journal* **350 Pt 2**, 563-568
278. Talanian, R. V., Quinlan, C., Trautz, S., Hackett, M. C., Mankovich, J. A., Banach, D., Ghayur, T., Brady, K. D., and Wong, W. W. (1997) Substrate specificities of caspase family proteases. *The Journal of biological chemistry* **272**, 9677-9682
279. Xu, G., Cirilli, M., Huang, Y., Rich, R. L., Myszka, D. G., and Wu, H. (2001) Covalent inhibition revealed by the crystal structure of the caspase-8/p35 complex. *Nature* **410**, 494-497
280. Hacker, G. (2000) The morphology of apoptosis. *Cell and tissue research* **301**, 5-17

281. Taylor, R. C., Cullen, S. P., and Martin, S. J. (2008) Apoptosis: controlled demolition at the cellular level. *Nature reviews. Molecular cell biology* **9**, 231-241
282. Luthi, A. U., and Martin, S. J. (2007) The CASBAH: a searchable database of caspase substrates. *Cell death and differentiation* **14**, 641-650
283. Takahashi, A., Alnemri, E. S., Lazebnik, Y. A., Fernandes-Alnemri, T., Litwack, G., Moir, R. D., Goldman, R. D., Poirier, G. G., Kaufmann, S. H., and Earnshaw, W. C. (1996) Cleavage of lamin A by Mch2 alpha but not CPP32: multiple interleukin 1 beta-converting enzyme-related proteases with distinct substrate recognition properties are active in apoptosis. *Proceedings of the National Academy of Sciences of the United States of America* **93**, 8395-8400
284. Orth, K., Chinnaiyan, A. M., Garg, M., Froelich, C. J., and Dixit, V. M. (1996) The CED-3/ICE-like protease Mch2 is activated during apoptosis and cleaves the death substrate lamin A. *The Journal of biological chemistry* **271**, 16443-16446
285. Lazebnik, Y. A., Takahashi, A., Moir, R. D., Goldman, R. D., Poirier, G. G., Kaufmann, S. H., and Earnshaw, W. C. (1995) Studies of the lamin proteinase reveal multiple parallel biochemical pathways during apoptotic execution. *Proceedings of the National Academy of Sciences of the United States of America* **92**, 9042-9046
286. Enari, M., Sakahira, H., Yokoyama, H., Okawa, K., Iwamatsu, A., and Nagata, S. (1998) A caspase-activated DNase that degrades DNA during apoptosis, and its inhibitor ICAD. *Nature* **391**, 43-50
287. Liu, X., Li, P., Widlak, P., Zou, H., Luo, X., Garrard, W. T., and Wang, X. (1998) The 40-kDa subunit of DNA fragmentation factor induces DNA fragmentation and chromatin condensation during apoptosis. *Proceedings of the National Academy of Sciences of the United States of America* **95**, 8461-8466
288. Sakahira, H., Enari, M., and Nagata, S. (1998) Cleavage of CAD inhibitor in CAD activation and DNA degradation during apoptosis. *Nature* **391**, 96-99
289. Kaufmann, S. H., Desnoyers, S., Ottaviano, Y., Davidson, N. E., and Poirier, G. G. (1993) Specific proteolytic cleavage of poly(ADP-ribose) polymerase: an early marker of chemotherapy-induced apoptosis. *Cancer research* **53**, 3976-3985
290. Lazebnik, Y. A., Kaufmann, S. H., Desnoyers, S., Poirier, G. G., and Earnshaw, W. C. (1994) Cleavage of poly(ADP-ribose) polymerase by a proteinase with properties like ICE. *Nature* **371**, 346-347
291. Tewari, M., Quan, L. T., O'Rourke, K., Desnoyers, S., Zeng, Z., Beidler, D. R., Poirier, G. G., Salvesen, G. S., and Dixit, V. M. (1995) Yama/CPP32 beta, a mammalian homolog of CED-3, is a CrmA-inhibitable protease that cleaves the death substrate poly(ADP-ribose) polymerase. *Cell* **81**, 801-809
292. Rao, L., Perez, D., and White, E. (1996) Lamin proteolysis facilitates nuclear events during apoptosis. *The Journal of cell biology* **135**, 1441-1455
293. Fischer, U., Janicke, R. U., and Schulze-Osthoff, K. (2003) Many cuts to ruin: a comprehensive update of caspase substrates. *Cell death and differentiation* **10**, 76-100
294. Ghayur, T., Banerjee, S., Hugunin, M., Butler, D., Herzog, L., Carter, A., Quintal, L., Sekut, L., Talanian, R., Paskind, M., Wong, W., Kamen, R., Tracey, D., and Allen, H. (1997) Caspase-1 processes IFN-gamma-inducing factor and regulates LPS-induced IFN-gamma production. *Nature* **386**, 619-623

295. Martinon, F., Burns, K., and Tschopp, J. (2002) The inflammasome: a molecular platform triggering activation of inflammatory caspases and processing of proIL-beta. *Molecular cell* **10**, 417-426
296. Martinon, F., and Tschopp, J. (2004) Inflammatory caspases: linking an intracellular innate immune system to autoinflammatory diseases. *Cell* **117**, 561-574
297. Yoneyama, M., Kikuchi, M., Natsukawa, T., Shinobu, N., Imaizumi, T., Miyagishi, M., Taira, K., Akira, S., and Fujita, T. (2004) The RNA helicase RIG-I has an essential function in double-stranded RNA-induced innate antiviral responses. *Nature immunology* **5**, 730-737
298. O'Neill, L. A., and Bowie, A. G. (2007) The family of five: TIR-domain-containing adaptors in Toll-like receptor signalling. *Nature reviews. Immunology* **7**, 353-364
299. Kawai, T., and Akira, S. (2007) TLR signaling. *Seminars in immunology* **19**, 24-32
300. Janeway, C. A., Jr. (1992) The immune system evolved to discriminate infectious nonself from noninfectious self. *Immunology today* **13**, 11-16
301. Medzhitov, R., and Janeway, C. A., Jr. (2002) Decoding the patterns of self and nonself by the innate immune system. *Science* **296**, 298-300
302. Medzhitov, R., and Janeway, C. A., Jr. (1997) Innate immunity: impact on the adaptive immune response. *Current opinion in immunology* **9**, 4-9
303. Inohara, Chamaillard, McDonald, C., and Nunez, G. (2005) NOD-LRR proteins: role in host-microbial interactions and inflammatory disease. *Annual review of biochemistry* **74**, 355-383
304. Reed, J. C. (2004) Apoptosis mechanisms: implications for cancer drug discovery. *Oncology (Williston Park, N.Y.)* **18**, 11-20
305. Mariathasan, S., Newton, K., Monack, D. M., Vucic, D., French, D. M., Lee, W. P., Roose-Girma, M., Erickson, S., and Dixit, V. M. (2004) Differential activation of the inflammasome by caspase-1 adaptors ASC and Ipaf. *Nature* **430**, 213-218
306. Yamin, T. T., Ayala, J. M., and Miller, D. K. (1996) Activation of the native 45-kDa precursor form of interleukin-1-converting enzyme. *The Journal of biological chemistry* **271**, 13273-13282
307. Gu, Y., Kuida, K., Tsutsui, H., Ku, G., Hsiao, K., Fleming, M. A., Hayashi, N., Higashino, K., Okamura, H., Nakanishi, K., Kurimoto, M., Tanimoto, T., Flavell, R. A., Sato, V., Harding, M. W., Livingston, D. J., and Su, M. S. (1997) Activation of interferon-gamma inducing factor mediated by interleukin-1beta converting enzyme. *Science* **275**, 206-209
308. Nadiri, A., Wolinski, M. K., and Saleh, M. (2006) The inflammatory caspases: key players in the host response to pathogenic invasion and sepsis. *J Immunol* **177**, 4239-4245
309. Saleh, M., Mathison, J. C., Wolinski, M. K., Bensinger, S. J., Fitzgerald, P., Droin, N., Ulevitch, R. J., Green, D. R., and Nicholson, D. W. (2006) Enhanced bacterial clearance and sepsis resistance in caspase-12-deficient mice. *Nature* **440**, 1064-1068
310. Bossy-Wetzel, E., Bakiri, L., and Yaniv, M. (1997) Induction of apoptosis by the transcription factor c-Jun. *Embo J* **16**, 1695-1709
311. Estus, S., Zaks, W. J., Freeman, R. S., Gruda, M., Bravo, R., and Johnson, E. M., Jr. (1994) Altered gene expression in neurons during programmed cell death: identification of c-jun as necessary for neuronal apoptosis. *The Journal of cell biology* **127**, 1717-1727

312. Ham, J., Babij, C., Whitfield, J., Pfarr, C. M., Lallemand, D., Yaniv, M., and Rubin, L. L. (1995) A c-Jun dominant negative mutant protects sympathetic neurons against programmed cell death. *Neuron* **14**, 927-939
313. Behrens, A., Sibilia, M., and Wagner, E. F. (1999) Amino-terminal phosphorylation of c-Jun regulates stress-induced apoptosis and cellular proliferation. *Nature genetics* **21**, 326-329
314. Eferl, R., Sibilia, M., Hilberg, F., Fuchsbichler, A., Kufferath, I., Guertl, B., Zenz, R., Wagner, E. F., and Zatloukal, K. (1999) Functions of c-Jun in liver and heart development. *The Journal of cell biology* **145**, 1049-1061
315. Gurzov, E. N., Ortis, F., Bakiri, L., Wagner, E. F., and Eizirik, D. L. (2008) JunB Inhibits ER Stress and Apoptosis in Pancreatic Beta Cells. *PloS one* **3**, e3030
316. Yogev, O., Goldberg, R., Anzi, S., and Shaulian, E. (2010) Jun proteins are starvation-regulated inhibitors of autophagy. *Cancer research* **70**, 2318-2327
317. Bai, R. Y., Ouyang, T., Miething, C., Morris, S. W., Peschel, C., and Duyster, J. (2000) Nucleophosmin-anaplastic lymphoma kinase associated with anaplastic large-cell lymphoma activates the phosphatidylinositol 3-kinase/Akt antiapoptotic signaling pathway. *Blood* **96**, 4319-4327
318. Slupianek, A., Nieborowska-Skorska, M., Hoser, G., Morrione, A., Majewski, M., Xue, L., Morris, S. W., Wasik, M. A., and Skorski, T. (2001) Role of phosphatidylinositol 3-kinase-Akt pathway in nucleophosmin/anaplastic lymphoma kinase-mediated lymphomagenesis. *Cancer research* **61**, 2194-2199
319. Rassidakis, G. Z., Sarris, A. H., Herling, M., Ford, R. J., Cabanillas, F., McDonnell, T. J., and Medeiros, L. J. (2001) Differential expression of BCL-2 family proteins in ALK-positive and ALK-negative anaplastic large cell lymphoma of T/null-cell lineage. *Am J Pathol* **159**, 527-535
320. Drakos, E., Rassidakis, G. Z., Lai, R., Herling, M., O'Connor, S. L., Schmitt-Graeff, A., McDonnell, T. J., and Medeiros, L. J. (2004) Caspase-3 activation in systemic anaplastic large-cell lymphoma. *Mod Pathol* **17**, 109-116
321. Oyarzo, M. P., Drakos, E., Atwell, C., Amin, H. M., Medeiros, L. J., and Rassidakis, G. Z. (2006) Intrinsic apoptotic pathway in anaplastic large cell lymphoma. *Human pathology* **37**, 874-882
322. Imai, S., Sugiura, M., Oikawa, O., Koizumi, S., Hirao, M., Kimura, H., Hayashibara, H., Terai, N., Tsutsumi, H., Oda, T., Chiba, S., and Osato, T. (1996) Epstein-Barr virus (EBV)-carrying and -expressing T-cell lines established from severe chronic active EBV infection. *Blood* **87**, 1446-1457
323. Clements, G. B., Klein, G., and Povey, S. (1975) Production by EBV infection of an EBNA-positive subline from an EBNA-negative human lymphoma cell line without detectable EBV DNA. *International journal of cancer. Journal international du cancer* **16**, 125-133
324. Ben-Bassat, H., Goldblum, N., Mitrani, S., Goldblum, T., Yoffey, J. M., Cohen, M. M., Bentwich, Z., Ramot, B., Klein, E., and Klein, G. (1977) Establishment in continuous culture of a new type of lymphocyte from a "Burkitt like" malignant lymphoma (line D.G.-75). *International journal of cancer. Journal international du cancer* **19**, 27-33
325. Schneider, U., Schwenk, H. U., and Bornkamm, G. (1977) Characterization of EBV-genome negative "null" and "T" cell lines derived from children with acute lymphoblastic leukemia and leukemic transformed non-Hodgkin lymphoma. *International journal of cancer. Journal international du cancer* **19**, 621-626

326. Northrop, J. P., Ullman, K. S., and Crabtree, G. R. (1993) Characterization of the nuclear and cytoplasmic components of the lymphoid-specific nuclear factor of activated T cells (NF-AT) complex. *The Journal of biological chemistry* **268**, 2917-2923
327. Fischer, P., Nacheva, E., Mason, D. Y., Sherrington, P. D., Hoyle, C., Hayhoe, F. G., and Karpas, A. (1988) A Ki-1 (CD30)-positive human cell line (Karpas 299) established from a high-grade non-Hodgkin's lymphoma, showing a 2;5 translocation and rearrangement of the T-cell receptor beta-chain gene. *Blood* **72**, 234-240
328. Hsu, S. M., Xie, S. S., and Hsu, P. L. (1990) Cultured Reed-Sternberg cells HDLM-1 and KM-H2 can be induced to become histiocytelike cells. H-RS cells are not derived from lymphocytes. *Am J Pathol* **137**, 353-367
329. Fisher, R. I., Bates, S. E., Bostick-Bruton, F., Tuteja, N., and Diehl, V. (1984) Neoplastic cells obtained from Hodgkin's disease function as accessory cells for mitogen-induced human T cell proliferative responses. *J Immunol* **132**, 2672-2677
330. Morgan, R., Smith, S. D., Hecht, B. K., Christy, V., Mellentin, J. D., Warnke, R., and Cleary, M. L. (1989) Lack of involvement of the c-fms and N-myc genes by chromosomal translocation t(2;5)(p23;q35) common to malignancies with features of so-called malignant histiocytosis. *Blood* **73**, 2155-2164
331. Hanahan, D. (1983) Studies on transformation of Escherichia coli with plasmids. *Journal of molecular biology* **166**, 557-580
332. Katoh, K., Misawa, K., Kuma, K., and Miyata, T. (2002) MAFFT: a novel method for rapid multiple sequence alignment based on fast Fourier transform. *Nucleic acids research* **30**, 3059-3066
333. Caffrey, D. R., Dana, P. H., Mathur, V., Ocano, M., Hong, E. J., Wang, Y. E., Somaroo, S., Caffrey, B. E., Potluri, S., and Huang, E. S. (2007) PFAAT version 2.0: a tool for editing, annotating, and analyzing multiple sequence alignments. *BMC bioinformatics* **8**, 381
334. Murphy, L. O., Smith, S., Chen, R. H., Fingar, D. C., and Blenis, J. (2002) Molecular interpretation of ERK signal duration by immediate early gene products. *Nature cell biology* **4**, 556-564
335. Ho, S. N., Hunt, H. D., Horton, R. M., Pullen, J. K., and Pease, L. R. (1989) Site-directed mutagenesis by overlap extension using the polymerase chain reaction. *Gene* **77**, 51-59
336. Wasilenko, S. T., Meyers, A. F., Vander Helm, K., and Barry, M. (2001) Vaccinia virus infection disarms the mitochondrion-mediated pathway of the apoptotic cascade by modulating the permeability transition pore. *Journal of virology* **75**, 11437-11448
337. Song, J., Tan, H., Shen, H., Mahmood, K., Boyd, S. E., Webb, G. I., Akutsu, T., and Whisstock, J. C. (2010) Cascleave: towards more accurate prediction of caspase substrate cleavage sites. *Bioinformatics* **26**, 752-760
338. Flygare, J., Hellgren, D., and Wennborg, A. (2000) Caspase-3 mediated cleavage of HsRad51 at an unconventional site. *European journal of biochemistry / FEBS* **267**, 5977-5982
339. Bradford, M. M. (1976) A rapid and sensitive method for the quantitation of microgram quantities of protein utilizing the principle of protein-dye binding. *Analytical biochemistry* **72**, 248-254

340. Czekanska, E. M. (2011) Assessment of cell proliferation with resazurin-based fluorescent dye. *Methods Mol Biol* **740**, 27-32
341. Garcia-Calvo, M., Peterson, E. P., Leiting, B., Ruel, R., Nicholson, D. W., and Thornberry, N. A. (1998) Inhibition of human caspases by peptide-based and macromolecular inhibitors. *The Journal of biological chemistry* **273**, 32608-32613
342. Han, Y., Amin, H. M., Frantz, C., Franko, B., Lee, J., Lin, Q., and Lai, R. (2006) Restoration of shp1 expression by 5-AZA-2'-deoxycytidine is associated with downregulation of JAK3/STAT3 signaling in ALK-positive anaplastic large cell lymphoma. *Leukemia* **20**, 1602-1609
343. Hsu, F. Y., Zhao, Y., Anderson, W. F., and Johnston, P. B. (2007) Downregulation of NPM-ALK by siRNA causes anaplastic large cell lymphoma cell growth inhibition and augments the anti cancer effects of chemotherapy in vitro. *Cancer Invest* **25**, 240-248
344. Holtick, U., Vockerodt, M., Pinkert, D., Schoof, N., Sturzenhofecker, B., Kussebi, N., Lauber, K., Wesselborg, S., Loffler, D., Horn, F., Trumper, L., and Kube, D. (2005) STAT3 is essential for Hodgkin lymphoma cell proliferation and is a target of tyrphostin AG17 which confers sensitization for apoptosis. *Leukemia* **19**, 936-944
345. Mechta-Grigoriou, F., Gerald, D., and Yaniv, M. (2001) The mammalian Jun proteins: redundancy and specificity. *Oncogene* **20**, 2378-2389
346. Nikolakaki, E., Coffer, P. J., Hemelsoet, R., Woodgett, J. R., and Defize, L. H. (1993) Glycogen synthase kinase 3 phosphorylates Jun family members in vitro and negatively regulates their transactivating potential in intact cells. *Oncogene* **8**, 833-840
347. Dephoure, N., Zhou, C., Villen, J., Beausoleil, S. A., Bakalarski, C. E., Elledge, S. J., and Gygi, S. P. (2008) A quantitative atlas of mitotic phosphorylation. *Proceedings of the National Academy of Sciences of the United States of America* **105**, 10762-10767
348. Brown, P. H., Alani, R., Preis, L. H., Szabo, E., and Birrer, M. J. (1993) Suppression of oncogene-induced transformation by a deletion mutant of c-jun. *Oncogene* **8**, 877-886
349. Brown, P. H., Chen, T. K., and Birrer, M. J. (1994) Mechanism of action of a dominant-negative mutant of c-Jun. *Oncogene* **9**, 791-799
350. Liu, Y., Lu, C., Shen, Q., Munoz-Medellin, D., Kim, H., and Brown, P. H. (2004) AP-1 blockade in breast cancer cells causes cell cycle arrest by suppressing G1 cyclin expression and reducing cyclin-dependent kinase activity. *Oncogene* **23**, 8238-8246
351. Shimizu, Y., Kinoshita, I., Kikuchi, J., Yamazaki, K., Nishimura, M., Birrer, M. J., and Dosaka-Akita, H. (2008) Growth inhibition of non-small cell lung cancer cells by AP-1 blockade using a cJun dominant-negative mutant. *British journal of cancer* **98**, 915-922
352. Tichelaar, J. W., Yan, Y., Tan, Q., Wang, Y., Estensen, R. D., Young, M. R., Colburn, N. H., Yin, H., Goodin, C., Anderson, M. W., and You, M. (2010) A dominant-negative c-jun mutant inhibits lung carcinogenesis in mice. *Cancer prevention research (Philadelphia, Pa.)* **3**, 1148-1156

353. Hennigan, R. F., and Stambrook, P. J. (2001) Dominant negative c-jun inhibits activation of the cyclin D1 and cyclin E kinase complexes. *Molecular biology of the cell* **12**, 2352-2363
354. Feng, Z., Li, L., Ng, P. Y., and Porter, A. G. (2002) Neuronal differentiation and protection from nitric oxide-induced apoptosis require c-Jun-dependent expression of NCAM140. *Molecular and cellular biology* **22**, 5357-5366
355. Madireddi, M. T., Dent, P., and Fisher, P. B. (2000) AP-1 and C/EBP transcription factors contribute to mda-7 gene promoter activity during human melanoma differentiation. *Journal of cellular physiology* **185**, 36-46
356. Cooper, S. J., MacGowan, J., Ranger-Moore, J., Young, M. R., Colburn, N. H., and Bowden, G. T. (2003) Expression of dominant negative c-jun inhibits ultraviolet B-induced squamous cell carcinoma number and size in an SKH-1 hairless mouse model. *Molecular cancer research : MCR* **1**, 848-854
357. Han, B., Rorke, E. A., Adhikary, G., Chew, Y. C., Xu, W., and Eckert, R. L. (2012) Suppression of AP1 transcription factor function in keratinocyte suppresses differentiation. *PloS one* **7**, e36941
358. Li, J. J., Rhim, J. S., Schlegel, R., Vousden, K. H., and Colburn, N. H. (1998) Expression of dominant negative Jun inhibits elevated AP-1 and NF-kappaB transactivation and suppresses anchorage independent growth of HPV immortalized human keratinocytes. *Oncogene* **16**, 2711-2721
359. Thompson, E. J., MacGowan, J., Young, M. R., Colburn, N., and Bowden, G. T. (2002) A dominant negative c-jun specifically blocks okadaic acid-induced skin tumor promotion. *Cancer research* **62**, 3044-3047
360. Fletcher, J. I., Haber, M., Henderson, M. J., and Norris, M. D. (2010) ABC transporters in cancer: more than just drug efflux pumps. *Nat Rev Cancer* **10**, 147-156
361. Igney, F. H., and Krammer, P. H. (2002) Death and anti-death: tumour resistance to apoptosis. *Nat Rev Cancer* **2**, 277-288
362. Holcik, M., and Sonenberg, N. (2005) Translational control in stress and apoptosis. *Nature reviews. Molecular cell biology* **6**, 318-327
363. Wasilenko, S. T., Banadyga, L., Bond, D., and Barry, M. (2005) The vaccinia virus F1L protein interacts with the proapoptotic protein Bak and inhibits Bak activation. *Journal of virology* **79**, 14031-14043
364. Kurokawa, M., and Kornbluth, S. (2009) Caspases and kinases in a death grip. *Cell* **138**, 838-854
365. Emoto, Y., Manome, Y., Meinhardt, G., Kisaki, H., Kharbanda, S., Robertson, M., Ghayur, T., Wong, W. W., Kamen, R., Weichselbaum, R., and et al. (1995) Proteolytic activation of protein kinase C delta by an ICE-like protease in apoptotic cells. *Embo J* **14**, 6148-6156
366. Coleman, M. L., Sahai, E. A., Yeo, M., Bosch, M., Dewar, A., and Olson, M. F. (2001) Membrane blebbing during apoptosis results from caspase-mediated activation of ROCK I. *Nature cell biology* **3**, 339-345
367. Sebbagh, M., Renvoize, C., Hamelin, J., Riche, N., Bertoglio, J., and Breard, J. (2001) Caspase-3-mediated cleavage of ROCK I induces MLC phosphorylation and apoptotic membrane blebbing. *Nature cell biology* **3**, 346-352
368. Cardone, M. H., Salvesen, G. S., Widmann, C., Johnson, G., and Frisch, S. M. (1997) The regulation of anoikis: MEKK-1 activation requires cleavage by caspases. *Cell* **90**, 315-323

369. Deak, J. C., Cross, J. V., Lewis, M., Qian, Y., Parrott, L. A., Distelhorst, C. W., and Templeton, D. J. (1998) Fas-induced proteolytic activation and intracellular redistribution of the stress-signaling kinase MEKK1. *Proceedings of the National Academy of Sciences of the United States of America* **95**, 5595-5600
370. Widmann, C., Gerwins, P., Johnson, N. L., Jarpe, M. B., and Johnson, G. L. (1998) MEK kinase 1, a substrate for DEVD-directed caspases, is involved in genotoxin-induced apoptosis. *Molecular and cellular biology* **18**, 2416-2429
371. Widmann, C., Gibson, S., and Johnson, G. L. (1998) Caspase-dependent cleavage of signaling proteins during apoptosis. A turn-off mechanism for anti-apoptotic signals. *The Journal of biological chemistry* **273**, 7141-7147
372. Bachelder, R. E., Wendt, M. A., Fujita, N., Tsuruo, T., and Mercurio, A. M. (2001) The cleavage of Akt/protein kinase B by death receptor signaling is an important event in detachment-induced apoptosis. *The Journal of biological chemistry* **276**, 34702-34707
373. Xu, J., Liu, D., and Songyang, Z. (2002) The role of Asp-462 in regulating Akt activity. *The Journal of biological chemistry* **277**, 35561-35566
374. Crouch, D. H., Fincham, V. J., and Frame, M. C. (1996) Targeted proteolysis of the focal adhesion kinase pp125 FAK during c-MYC-induced apoptosis is suppressed by integrin signalling. *Oncogene* **12**, 2689-2696
375. Wen, L. P., Fahrni, J. A., Troie, S., Guan, J. L., Orth, K., and Rosen, G. D. (1997) Cleavage of focal adhesion kinase by caspases during apoptosis. *The Journal of biological chemistry* **272**, 26056-26061
376. Santoro, M. F., Annand, R. R., Robertson, M. M., Peng, Y. W., Brady, M. J., Mankovich, J. A., Hackett, M. C., Ghayur, T., Walter, G., Wong, W. W., and Giegel, D. A. (1998) Regulation of protein phosphatase 2A activity by caspase-3 during apoptosis. *The Journal of biological chemistry* **273**, 13119-13128
377. Huang, H. S., and Lee, E. Y. (2008) Protein phosphatase-1 inhibitor-3 is an in vivo target of caspase-3 and participates in the apoptotic response. *The Journal of biological chemistry* **283**, 18135-18146
378. Degli Esposti, M., Ferry, G., Masdehors, P., Boutin, J. A., Hickman, J. A., and Dive, C. (2003) Post-translational modification of Bid has differential effects on its susceptibility to cleavage by caspase 8 or caspase 3. *The Journal of biological chemistry* **278**, 15749-15757
379. Lu, W., Lee, H. K., Xiang, C., Finniss, S., and Brodie, C. (2007) The phosphorylation of tyrosine 332 is necessary for the caspase 3-dependent cleavage of PKCdelta and the regulation of cell apoptosis. *Cell Signal* **19**, 2165-2173
380. Dix, M. M., Simon, G. M., Wang, C., Okerberg, E., Patricelli, M. P., and Cravatt, B. F. (2012) Functional interplay between caspase cleavage and phosphorylation sculpts the apoptotic proteome. *Cell* **150**, 426-440
381. Ravi, R., Bedi, A., and Fuchs, E. J. (1998) CD95 (Fas)-induced caspase-mediated proteolysis of NF-kappaB. *Cancer research* **58**, 882-886
382. Levkau, B., Scatena, M., Giachelli, C. M., Ross, R., and Raines, E. W. (1999) Apoptosis overrides survival signals through a caspase-mediated dominant-negative NF-kappa B loop. *Nature cell biology* **1**, 227-233
383. Barkett, M., Dooher, J. E., Lemonnier, L., Simmons, L., Scarpati, J. N., Wang, Y., and Gilmore, T. D. (2001) Three mutations in v-Rel render it resistant to

cleavage by cell-death protease caspase-3. *Biochimica et biophysica acta* **1526**, 25-36

384. King, P., and Goodbourn, S. (1998) STAT1 is inactivated by a caspase. *The Journal of biological chemistry* **273**, 8699-8704
385. Darnowski, J. W., Goulette, F. A., Guan, Y. J., Chatterjee, D., Yang, Z. F., Cousens, L. P., and Chin, Y. E. (2006) Stat3 cleavage by caspases: impact on full-length Stat3 expression, fragment formation, and transcriptional activity. *The Journal of biological chemistry* **281**, 17707-17717
386. Charvet, C., Alberti, I., Luciano, F., Jacquel, A., Bernard, A., Auberger, P., and Deckert, M. (2003) Proteolytic regulation of Forkhead transcription factor FOXO3a by caspase-3-like proteases. *Oncogene* **22**, 4557-4568
387. De Maria, R., Zeuner, A., Eramo, A., Domenichelli, C., Bonci, D., Grignani, F., Srinivasula, S. M., Alnemri, E. S., Testa, U., and Peschle, C. (1999) Negative regulation of erythropoiesis by caspase-mediated cleavage of GATA-1. *Nature* **401**, 489-493
388. Krippner-Heidenreich, A., Walsemann, G., Beyrouthy, M. J., Speckgens, S., Kraft, R., Thole, H., Talanian, R. V., Hurt, M. M., and Luscher, B. (2005) Caspase-dependent regulation and subcellular redistribution of the transcriptional modulator YY1 during apoptosis. *Molecular and cellular biology* **25**, 3704-3714
389. Zhao, M., Duan, X. F., Wen, D. H., and Chen, G. Q. (2009) PU.1, a novel capase-3 substrate, partially contributes to chemotherapeutic agents-induced apoptosis in leukemic cells. *Biochem Bioph Res Co* **382**, 508-513
390. Gordon, S., Akopyan, G., Garban, H., and Bonavida, B. (2006) Transcription factor YY1: structure, function, and therapeutic implications in cancer biology. *Oncogene* **25**, 1125-1142
391. Wang, Z. Q., Stingl, L., Morrison, C., Jantsch, M., Los, M., Schulze-Osthoff, K., and Wagner, E. F. (1997) PARP is important for genomic stability but dispensable in apoptosis. *Genes & development* **11**, 2347-2358
392. Oliver, F. J., de la Rubia, G., Rolli, V., Ruiz-Ruiz, M. C., de Murcia, G., and Murcia, J. M. (1998) Importance of poly(ADP-ribose) polymerase and its cleavage in apoptosis. Lesson from an uncleavable mutant. *The Journal of biological chemistry* **273**, 33533-33539
393. Ferrari, D., Stepczynska, A., Los, M., Wesselborg, S., and Schulze-Osthoff, K. (1998) Differential regulation and ATP requirement for caspase-8 and caspase-3 activation during CD95- and anticancer drug-induced apoptosis. *The Journal of experimental medicine* **188**, 979-984
394. Los, M., Mozoluk, M., Ferrari, D., Stepczynska, A., Stroh, C., Renz, A., Herceg, Z., Wang, Z. Q., and Schulze-Osthoff, K. (2002) Activation and caspase-mediated inhibition of PARP: a molecular switch between fibroblast necrosis and apoptosis in death receptor signaling. *Molecular biology of the cell* **13**, 978-988
395. Filipovic, D. M., Meng, X., and Reeves, W. B. (1999) Inhibition of PARP prevents oxidant-induced necrosis but not apoptosis in LLC-PK1cells. *American Journal of Physiology - Renal Physiology* **277**, F428-F436
396. Rajani, D. K., Walch, M., Martinvalet, D., Thomas, M. P., and Lieberman, J. (2012) Alterations in RNA processing during immune-mediated programmed cell death. *Proceedings of the National Academy of Sciences of the United States of America* **109**, 8688-8693

397. Chun, H. J., Zheng, L., Ahmad, M., Wang, J., Speirs, C. K., Siegel, R. M., Dale, J. K., Puck, J., Davis, J., Hall, C. G., Skoda-Smith, S., Atkinson, T. P., Straus, S. E., and Lenardo, M. J. (2002) Pleiotropic defects in lymphocyte activation caused by caspase-8 mutations lead to human immunodeficiency. *Nature* **419**, 395-399
398. Salmena, L., Lemmers, B., Hakem, A., Matysiak-Zablocki, E., Murakami, K., Au, P. Y., Berry, D. M., Tamblyn, L., Shehabeldin, A., Migon, E., Wakeham, A., Bouchard, D., Yeh, W. C., McGlade, J. C., Ohashi, P. S., and Hakem, R. (2003) Essential role for caspase 8 in T-cell homeostasis and T-cell-mediated immunity. *Genes & development* **17**, 883-895
399. Bidere, N., Su, H. C., and Lenardo, M. J. (2006) Genetic disorders of programmed cell death in the immune system. *Annual review of immunology* **24**, 321-352
400. Kennedy, N. J., Kataoka, T., Tschopp, J., and Budd, R. C. (1999) Caspase activation is required for T cell proliferation. *The Journal of experimental medicine* **190**, 1891-1896
401. Alam, A., Cohen, L. Y., Aouad, S., and Sekaly, R. P. (1999) Early activation of caspases during T lymphocyte stimulation results in selective substrate cleavage in nonapoptotic cells. *The Journal of experimental medicine* **190**, 1879-1890
402. Micheau, O., Thome, M., Schneider, P., Holler, N., Tschopp, J., Nicholson, D. W., Briand, C., and Grutter, M. G. (2002) The long form of FLIP is an activator of caspase-8 at the Fas death-inducing signaling complex. *The Journal of biological chemistry* **277**, 45162-45171
403. Tschopp, J., Irmler, M., and Thome, M. (1998) Inhibition of fas death signals by FLIPs. *Current opinion in immunology* **10**, 552-558
404. Boatright, K. M., Deis, C., Denault, J. B., Sutherlin, D. P., and Salvesen, G. S. (2004) Activation of caspases-8 and -10 by FLIP(L). *The Biochemical journal* **382**, 651-657
405. Chang, D. W., Xing, Z., Pan, Y., Algeciras-Schimnich, A., Barnhart, B. C., Yaish-Ohad, S., Peter, M. E., and Yang, X. (2002) c-FLIP(L) is a dual function regulator for caspase-8 activation and CD95-mediated apoptosis. *EMBO J* **21**, 3704-3714
406. Irmler, M., Thome, M., Hahne, M., Schneider, P., Hofmann, K., Steiner, V., Bodmer, J. L., Schroter, M., Burns, K., Mattmann, C., Rimoldi, D., French, L. E., and Tschopp, J. (1997) Inhibition of death receptor signals by cellular FLIP. *Nature* **388**, 190-195
407. Dohrman, A., Kataoka, T., Cuenin, S., Russell, J. Q., Tschopp, J., and Budd, R. C. (2005) Cellular FLIP (long form) regulates CD8+ T cell activation through caspase-8-dependent NF-kappa B activation. *J Immunol* **174**, 5270-5278
408. Kataoka, T., and Tschopp, J. (2004) N-terminal fragment of c-FLIP(L) processed by caspase 8 specifically interacts with TRAF2 and induces activation of the NF-kappaB signaling pathway. *Molecular and cellular biology* **24**, 2627-2636
409. Su, H., Bidere, N., Zheng, L., Cubre, A., Sakai, K., Dale, J., Salmena, L., Hakem, R., Straus, S., and Lenardo, M. (2005) Requirement for caspase-8 in NF-kappaB activation by antigen receptor. *Science* **307**, 1465-1468
410. Bidere, N., Snow, A. L., Sakai, K., Zheng, L., and Lenardo, M. J. (2006) Caspase-8 regulation by direct interaction with TRAF6 in T cell receptor-induced NF-kappaB activation. *Current biology : CB* **16**, 1666-1671
411. Nakayama, K. I., and Nakayama, K. (2006) Ubiquitin ligases: cell-cycle control and cancer. *Nat Rev Cancer* **6**, 369-381

412. Yan, X. X., Najbauer, J., Woo, C. C., Dashtipour, K., Ribak, C. E., and Leon, M. (2001) Expression of active caspase-3 in mitotic and postmitotic cells of the rat forebrain. *The Journal of comparative neurology* **433**, 4-22
413. Hsu, S. L., Yu, C. T., Yin, S. C., Tang, M. J., Tien, A. C., Wu, Y. M., and Huang, C. Y. (2006) Caspase 3, periodically expressed and activated at G2/M transition, is required for nocodazole-induced mitotic checkpoint. *Apoptosis : an international journal on programmed cell death* **11**, 765-771
414. Swe, M., and Sit, K. H. (2000) zVAD-fmk and DEVD-cho induced late mitosis arrest and apoptotic expressions. *Apoptosis : an international journal on programmed cell death* **5**, 29-36
415. Hashimoto, T., Kikkawa, U., and Kamada, S. (2011) Contribution of caspase(s) to the cell cycle regulation at mitotic phase. *PloS one* **6**, e18449
416. Hashimoto, T., Yamauchi, L., Hunter, T., Kikkawa, U., and Kamada, S. (2008) Possible involvement of caspase-7 in cell cycle progression at mitosis. *Genes to cells : devoted to molecular & cellular mechanisms* **13**, 609-621
417. Jacobs-Helber, S. M., Abutin, R. M., Tian, C., Bondurant, M., Wickrema, A., and Sawyer, S. T. (2002) Role of JunB in erythroid differentiation. *The Journal of biological chemistry* **277**, 4859-4866
418. Mehic, D., Bakiri, L., Ghannadan, M., Wagner, E. F., and Tschachler, E. (2005) Fos and jun proteins are specifically expressed during differentiation of human keratinocytes. *The Journal of investigative dermatology* **124**, 212-220
419. Bessis, M., and Weed, R. I. (1973) The structure of normal and pathologic erythrocytes. *Advances in biological and medical physics* **14**, 35-91
420. Seki, M., and Shirasawa, H. (1965) Role of the reticular cells during maturation process of the erythroblast. 3. The fate of phagocytized nucleus. *Acta pathologica japonica* **15**, 387-405
421. Seki, M., Yoneyama, T., and Shirasawa, H. (1965) Role of the reticular cells during maturation process of the erythroblast. II. Further observation on the denucleation process of erythroblast. *Acta pathologica japonica* **15**, 303-316
422. Seki, M., Yoneyama, T., and Shirasawa, H. (1965) Role of the reticular cells during maturation process of the erythroblast. I. Denucleation of erythroblast by reticular cell; electron microscopic study. *Acta pathologica japonica* **15**, 295-301
423. Carlile, G. W., Smith, D. H., and Wiedmann, M. (2004) Caspase-3 has a nonapoptotic function in erythroid maturation. *Blood* **103**, 4310-4316
424. Zermati, Y., Garrido, C., Amsellem, S., Fishelson, S., Bouscary, D., Valensi, F., Varet, B., Solary, E., and Hermine, O. (2001) Caspase activation is required for terminal erythroid differentiation. *The Journal of experimental medicine* **193**, 247-254
425. McCall, C. A., and Cohen, J. J. (1991) Programmed cell death in terminally differentiating keratinocytes: role of endogenous endonuclease. *The Journal of investigative dermatology* **97**, 111-114
426. Weil, M., Raff, M. C., and Braga, V. M. (1999) Caspase activation in the terminal differentiation of human epidermal keratinocytes. *Current biology : CB* **9**, 361-364
427. Sordet, O., Rebe, C., Plenchette, S., Zermati, Y., Hermine, O., Vainchenker, W., Garrido, C., Solary, E., and Dubrez-Daloz, L. (2002) Specific involvement of

caspases in the differentiation of monocytes into macrophages. *Blood* **100**, 4446-4453

428. Rebe, C., Cathelin, S., Launay, S., Filomenko, R., Prevotat, L., L'Ollivier, C., Gyan, E., Micheau, O., Grant, S., Dubart-Kupperschmitt, A., Fontenay, M., and Solary, E. (2007) Caspase-8 prevents sustained activation of NF-kappaB in monocytes undergoing macrophagic differentiation. *Blood* **109**, 1442-1450
429. Cathelin, S., Rebe, C., Haddaoui, L., Simioni, N., Verdier, F., Fontenay, M., Launay, S., Mayeux, P., and Solary, E. (2006) Identification of proteins cleaved downstream of caspase activation in monocytes undergoing macrophage differentiation. *The Journal of biological chemistry* **281**, 17779-17788
430. Zeuner, A., Eramo, A., Testa, U., Felli, N., Pelosi, E., Mariani, G., Srinivasula, S. M., Alnemri, E. S., Condorelli, G., Peschle, C., and De Maria, R. (2003) Control of erythroid cell production via caspase-mediated cleavage of transcription factor SCL/Tal-1. *Cell death and differentiation* **10**, 905-913
431. Franchi, L., Eigenbrod, T., Munoz-Planillo, R., and Nunez, G. (2009) The inflammasome: a caspase-1-activation platform that regulates immune responses and disease pathogenesis. *Nature immunology* **10**, 241-247
432. Rajput, A., Kovalenko, A., Bogdanov, K., Yang, S. H., Kang, T. B., Kim, J. C., Du, J., and Wallach, D. (2011) RIG-I RNA helicase activation of IRF3 transcription factor is negatively regulated by caspase-8-mediated cleavage of the RIP1 protein. *Immunity* **34**, 340-351
433. Ben Moshe, T., Barash, H., Kang, T. B., Kim, J. C., Kovalenko, A., Gross, E., Schuchmann, M., Abramovitch, R., Galun, E., and Wallach, D. (2007) Role of caspase-8 in hepatocyte response to infection and injury in mice. *Hepatology (Baltimore, Md.)* **45**, 1014-1024
434. Oberst, A., and Green, D. R. (2011) It cuts both ways: reconciling the dual roles of caspase 8 in cell death and survival. *Nature reviews. Molecular cell biology* **12**, 757-763
435. Gomard, T., Michaud, H. A., Tempe, D., Thiolon, K., Pelegrin, M., and Piechaczyk, M. (2010) An NF-kappaB-dependent role for JunB in the induction of proinflammatory cytokines in LPS-activated bone marrow-derived dendritic cells. *PloS one* **5**, e9585